SYNTHESIS AND CHARACTERIZATION OF MECHANICAL, THERMAL AND FLAMMABILITY PROPERTIES OF EPOXY BASED NANOCOMPOSITES

A THESIS SUBMITTED TO
THE GRADUATE SCHOOL OF NATURAL AND APPLIED SCIENCES
OF
MIDDLE EAST TECHNICAL UNIVERSITY

BY

ERHAN KOP

IN PARTIAL FULFILLMENT OF THE REQUIREMENTS
FOR
THE DEGREE OF MASTER SCIENCE
IN
CHEMICAL ENGINEERING

DECEMBER 2007

Approval of the thesis:

SYNTHESIS AND CHARACTERIZATION OF MECHANICAL, THERMAL AND FLAMMABILITY PROPERTIES OF EPOXY BASED NANOCOMPOSITES

Submitted by **ERHAN KOP** in partial fulfillment of the requirements for the degree of **Master of Science in Chemical Engineering Department, Middle East Technical University** by,

Prof. Dr. Canan ÖZGEN _____
Dean, **Graduate School of Natural and Applied Sciences**

Prof. Dr. Gürkan KARAKAŞ _____
Head of Department, **Chemical Engineering Dept., METU**

Prof. Dr. Ülkü YILMAZER _____
Supervisor, **Chemical Engineering Dept., METU**

Examining Committee Members

Prof. Dr. Güngör GÜNDÜZ _____
Chemical Engineering Dept., METU

Prof. Dr. Ülkü YILMAZER _____
Chemical Engineering Dept., METU

Prof. Dr. Cevdet KAYNAK _____
Metallurgical and Materials Engineering Dept., METU

Assoc. Prof. Dr. Göknur BAYRAM _____
Chemical Engineering Dept., METU

Dr. Cevdet ÖZTİN _____
Chemical Engineering Dept., METU

Date: _____

I hereby declare that all information in this document has been obtained and presented in accordance with academic rules and ethical conduct. I also declare that, as required by these rules and conduct, I have fully cited and referenced all material and results that are not original to this work.

Name, Last name : Erhan KOP

Signature :

ABSTRACT

SYNTHESIS AND CHARACTERIZATION OF MECHANICAL, THERMAL AND FLAMMABILITY PROPERTIES OF EPOXY BASED NANOCOMPOSITES

Kop, Erhan

M.S., Department of Chemical Engineering

Supervisor: Prof. Dr. Ülkü YILMAZER

December 2007, 118 pages

Polymer-clay nanocomposites have received a lot of attention because of outstanding improvements in properties when compared with neat polymeric materials. The aim of this study was to prepare epoxy-clay nanocomposites by mixing organically modified montmorillonite with an epoxy resin and to investigate the effects of clay content on the mechanical, thermal and flammability properties of the resultant nanocomposites. The production of the epoxy-clay nanocomposites was accomplished by in-situ polymerization. In the nanocomposite synthesis, organically modified clay content was varied from 1 wt.% to 9 wt.%. Araldite LY556 epoxy resin, Aradur 918 anhydride hardener, and DY070 imidazole type accelerator were used in the epoxy system. Closite 30B, an organoclay modified with methyl, tallow, bis-2-hydroxyethyl, quaternary ammonium chloride (MT2EtOH), was used as the clay material.

X-ray diffraction results showed that d-spacing between the platelets of organoclay increased from 1.80 nm to 4.4 nm. The microstructures

of nanocomposites were investigated by scanning electron microscopy (SEM). The SEM micrographs indicated that at 1 wt.% clay loading, no clay aggregates were observed. On the other hand, beyond 1 wt.% clay loading, formation of clay agglomerations was observed. Tensile strength and tensile strain values of nanocomposites decreased with clay loading. The tensile strength value of neat epoxy resin decreased from 55 MPa to 29 MPa with 9 % clay loading. On the other hand, Young's modulus increased with clay content and a maximum value was obtained at 5 wt. % clay loading. At 9 % clay loading, Young's modulus value was 26 % higher than that of the neat epoxy resin. Impact strength property had a minimum value at 7 wt. % clay content. Flexural strength and flexural strain at break property behaved in a similar trend. They had a minimum value at 5 % clay loading. At this clay loading, flexural strength value became approximately 43 % lower compared to the flexural strength of the neat epoxy resin. On the other hand, at 9 wt.% clay loading flexural modulus value increased approximately 48 % compared to the pure epoxy resin.

Up to 7 wt.% clay ratio, initial decomposition temperature of epoxy resin was slightly improved. Also, according to TGA results, amount of char formation increased with clay loading. DSC results indicate that Tg of the cured nanocomposite resins decreased from 147 ^{o}C to 129 ^{o}C with 9 wt. % clay loading. The flammability of neat epoxy resin was not significantly affected with Cloisite 30B addition.

Keywords: Nanocomposite, Epoxy Resin, Montmorillonite, In-situ Polymerization, Flammability

ÖZ

EPOKSİ ESASLI NANOKOMPOZİTLERİN SENTEZİ VE MEKANİK, ISIL VE YANABİLİRLİK ÖZELLİKLERİNİN KARAKTERİZASYONU

Kop, Erhan

Yüksek Lisans, Kimya Mühendisliği Bölümü

Tez Yöneticisi: Prof. Dr. Ülkü YILMAZER

Aralık 2007, 118 sayfa

Saf polimerik malzemelerle karşılaştırıldığında özelliklerindeki göze çarpan iyileşme etkileri nedeniyle polymer-kil nanokompozitleri büyük önem kazanmıştır. Bu çalışmanın amacı organik olarak modifiye edilmiş montmorillonit kili epoksi reçine ile karıştırarak epoksi/kil nanokompozit sistemleri hazırlamak ve elde edilen nanokompozitlerin mekanik, ısıl ve yanabilirlik özelliklerine inorganik dolgunun etkisini incelemektir. Epoksi-kil nanokompozitlerin üretimi yerinde polimerizasyon ile gerçekleştirilmiştir. Nanokompozit sentezlerinde organik olarak modifiye kil kütlece %1 ve % 9 oranlarında kullanılmıştır. Kullanılan epoksi reçine, Araldite LY556 epoksi, Aradur 918 anhidrit sertleştirici ve DY070 imidazol hızlandırıcıdan oluşmaktadır. Kil malzeme olarak metal, tallov, bis-2-hidroksietil, kuaterner amonyum klorit (MT2EtOH) ile modifiye edilmiş Cloisite 30B kullanılmıştır.

X-ışını kırınım sonuçları, kilin plakacıkları arasındaki d-boşluğunun 1.80nm'den 4.4 nm'ye çıktığını göstermektedir. Nanokompozitlerin

mikro yapıları taramalı elektron mikroskopu (SEM) ile incelendi. SEM grafikleri, ağırlıkça % 1 kil yüklemesinde kil topaklanması gözlenmemiştir. Fakat, ağırlıkça % 1'den daha yüksek kil yüklemelerinde, kil topaklanmalarının oluştuğu gözlenmiştir. Nano-kompozitlerin çekme dayanımı ve kopmada uzama değerleri kil yüklemesi ile azalmıştır. Saf epoksi reçinenin çekme dayanımı kütlece % 9 kil yükleme ile 55MPa'dan 29MPa'a düşmüştür. Fakat, Young modülü değeri kil miktarı ile artmıştır ve en yüksek değer kütlece % 5 kil yüklemesi ile elde edilmiştir. % 9 kil yüklemesinde, Young modülü değeri saf epoksi reçineye göre % 26 artmıştır. Malzeme kütlece % 7 kil içerdiği durumda en düşük darbe dayanımına sahiptir. Eğilmedeki dayanım ve kopma özellikleri benzer eğilimler göstermiştir. Bu veriler, kütlece % 5 kil yüklemesinde en düşük değere sahiplerdir. Bu kil yüklemesiyle, eğilme dayanımı değeri saf epoksinin sahip olduğuna göre yaklaşık % 43 daha düşük olmuştur. Öte yandan, kütlece % 9 kil içeren nanokompozit malzemenin eğilme modülü saf epoksinin değerine göre % 48 artmıştır.

Epoksi reçinenin ilk bozunma sıcaklığı kütlece % 7 kil oranına kadar çok az miktarda iyileşmiştir. Bununla birlikte TGA sonuçlarına göre kil yüklemesi ile birlikte cüruf oluşma miktarı artmaktadır. DSC analizi sonucunda kürleştirilmiş nanokompozitin Tg değeri kütlece % 9 kil yüklemesi ile 147 ^{o}C'den 129 ^{o}C' ye düşmüştür. Saf epoksi reçinenin yanabilirliği Cloisite 30B eklenmesinden etkilenmemiştir.

Anahtar Kelimeler: Nanokompozit, Epoksi Reçine, Montmorillonit, Yerinde Polimerizasyon, Yanabilirlik

To The Turkish Martyrs Who Were Killed In The Terrorist Attacks

ACKNOWLEDGMENTS

I wish to express my sincere appreciation to Prof. Dr. Ülkü YILMAZER for his guidance, advice, encouragement and insight throughout this study.

This study was carried out at The Scientific and Technological Research Council of Turkey - Defense Industries Research and Development Institute (TÜBİTAK-SAGE) as a part of the nanocomposite development studies. I would like to thank TÜBİTAK-SAGE for the financial support.

I would like to thank Hüsnü KAŞIKÇI, Head of Polymeric Materials Division of TUBİTAK-SAGE for his support during the progress of this study.

I would like to thank Dr. Isıl IŞIK and Dr. Elif ÖZTÜRK for their support during writing of this thesis.

I am also grateful to my wife for her unlimited support, patience and love during this work.

TABLE OF CONTENTS

LIST OF TABLES

TABLES

LIST OF FIGURES

FIGURES

CHAPTER 1

INTRODUCTION

A composite material is a combination of two or more distinct materials usually a binder material (matrix) and reinforcement. In general, resultant properties of a composite material are better than those of constituent materials, and it has recognizable interphases. There are different types of classification for composite materials. They can be classified according to filler dimensions as macrocomposite, microcomposite and nanocomposite.

Epoxy based nanocomposites have attracted great interest from both scientific and industrial views. Epoxy resin by itself finds wide applications including: coatings, electrical, automative, marine, military and civil infrastructure. They have excellent chemical resistance, good mechanical properties and good adhesion to many substrates. The term, epoxy resin, is used for both prepolymer and cured resin. An epoxy is a short chain oligomer containing epoxy group, three membered ring. Epoxy resins are used in the body of composite materials such as fibre composites and honeycomb structures [1]. Recently, to improve the properties of the epoxy resin, nano particles have been incorporated in it [2]. Epoxy-clay nanocomposites are prepared by well distribution and intercalation or exfoliation of the clay minerals in an epoxy matrix. In order to call a material as a nanocomposite, clay platelets must be present in nano dimension (10^{-9} m) in the resultant composite. Clay is a layered silicate having 1-100 nm in thickness with 10-1000 aspect ratios [3]. Nanocomposites have unique advantages when compared with traditional composites; these include barrier properties, mechanical properties [4, 5, 6], gas impermeability and also increased thermal

stability [7, 8]. These are caused by the larger surface area of clay minerals per volume in matrix material. Many important chemical and physical interactions are governed by surfaces. Other important properties include flame retardancy [9], scratch/wear resistance, as well as optical and electrical properties. In contrast to conventional composites, these properties are obtained at low filler loadings (between 1 and 5 wt %) [5, 10]. So, nanocomposites can be processed by using conventional techniques suitable for neat polymers. However, it is not possible to have highly exfoliated structures at high clay loadings. At high filler contents, polymers behave as conventional composites. The optimum clay amount that is needed for nanocomposite formation must be determined by experiments. In the fabrication of the nanocomposites, various types of fillers can be used. These are clay minerals, nanotubes, nanofibers and spherical particles in nano dimensions. Despite the progress in nanocomposites, high performance fiber reinforced composite market has been affected little.

Initially, thermoplastics were used in the development of the nanocomposites. The first nanocomposite material was demonstrated by Toyota researchers [11]. Recently, thermosets have begun to be applied to nanocomposites. But, difficulties are observed in the development of the clay-polymer nanocomposites with thermosetting polymers. By the incorporation of the nanoclays into the epoxy matrix, one of the most common thermosets, different effects are observed according to type of epoxy resin.

The aim of this study was to prepare epoxy-clay nanocomposites by mixing organically modified smectite clay with an epoxy resin and to investigate effects of inorganic content on the morphology, mechanical, thermal and flammability properties of the resultant nanocomposite. The fabrication of the epoxy-clay nanocomposite was accomplished by the mixing of epoxy resin (Part A) with Cloisite 30B. Then, in-situ polymerization took place with the addition of the hardener (Part B). In the study, clay content was varied from 1 to 9

wt. % by weight. Epoxy resin was diglycidyl ether Bisphenol-A epoxy resin. Clay type was the montmorillonite modified by alkylammonium ions. The modified clay layers prevent agglomeration and are more compatible with the organic matrix [12]. Otherwise, agglomerated clays cause incomplete exfoliation and inhomogeneous dispersion of the nanoplatelets [13].

The effects of the clay minerals on the properties of final nanocomposite material were investigated by morphological, mechanical, thermal and flammability tests. Morphological tests were performed by X-ray diffraction (XRD) and scanning electron microscope (SEM) analysis. Wide-angle x-ray diffraction (WAXD) was used to determine the intercalation or degree of exfoliation in the nanocomposites. The peaks observed in the diffractogram indicate the d-spacings between the clay platelets. SEM analyses was performed to to determine the clay particles and microbubbles and their distribution in the matrix. Mechanical properties were determined by tensile, impact and flexural tests. Thermal properties of the nanocomposites were investigated by thermogravimetric analysis (TGA) and differential scanning calorimeter (DSC). TGA results were used to observe the changes in the decomposition temperature and amount of weight remaining after the analyses. DSC was used to evaluate the change in the Tg of neat epoxy resin by the addition of Cloisite 30B. Also, flammability of the neat epoxy resin and its nanocomposites were investigated.

CHAPTER 2

BACKGROUND

2.1 Composite Material

A composite material is a combination of two or more distinct materials: usually a binder material (matrix) and reinforcement. In a composite structure, the constituent materials do not dissolve in each other and recognizable interfaces are present between the phases. They just stick to each other. Hence, in a composite material, the constituent materials retain their identities. Structure of a typical composite is shown in Figure 2.1. Matrix material is low modulus material; on the other hand, reinforcing elements usually have strength and stiffness 10-1000 times higher than that. Resultant properties of composite material transcend that of constituent materials [14, 15, 16].

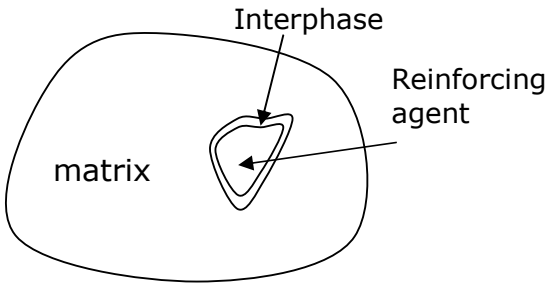

Figure 2.1 Schematic of composite structure

Composite materials have been used since early times. They were used to improve the properties of some conventional weapons. For example: Mongolians used wood and cow tendons glued together in stretched parts of arcs. Also, cannons which had wooden barrels bound with brass to increase the pressure resistance of a hollow cylinder [16].

There are three different types of composites which are macrocomposite, microcomposite and nanocomposite. Macrocomposites are conventional composites such as glass, carbon and Kevlar reinforced polymers. Macrocomposites are more superior to microcomposites. Polymeric resin with clay not intercalated forms microcomposites. The nanocomposites, new materials, are comprised of matrix and reinforcing agent having dimensions between 1 nm to 100 nm. Nanocomposites have rather different physical properties than conventional composites with lower filler content. Most effective type of composite at low filler loading is the nanocomposite [16].

Not all of the fillers have reinforcing effect. Sometimes particles are added to extend the materials, instead of reinforcing the material. These types of materials are generally called as filled systems. Filler particles are usually used to lower the cost of material rather than reinforcement, so filled systems are not considered as composites. Nevertheless, in some cases fillers can also reinforce the matrix material [14, 17].

The most important features of the composites are high stiffness, low density, corrosion resistance, long fatigue lives, tailorable properties (For example; thermal expansion), and ability to fabricate complicated parts. Composite materials can maintain stealth property to the military structures. This is a very important property for aircrafts and missiles. With these materials, aircrafts become transparent when exposed to radar [14].

The reinforcing agents in composites are stronger than the continuous matrix phase. In composite materials, reinforcement is generally provided by the addition of a significant volume fraction (10 % or more) discontinuous phase [14, 17].

Composite materials can be classified according to two aspects. Composites are firstly classified based on the matrix constituent. They are called by the part which is mostly present in the composite. The composite classes depending on matrix constituents are listed below:

- Organic-Matrix Composites (OMCs)
- Metal-Matrix Composites (MMCs)
- Ceramic-Matrix Composites (CMCs)

The other classification is done according to dimensions of filler. The composite with filler which is in micron or bigger dimension is called macrocomposite, and composite with filler in molecular dimension is called nanocomposite. Polymers with fillers in micron dimensions and polymer blends are called as microcomposite. In polymer blends, there is no chemical interaction between the polymer molecules, they are just physically mixed [14, 15]. In this study, epoxy-clay nanocomposite will be synthesized.

2.1.1 Metal Matrix Composites (MMCs)

Development of MMCs began in the 1950s and early 1960s. The advantages of metals are still observed in the composite forms. Also, metal fillers provide additional structural efficiency to the final material.

Although these types of composites were very expensive and had marginal reproducibility, important applications were established, including 243 structural components on the space shuttle orbiters [14].

MMCs can be classified according to form of reinforcing agents such as article-reinforced, whisker-reinforced, tow-based and monofilamant reinforced. Aluminum, magnesium, iron, titanium and copper can be used as matrix materials. MMCs find many applications in the automotive, thermal management, tribology, and aerospace industries. Especially, monofilament-reinforced titanium MMCs were developed for the aerospace applications where high-temperature resistance is needed. Moreover, new MMC insertions in the ground transportation, industrial, and thermal management/ electronic packaging industries are being used [14, 15].

2.1.2 Ceramic Matrix Composites (CMCs)

Ceramic-matrix composites are advanced engineering materials used in structural applications. They are formed by the addition of discontinuous particulate or continuous fiber reinforcement typically to matrix material including polycrystalline ceramic, glass, or glass-ceramic matrix. In this type of composite, the most important matrix materials are alumina (Al_2O_3), silicon nitride (Si_3N_4), mullite ($3Al_2O_3.2SiO_2$), and aluminosilicate matrices. Beside these, important reinforcements include SiC, zirconia (ZrO_2), and titanium carbide (TiC).

Ceramics are very attractive materials for wide variety of applications in aerospace and industrial sectors, because of their high-temperature stability, corrosion resistance, and toughness properties. But, they are very susceptible to flaws which can cause catastrophic failure. This disadvantage can be overcome by the addition of reinforcements in ceramic materials [14, 15, 18].

2.1.3 Organic-Matrix Composites (OMCs)

The organic-matrix composites are divided into two classes which are polymer-matrix composites (PMCs) and carbon-matrix composites usually referred as carbon-carbon composites [14].

2.1.3.1 Carbon-Matrix Composite

Carbon-matrix composites are typically formed from PMCs by including the extra steps of carbonizing and densifying the original polymer matrix. Hence, C/C composites are used in high temperature applications. Mechanical properties of carbon matrix composites do not degrade until 2200 °C. Conversely, the main drawback is high cost of material and fabrication. They find wide application areas in aerospace and military systems [14, 15].

2.1.3.2 Polymer-Matrix Composite (PMCs)

PMCs are the most widely used composite materials in the world. In this type of composites, polymer based resins are used as a matrix material in combination with reinforcing agents. The ratio of the matrix material to the reinforcement is usually in the range of 1:2 and 2:1. They are extensively used in industrial, military, aerospace and automobile applications. The main advantage of these composites is the easy fabrication of large complex shapes [14, 15].

Usually combination of a matrix and a reinforcing agent has synergistic effects on the final properties of the resultant composite material. In a fiber reinforced polymeric composite, while the fiber provides the high strength and modulus, the matrix constituent provides uniform load distribution and protects the surface of the composite from abrasion

and weathering effects, both of which can initiate fracture. A good adhesion between the polymer and the reinforcing agent must be maintained to allow uniform load transfer. A coupling agent to improve adhesion is also applied to some types of the reinforcing agents. Nonetheless, depending on design requirements, adhesion may be needed as minimal in some applications [14, 15].

In PMCs applications, both thermoplastic and thermoset polymers can be used as a matrix constituent. PMC with thermoplastic polymers soften upon heating. Consequently, service temperature for the thermoplastic PMC is limited, i.e., usually they are not suitable for high temperature applications. Conversely, thermoset PMC can not be reshaped after curing process. Because, thermoset PMCs have crosslinked molecular structure which is an insoluble and infusible three-dimensional network [15].

PMCs were developed during the World War II as a result of efforts to produce materials with higher specific strength and stiffness values than existing structural materials. Metal alloys, used in aerospace industry, may be subject to corrosion and fatigue damage. PMCs overcome these disadvantages. By the end of the war, glass-fiber reinforced plastics were used in many military applications such as rocket motor case, structural aircraft parts. In the 1960s, PMCs were begun to be used in commercial applications. By this way, cost of the products was lowered and consumers became more familiar with composite materials. During the Cold War, sufficient resources were allocated for the research and development of high technology composite materials. After successful application of PMCs in military aircraft, new applications in the commercial industry were also found [14, 19].

Recently, PMC materials are applied to structures of the next-generation U.S. tactical fighter aircraft. Beside this, most of the rocket

motor cases, body of ships, and military personal equipment are also made of PMC materials. The body of the B-2 bomber, shown in Figure 2.2, is comprised of different composite parts. By the design of outer surface geometry and use of special PMC materials, B-2 Bomber becomes invisible by Radar. There are also many aircrafts that consist of high percentage of composite materials, and it is still continued to research new ways to decrease the weight of the composite bodies [14, 15, 20].

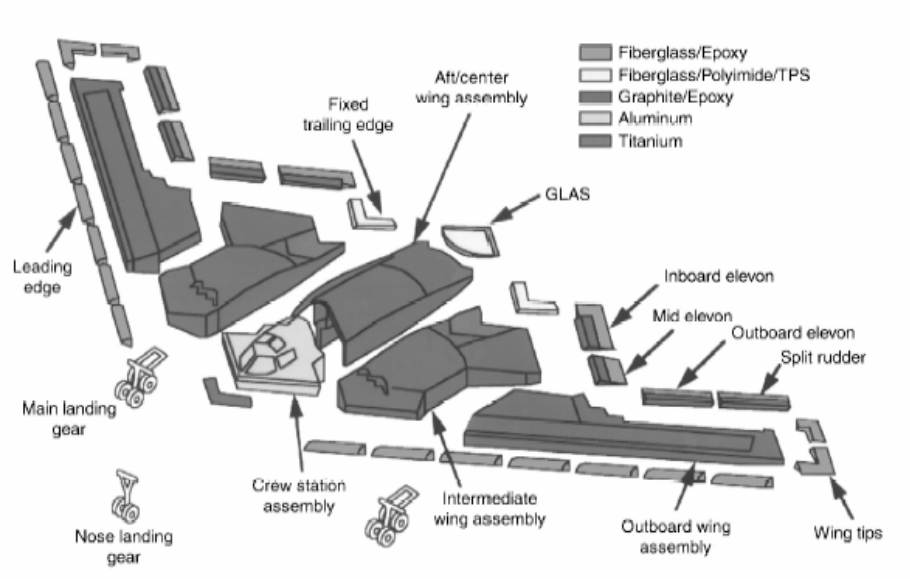

Figure 2.2 Composite applications in the U. S. Air Force B-2 advanced "stealth" bomber [14]

2.1.3.2.1 Polymeric Matrices

As mentioned before, the main role of the matrix resin is to eliminate stress concentrations by uniform load distribution to the reinforcing agents. This increases damage tolerance and provides long term durability. Moreover, matrix determines the hot / wet performance. In the design step of a polymeric matrix composite, susceptibility of matrix material to hot/wet environment must be taken into

consideration. The performance of a composite material in a hot environment strongly depends on matrix material [15, 20].

A variety of thermosetting and thermoplastic resins are used as matrix materials. The selection of the matrix resin includes; design requirements of final product, ability to wet the surface of reinforcing agents, considering composite processing [20].

Thermoset polymers are most widely used matrix materials in PMCs. They can not be reshaped once reacted and cured. Thermosetting resins are low molecular weight telechelic (carrying functionalized end groups) oligomers which need a catalyst, and/or hardening agent or elevated temperatures (>100 ^{o}C) to be cured. After the curing process, a rigid and a highly crosslinked network is formed. If maximum mechanical properties are needed, post curing process is applied to the resin. In most of the cases, volatile materials are released during the curing process [14, 20, 21].

The most common used thermosetting systems are unsaturated polyesters, vinyl esters, epoxies, phenolics, bismaleimides (BMI), polyimides (PI) and cyanate ester resins [14, 20].

2.2 Nanocomposites

Nanocomposites are new types of materials and find wide range of application areas. Nanocomposites have many advantages when compared with traditional types of composite materials. Although they are similar to normal composite materials, the filler sizes are in the range of nanometers. A nanometer scale is simply a range between the micro and molecular dimensions. At low filler loading range, generally improved properties are obtained. These performance improvements can be achieved at a lower cost than by other means.

2.2.1 Polymer-Clay Nanocomposites

The first commercial application of the polymer-clay nanocomposites has begun by the use of nylon6/clay nanocomposites on Toyota cars in 1991. By this work, it was seen that wide range of engineering properties of nylon 6 were improved with clay. Since this achievement, researchers have carried out to develop different polymer-clay nanocomposites. Today, almost all of the engineering polymers are used in the production of the polymer/clay nanocomposites. These polymers include polypropylene (PP), polyethylene, polystyrene (PS), polyvinylchloride (PVC), polycarbonate, polyamide, epoxy resins, polyimide (PI), phenolic resin, etc [1, 26].

Polymer-clay nanocomposites have been receiving great attention in many applications. They are similar to conventional composite materials in that both conventional composites and polymer clay nanocomposites include filler to obtain improved properties. On the other hand, fillers in the polymer/clay nanocomposites are in nano dimension in one direction and have better properties in lower filler loadings (1-5 %). Polymer-clay nanocomposites are accomplished only when silicate layers are broken down individually in polymer matrix as shown in Figure 2.3. In addition, when compared with pristine resins, polymer clay nanocomposites have better mechanical, thermal, flammability and barrier properties. These improvements are achieved by large surface area to volume ratio of well distributed and exfoliated clay minerals [1, 26].

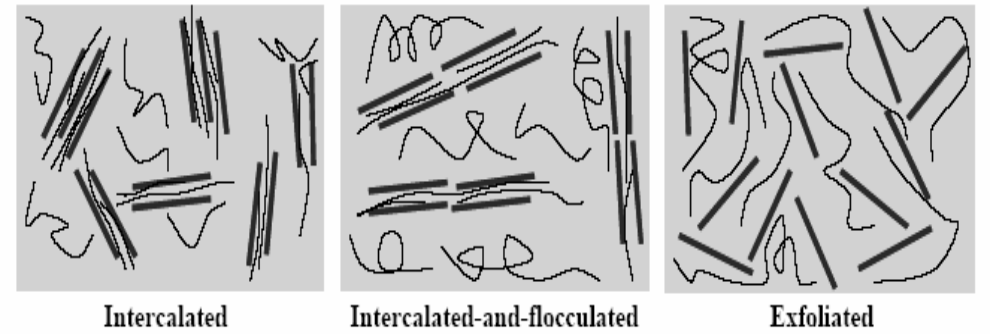

Figure 2.3 Schematic illustration of three different types of polymer-clay nanocomposites

The major aim in the production of the nanocomposite is to separate silicate layers in the matrix. By this way, nanoclays are formed in the matrix and these nanoparticles maintain excellent mechanical properties in matrix system [26].

Addition of clay minerals into the polymer system does not affect optical clarity of the resultant polymer clay nanocomposite so that the thickness of each silicate layer is smaller than the wavelength of the visible light. Conventional composites are opaque but well exfoliated polymer clay nanocomposites are optically clear [26].

While most other nanotechnologies are still in the concept, polymer-clay nanocomposites can be applied immediately for commercial applications. Today, these materials are used in many applications [26].

Polymer clay nanocomposites find wide applications in automotive and food industries. In automotive applications, they are used in timing belt covers, engine covers, step assistant, fuel lines and doors. Their barrier properties make them useful in food packaging applications. They are used in beverage applications. The use of polymer clay nanocomposite is still growing. Nanocomposites are planned to be used in many military applications [1, 26].

2.2.2 Clay Fillers

Clay is a phyllosilicate, natural or synthetic mineral. Polymer clay nanocomposites use smectite type clays including montmorillonite, hectorite, and synthetic mica as fillers. Smectite type clays have layered structures. Layers consist of tetrahedrally coordinated Si atoms and edge shared octahedral plane of either $AlOH_3$ or $MgOH_2$. Each layer of clays has approximately 1 nm thickness.

Although, mechanical properties of the layers are not known, it is estimated to be 50-400 times higher than that of polymeric matrix by modeling. Each layer is bonded to the other by weak van der Waals forces to form a clay particle. By using effective distribution techniques, very good improvements can be obtained in polymer properties [1, 26].

2.2.2.1 Montmorillonite

MMT clay shown in Figure 2.4 is a sandwich structure constructed of repeating triple-layer sheets composed of two tetrahedral silica sheets and one octahedral sheet of alumina in between. The thickness of the layers is 1 nm and the length is approximately 100 to several hundred nanometers [1, 26].

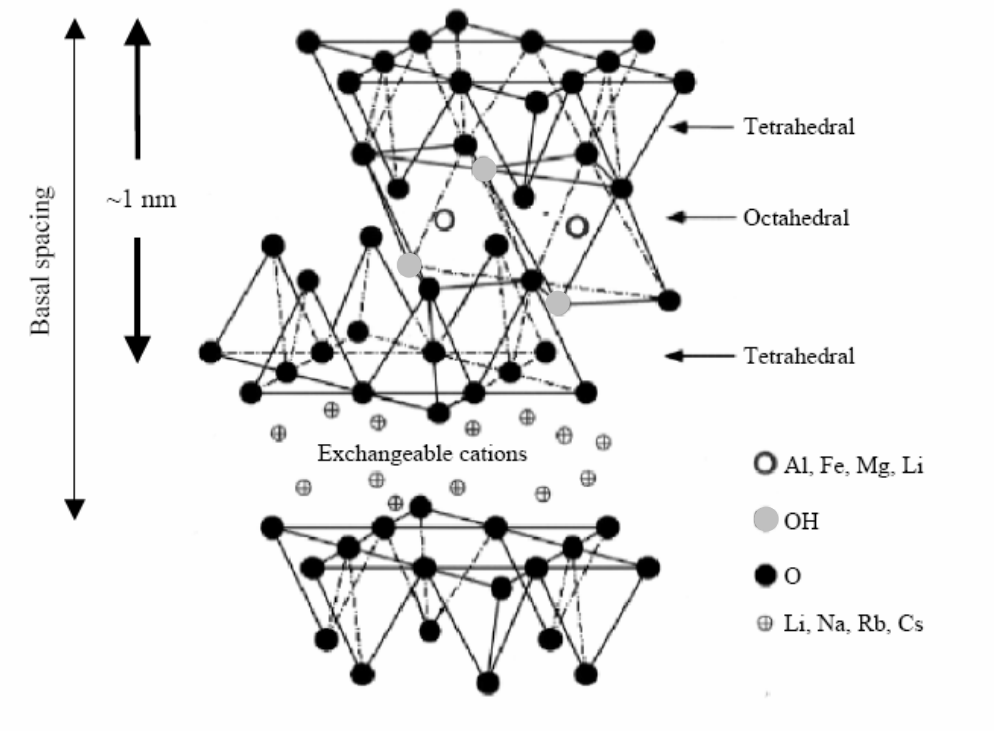

Figure 2.4 Structure of montmorillonite type clay

The gap between the layers is called as interlayer or gallery. Clay minerals are usually characterized by a surface charge and this is known as cation exchange capacity (CEC). It is generally shown as mequiv/100g of clay mineral. This charge varies from layer to layer, and average values must be considered for the crystal structure.

In the production of the polymer clay nanocomposites, there are two important characteristics related with the clay layers. These are the distribution of the clay layers individually and modification of the layer surfaces with ion exchange reactions.

Not all the polymer and clay mixtures result in nanocomposite structure. Pristine clay layers usually contain hydrated Na^+ or K^+ ions. Pristine clays are hydrophilic and they are compatible with only some

hydrophilic polymers. Hence, there are limited numbers of polymers that can form nanocomposites with these pristine clays. Clay minerals must be processed to form organophilic surfaces to be compatible with other polymers. Modification of the clay surfaces can be done by an ion-exchange reaction with cationic surfactants as shown in Figure 2.5. Different types of surfactants such as primary, secondary, tertiary and quaternary alkyl ammonium cations are available. These cations are used to improve the wetting characteristics with polymer matrix. Finally, interlayer becomes larger [26-28].

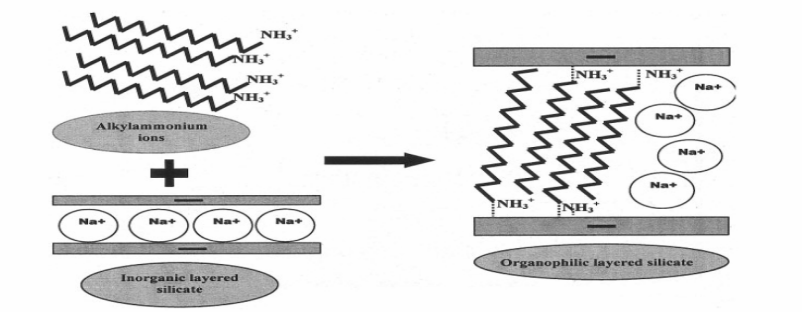

Figure 2.5 Intercalation of natural clay by substitution of alkyl ammonnium ions for organic Na^+ cations

2.2.3 Epoxy Resins

In the present study, epoxy resin is used as the matrix in the nanocomposite material. So, more detailed information will be given about epoxy resins.

The first production of epoxy resins was simultaneously made in Europe and in the United States in the late 1930s and early 1940s. However, the first synthesis of epoxy resin is often attributed to the Pierre Castan of Switzerland and S.O. Greenlee of the United States. They studied the reaction of Bisphenol-A with epichlorohydrin. The resultant resin is known as diglycidyl ether Bisphenol-A (DGEBA).

They firstly used the families of epoxy resins in casting and coating applications [14, 15, 24].

Since epoxy resins have unique properties, they are usually preferred in the structural and specialty composite applications. Epoxy systems usually include the base resin, curative and the modifiers. Although different types of base resins are present, today mainly DGEBA type resins are used. However, hardeners are available in variety of type, including amines, amides, merceptans, anhydrides, and Lewis acids and bases. In order to develop epoxy system formulations according to design requirements, these constituents of epoxy system must be understood well [22, 24].

Epoxies have many advantages over the other thermosets. They offer high strength, low shrinkage, excellent adhesion to various substrates, effective electrical insulation, chemical and solvent resistance, low cost, and low toxicity. They are easily cured without evolution of volatiles or by-products by a broad range of chemical species. Compatibility of epoxy resins with most substrates and their good wetting ability make them very suitable in many composites [14].

The starting materials of the epoxy are low molecular weight organic resins including epoxide groups, three membered rings. The most common epoxy resins are based on Bisphenol-A and epichlorohydrin shown in Figure 2.6.

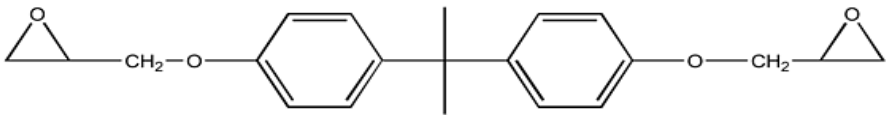

Figure 2.6 Chemical structure of diglycidyl ether of Bisphenol-A

Epoxy resins find wide application areas, i.e.; as adhesives, coatings, encapsulates, casting materials, potting compounds, and binders. They also find very important applications when combined with reinforcing agents to form structural composites. Epoxy technologies satisfy a variety of nonmetallic composite designs in commercial and military applications, including rocket motor tubes, flooring panels, ducting, vertical and horizontal stabilizers, wings, and even as fuselage. Also, they are used in many recreational applications such as, lightweight bicycle frames, golf clubs, snowboards, racing cars, and musical instruments. Depending on required physical and mechanical properties, epoxy resins can be formulated. For simplest applications, single epoxy resin with a curative is sufficient. On the other hand, when more requirements are needed, multiple epoxy resins, modifiers for toughness or flexibility or flame/smoke suppression, inert fillers for flow control or changing color, and different curatives have to be used [14].

In the selection of thermosetting resins, the following properties are taken into considerations:

- Tensile strength
- Tensile modulus
- Tensile strain
- Compressive strength
- Compressive modulus
- Notch sensitivity
- Impact resistance
- Heat deflection temperature (HDT)
- Glass transition temperature (T_g)
- Flammability
- Durability in service
- Material availability
- Ease of processing
- Price

Basic poxy resins are made mostly by the condensation of the epichlorohydrin and Bisphenol A. In the production of the epoxy resins, excess amount of epichlorohydrin is used to leave epoxy on each end

of the low Mw (900-3000) polymer. These two raw materials are reacted in a base (NaOH) to give linear epoxy resins. As a result of the condensation reaction, HCl is given out. The reaction mechanism is shown in Figure 2.7.

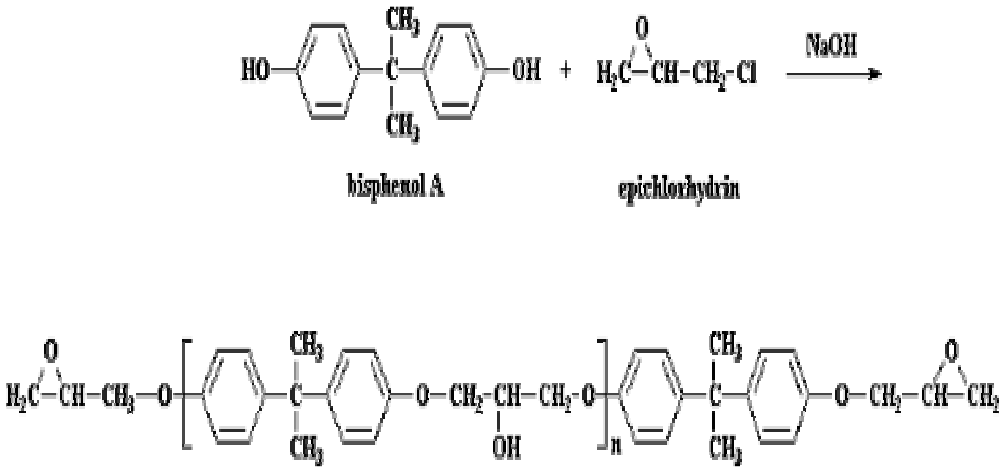

Figure 2.7 Reaction of Bisphenol-A and epichlorohidrin to form DGEBA

Here, *n* represents the number of repeating units in the prepolymer. Epoxy resins can be found in different forms (liquid, solid) according to *n*. In the prepolymer, n can be between 0 and 25. When the *n* is between the 0 and 1, the product is liquid. On the other hand, if *"n"* is 25, the epoxy resin becomes a hard plastic at room temperature. These types of epoxies have to be heated up and melted before they can be mixed with the other part of the epoxy mix.

In order to change the functionality and viscosity of the resin, different hydroxyl groups which can be used instead of Bisphenol A, including resorcinol, hydroquinone, glycols, glycerol, and butanol.

Base epoxy resin: epoxy resin can be described as low molecular weight organic liquid containing epoxide groups. An epoxide group, shown in Figure 2.8, is a three-membered ring consisting of one oxygen atom and two carbon atoms.

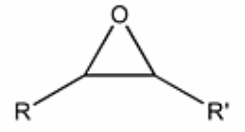

Figure 2.8 Basic chemical structure of epoxy group

There are various types of epoxy resins which are formed by the attachment of epoxy group to different base molecules. Because of the diversity of molecular structures and chemical processing, epoxies are widely used in commercial applications.

One of the most important benefits of epoxy resins is that they can be tailored according to design requirements. Epoxy systems can be tailored by selecting appropriate curing agent and modifier system.

There are two synthesis methods for production of epoxy resins in which the double bond is converted into an oxirane ring. These processes are;

- Dehydrohalogenation of a halohydrin intermediate
- Direct peracid epoxidation.

Although both synthesis methods are used to produce commercial epoxy resins, the former route is more common and allows producing a wide variety of materials. Except for cycloaliphatic resins,

epichlorohydrin is the most important raw material used as a precursor in the production of nearly all of the commercial epoxy resins [14].

Glass transition temperature (T_g) is the one of the most important design criteria in polymeric composite applications. T_g is the primary indicator of service and use temperature of epoxy resins. Below the T_g, only vibrational motion is present, whereas above the T_g, individiual molecular segments begin to move. Modulus of epoxy material below the T_g is higher than above the T_g. Moisture and solvents have negative effects on the T_g of epoxy resins. So, epoxies, intended to be used in such environments, must be designed accordingly.

T_g of a cured epoxy resin also depends on molecular structure. Molecular structure develops during cure and it is a function of crosslinking density, stiffness of polymer backbone, and intermolecular interactions. Consequently, T_g is strongly related to cure temperature. Epoxy systems cured at higher temperatures will have higher T_g value. On the other hand, epoxy systems have an ultimate T_g which can not be achieved by increasing cure temperature. It must be emphasized that molecular structure and other characteristics of cured epoxy resins are equally dependent on the base resin, the curing agent, and modifiers added to the system [14].

One of the important points in determining the suitable resin combination is the epoxy equivalent weight (EEW). Equation for EEW is given below, where W_R is the weight of the epoxy resin, and N_E is the number of epoxide groups. For a DGEBA type resin in which n=0, the molecular weight is 340. Because there are two epoxy groups per molecule, the EEW is calculated as 170.

$$EEW = \frac{(W_R)}{(N_E)} \tag{2.1}$$

EEW is used to determine the ratio of epoxy and curing agents in order to optimize the cured properties.

There are three main classes of epoxies, listed below:

- Phenolic glycidyl ethers
- Aromatic gycidyl amines
- Cycloaliphatics

Epoxy resin curatives: curatives or hardeners are used to build crosslinked structure by reacting with epoxy resins. Catalysts and accelerators are not correct terms for curatives and hardeners. Amines, amine derivatives and anhydrides are most common curing agents. [14]

Resin and curing agent combinations are determined depending on the application and end use requirements. By using different epoxy and curing agent combinations, following characteristics can be controlled [14]:

- System stability
- Cure kinetics
- Physical form
- Tg
- Mechanical performance
- Chemical resistance

Curing times of epoxy resins can range from seconds to days. In some heat activated systems, curing times can range from months to years at room temperature. Resins can be cured from 5 ^{o}C to 260 ^{o}C. Curatives are added to the epoxy resins in units of phr (parts curative per 100 parts of bis-A epoxy). Curing agent ratio can also be calculated as EEW. For example, diethylene triamine (DETA) has a

molecular weight of 103 and five active hydrogens. Then, the hydrogen equivalent is 20.6.

Epoxy resins have different curing periods which are;

- Room-temperature cure
- Room or elevated-temperature cure
- Elevated-temperature cure

2.2.3.1 Room Temperature Curing Agents

These types of curing agents are aliphatic amines, polyamides, and amidoamines [14].

Aliphatic amines are *c*ommonly used primary amines listed below;

- Diethylene triamine (DETA)
- Triethylene tetramine (TETA)
- Tetraethlylenepentamine (TEPA)
- N-aminoethyl-piperazine (N-AEP)

Even though these amines will cure at room temperature, to enhance some properties, an elevated-temperature cure or postcure should be applied [14]. Primary amines are highly exothermic curatives with less reactivity, and less toxicity than the pure amines.

Polyamides: they are classified as primary, secondary, or tertiary. They are condensation products of polyamines and dimer acids or fatty acids. The structure of a polyamide is given in Figure 2.9. Despite the fact that polyamides have excellent adhesion, low toxicity, and good toughness, they become dark color upon curing. Polyamides are often used for coatings, adhesives, and sealants [14].

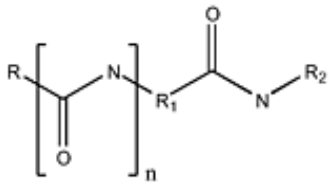

Figure 2.9 Chemical structure of a polyamide

Amidoamines: they consist of both amide and amine groups. They are formed by the reaction of monobasic carboxylic acids (usually the acids derived from C16–C19 fats and oils) and aliphatic polyamines. Amidoamines contain the imidazoline group which is a five-membered ring structure. This group gives more rigidity to the resulting polymer and higher T_g [14].

2.2.3.2 Room- or Elevated-Temperature Curing Agents

BF_3 and imidazoles: they can be cured safely at room temperature as well as at elevated temperatures. Pot life can range from hours to days. They are often used as accelerators with other curatives. The cured product has similar chemical resistance to that enhanced with aromatic amines. Also, T_gs can exceed 200 °C. Imidazoles are also used as accelerators in anhydride cures. Imidazoles are used usually in electronic, structural adhesive, automotive, and aerospace composite applications [14].

2.2.3.3 Elevated Temperature Curatives

These types of curing agents include aromatic amines and anhydrides. Aromatic amine curatives are in the form of fine powder, and used by blending and melting into the epoxy resin. The aromatic resins are

more expensive than aliphatic ones. The aromatic amines are generally used in high temperature applications. The reaction with this type of curative is slower because of lower nucleophilicity and steric effects [14].

4,4′-diaminodiphenyl methane (DADM, MDA, or DDM): it is the first curing agent used in industry. This curing agent is suspected as carcinogenic. So, less toxic ones such as methylene-bis(dimethylaniline) and methylene-bis(diisopropylaniline) (MPDA) are introduced to the industry and they are commercially available now. Diaminodiphenylsulfone (DDS), formed by replacement of methylene group with a sulfone, find wide application in aerospace industry [14].

Anhydrides: they are another major class of epoxy curatives which was used in this study. They are available in different physical forms. A complex reaction takes place between anhydride and epoxy resins. Anhydrides are generally used in epoxy formulations between 0.4 to 1.1 equivalents. Rate of the epoxy resins with anhydride is slower than with aliphatic amines and amides, so it is more convenient for the filament winding process. Long cure times and postcure profiles are necessary to obtain desired properties. Primary cure occurs in the range from 80 to 150^{o} C, and postcuring occurs at temperatures higher than primary curing temperature and up to 200^{o} C. Anhydride type curing agent is preferred when lower viscosity, non critical mixing ratio and long pot life are required. Polyanhydrides can offer excellent toughness and thermal shock resistance. But, moisture sensitivity, brittleness and limited formulation are the main disadvantages of using an anhydride curative. Anhydride type curing agents are mainly used in casting, potting, encapsulation, and filament winding applications [14].

2.2.3.4 Miscellaneous Curing Agents

Dicyandiamide (known as dicy): it is generally used as epoxy curative in composite applications. Selection of the appropriate grade is very important, because it affects the cost and properties of the cured resin. This curing agent is insoluble in epoxy resins at room temperature. The reaction does not take place until the temperature of the system becomes in the range of 80 – 90^{o} C. Hence, it can be used when the system to be bonded is suitable to be exposed the high temperatures [14].

Polysulfides, thiols and merceptants: these curatives are suitable to be used in adhesive applications since rapid cure is required. Common applications are industrial road marker adhesives and commercial patch kits [14].

2.2.3.5 Alternate Cure Methods

Radiation curing is an alternative method for curing. This method maintains lower cost and lower cycle times. There are different radiation sources; ultraviolet (UV), infrared (IR), or electron beam (EB). Rapid curing times, energy efficiency, dimensional stability, less pollution to the environment and no cure without radiation are advantages of the radiation curing. On the contrary, the disadvantages of the methods are large capital expense, difficulty in penetrating thick parts, and sensitivity of reaction to the impurities [14].

2.2.3.6 Accelerators For Epoxy Resins

They are used to catalyze the epoxy formation and increase the speed of the curing reaction. Accelerators, tertiary amines or imidazoles, are generally used in the range of 0.5% to 3.0%. Dimethylamino-methylphenol, benzyl-dimethylamine, phenylimidazole, and ethyl-methylimidazole are widely used accelerators [14].

2.2.4 Fillers and Reinforcing Agents

Reinforcing agents can be classified as particulate, fiber and woven types as given in Figure 2.10 [14, 17]. Fiber-reinforced composites can be further divided into those containing discontinuous or continuous fibers. Particulate reinforcements are present in the form of spheres, rods, flakes, and any other shapes in which lengths are approximately the same in all directions. However, some particulate fillers, used for the purpose of cost reduction rather than reinforcement, are not considered as reinforcing agents. Fiber reinforcements are considered as fillers having high aspect ratio, i.e.; length / breath. If the length of the fibers is not long enough, the properties of composite part will depend on the fiber length [17].

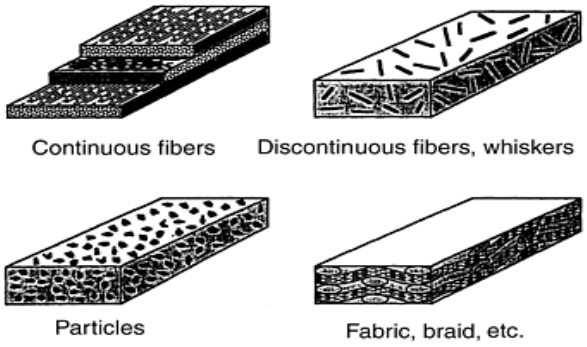

Figure 2.10 Common forms of fiber reinforcement.

Reinforcing agents can be selected according to design requirements. [14, 25]. The most common reinforcing agents are those in the fiber and their woven form such as fabric, braid. Woven form reinforcements are also made up from fiber type reinforcements. Thus, major emphasis will be given to the fiber reinforcements. The most common fiber reinforcement materials used in PMCs are glass, carbon and aramid. In some specific applications, boron, silicon carbide and other ceramic fibers are also used [14].

2.2.5 Fabrication Techniques

Different methods are developed to fabricate polymer clay nanocomposites. Appropriate fabrication method is selected according to the polymeric matrix. On the other hand, compatibility between the polymer and clay is also very important. If polymer and clay are not compatible, it is very difficult to obtain a nanocomposite structure. In such a case, pretreatment is essential to modify the surface of the silicate layers. Clays are hydrophilic in nature, thus they can be processed with water soluble polymers without pretreatment. But, most of the polymers are hydrophobic and they are not compatible with hydrophilic clays. So, clay modification is necessary before adding clay into polymer matrix. Clay is modified by using different chemicals to make them organophilic. There are various polymer-clay nanocomposite manufacturing techniques such as in-situ polymerization, solution induced intercalation, and melt processing.

In situ polymerization method: In this method, at first, clay layers are separated by the intercalation of polymer precursors into the galleries as shown in Figure 2.11. Then, by adding reacting monomer, polymerization begins and clay layers expand more. Polymerization can be initiated by different means, such as heat, radiation, solvent

and catalyst. This method is used by raw polymer manufacturers and it is also suitable for thermosetting polymers.

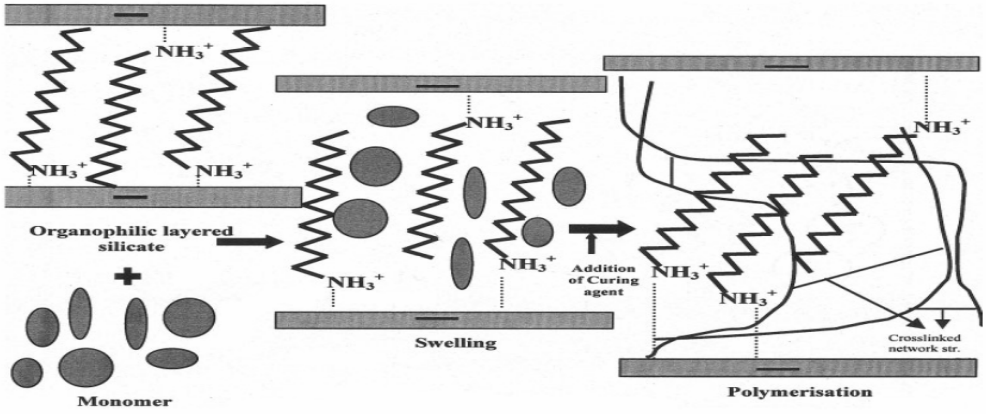

Figure 2.11 In-situ polymerization of epoxy resin with organoclay

The solution-induced intercalation method: In this method, silicate layers are separated by the migration of solvent between them. To achieve this, polymer precursor must be soluble in the solvent system. Clay layers can be swollen in various solvent systems such as water, chloroform or toluene. "Upon the addition of polymer into the solution, the polymer chains intercalate and displace the solvent within the interlayer are displaced" [26]. Then, solvents are removed and finally nanocomposite is obtained.

Melt Processing Method: In this method, intercalation occurs during the melting of matrix polymer. This method is not as efficient as the other methods for the nanocomposite production. Nanocomposites can be produced by using traditional methods such as extrusion and injection molding [28].

2.2.6 Characterization of Polymer-Clay Nanocomposites

2.2.6.1 Scanning Electron Microscopy (SEM)

The scanning electron microscope is mainly used to produce high-resolution and the improved depth-of-field images of sample surfaces. Another application is the chemical analysis of materials in micron-sized areas. The SEM provides better capabilities when compared with the optical microscope. Direct inspection and the three-dimesional images make the SEM a unique tool for failure studies and fracture research [14].

In the SEM analysis, sample preparation is the most important step. The test samples must be conductive. So, if the samples are not conductive, these must be covered with a thin layer of conductive material. The SEM uses electrons rather than light to form an image. A beam of electrons is formed by an electron gun at the top of the microscope. When the electron beam hits on the sample, backscattered and secondary electrons are emitted from the sample. A detector collects the backscattered and secondary electrons. These collected electrons are converted to the signal which is sent to a monitor similar to the television. And finally, the image of the sample is observed on the monitor [14].

Basic components of the scanning electron microscope is shown in Figure 2.12. the scanning electron microscope has different parts:

- Electron column
- Specimen chamber
- Vacuum pumping system
- Electronic control
- Imaging system

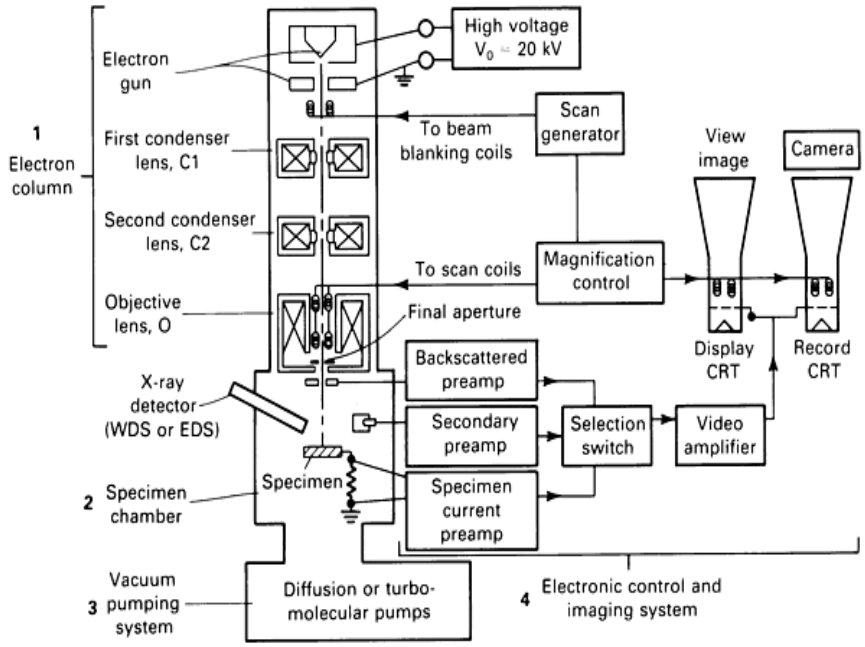

Figure 2.12 Basic components of the scanning electron microscope [14]

2.2.6.2 X-Ray Diffraction (XRD)

X-Ray diffraction (XRD) is the most widely used characterization technique by which various properties of metals related to the arrangements and distance of their atoms can be investigated. XRD techniques are also used for other crystalline materials, such as ceramics, geologic materials, and most inorganic chemical compounds [14].

The atoms are arranged in a crystal system as shown in Figure 2.13. Atom A is in the plane I and atom B is in the adjacent plane II. When an x-ray beam, an electromagnetic radiation, is directed onto a crystalline material, a number of beams come out from the sample (Figure 2.13). The angles and their relative intensities provide information about the lattice geometry, orientations, and arrangements of atoms in the crystal that make up the sample. If the

crystal system is a clay material, then each plane shows a layer and distance between them exhibits d-spacing or basal spacing [14].

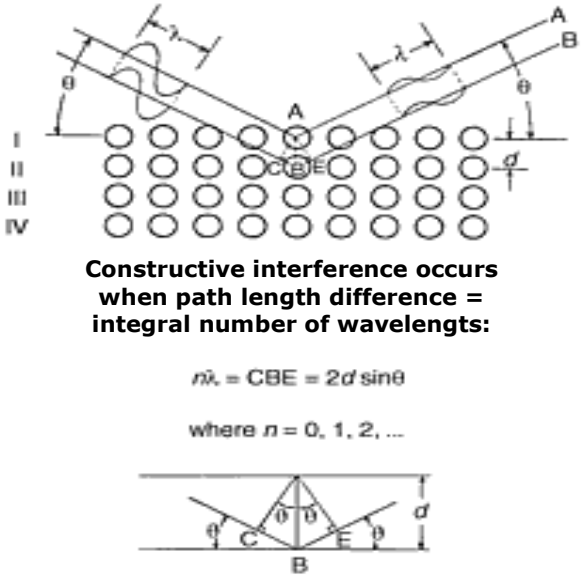

Figure 2.13 Bragg's law [14]

The constructive interference and stronger diffracted beams are resulted, only when the Bragg's law is satisfied [35].

$$n\lambda = 2d \sin\theta \qquad (2.3)$$

Where,

n = any integer

λ= wavelength of incident and diffracted beams

d = spacing of adjacent diffracting planes in the crystalline sample

θ= angle between incident beam and diffracting plane, as well as between the diffracting plane and the diffracted beam [35].

2.2.6.3 Mechanical Tests

Mechanical properties are one of the most important criteria in selection of materials in structural parts and in the design step to predict the performance of the material. The mechanical properties can be evaluated by using some standardized test methods to quantify their behavior. The results of the tests are used to make a decision for suitability of a material for a specific application. In this study, tensile, flexural and impact strength tests are performed to compare the structural properties of the neat epoxy resin and nanocomposite materials.

Tensile test is a short term measuring of how a material behaves under a tensile load. By the tensile test; tensile strength, strain at break and elastic modulus are determined. Flexural strength is another measure of material's strength obtained under bending load. Impact strength is a measure of energy absorbed by the material in a short time. These properties depend on the mechanical and environmental conditions [29].

Standard deviation of all mechanical properties was calculated by the following equation (2.2).

$$S = \sqrt{\frac{\Sigma X^2 - N\overline{X^2}}{N-1}} \qquad (2.2)$$

Where,

S = Standard deviation

X= Value of single observation

N = Number of observations

$\overline{X}$ = Arithmetic mean of the set of observations

Error bars were calculated according to standard deviations and added to the graphs.

2.2.6.3.1 Tensile Properties

Tensile property determination is one of the most widely used testing methods for mechanical properties of engineering plastics. This test is performed by applying an axial loading at a constant speed with an instrument. The test methods and specimens are defined according to ASTM D 638 standard [30]. A typical test sample is shown in Figure 2.14.

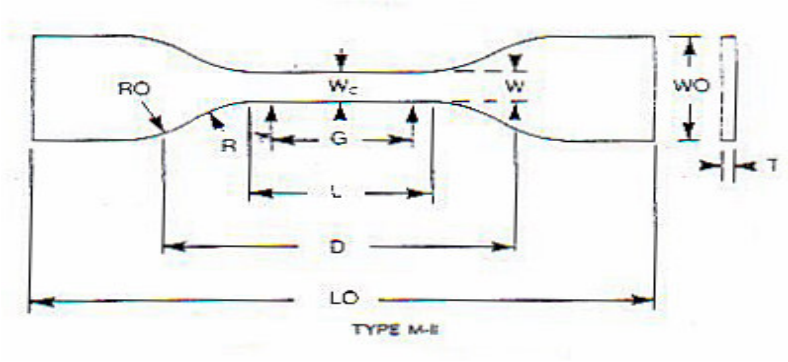

G :Gage length	R :Radius of fillet
L :Length of narrow section	RO :Outer radius
LO :Length overall	T :Thickness
W :Width of narrow section	D :Distance between the grips
WO:Width overall	

Figure 2.14 Tensile test specimen

As a result of tensile test, a stress-strain curve is obtained. A typical stress-strain curve is shown in Figure 2.15. Tensile strength is the maximum value obtained during the test, usually known as ultimate strength. Tensile strength is the maximum load divided by cross-sectional area with units such as N/m^2, or MPa.

Stress-strain behavior is highly affected by crosshead speed, ambient temperature, type of plastic, its molecular state and production methods. Below the T_g, polymer will be hard and brittle. So as the temperature increases, the tensile strength of a polymeric material decreases on the other hand brittleness decreases [14].

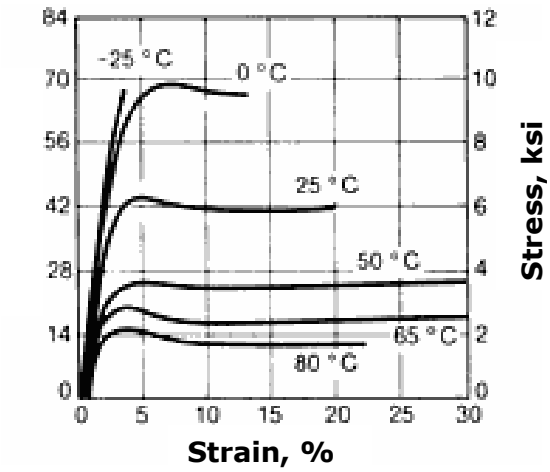

Figure 2.15 Typical stress – strain behaviour of a material at different temperatures [14]

2.2.6.3.2 Flexural Properties

The flexural strength of a material is the strength value of resistance under bending deformation. For materials that deform significantly but do not break, the load at yield, typically measured at 5% deformation/strain of the outer surface, is reported as the flexural

strength or flexural yield strength. The flexural strength is also one of the most important mechanical properties for polymers and composites. There are two methods for the determination of flexural strength: three-point loading and four-point loading. In a three-point flexural testing apparatus shown in Figure 2.16, load is applied by one supported beam to the center of the specimen. In this study, flexural strength test is performed according to ASTM D 790-03 with three point test apparatus [31].

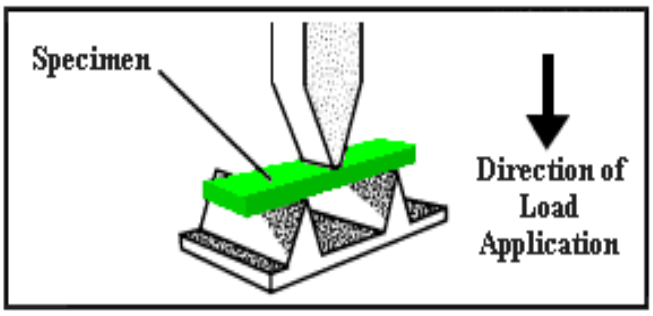

Figure 2.16 Flexural testing apparatus [32]

2.2.6.3.3 Impact Strength

Impact strength is the ability of material to withstand impact loading and it gives an idea about the brittleness of material. This property is determined by impact strength testing, measuring energy absorbed by material over a short period of time [29].

The impact strength of a material can be determined by using either Izod or Charpy impact test methods. Izod test is performed by impacting pendulum to a specimen on the notched side. On the other hand, Charpy impact is performed by impacting pendulum on the non-notched side. A typical test apparatus is shown in Figure 2.17. Impact test can be performed by the Gardner impact tester, which uses non-

notched samples. Gardner impact values are considered to be more definitive for the impact strength, while the Izod test is better to indicate notch sensitivity. The energy consumed to break test samples is in Joules. Generally, brittle materials have lower impact strength. Also, sensitivity to impact loading partly depends on environmental conditions. Hence, conditions have to be well defined when performing impact test [33].

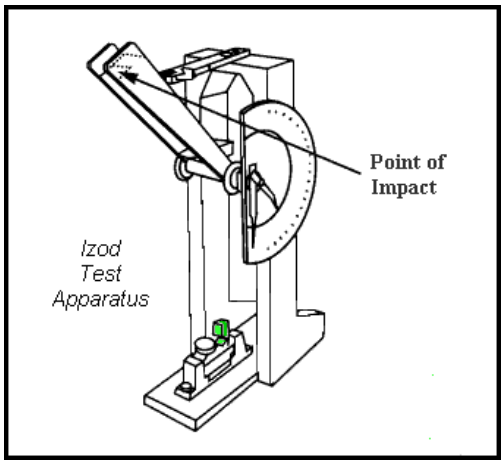

Figure 2.17 Typical impact testing apparatus

2.2.6.4 Thermal Analyses

Thermal analyses are used to characterize materials by measuring a physical or mechanical property as a function of temperature or time at a constant temperature or as a function of temperature. Gel points, T_g, expansion/contraction properties, reaction rates and cure kinetics, and polymer stability can be evaluated by thermal analyses. The most frequently used thermal analysis techniques are differential scanning calorimetry (DSC), thermogravimetric analysis (TGA), thermomechanical analysis (TMA), and rheological analysis. The TGA

analysis method is normally used to obtain the onset temperature of initial polymer, weight loss, as well as the extent of oxidative effects (in an air environment) or char formation (in an inert environment) [14].

2.2.6.4.1 Differential Scanning Calorimetry (DSC)

DSC analysis is used to characterize glass transition temperature (T_g), melting temperature (T_m), crystallization energy, resin curing, loss of solvents, and other processes involving an energy change. In general thermal characterization, DSC analysis technique may show an initial endotherm, assigned to the T_g, and either a second endotherm, indicating the T_m, or a pronounced exotherm that indicates a decomposition temperature. A schematic of a DSC thermogram is shown in Figure 2.18 [14].

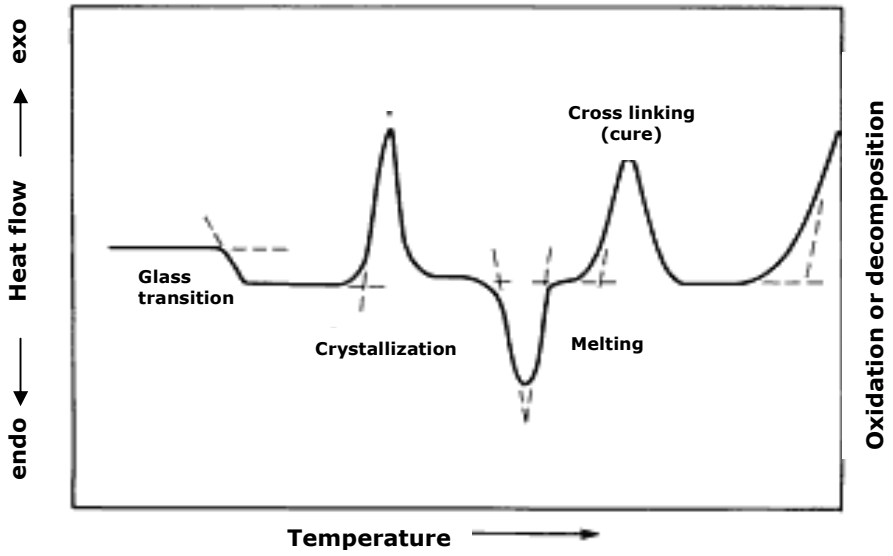

Figure 2.18 Schematic of differential scanning calorimetry thermogram

Differential scanning calorimeter measures the energy absorbed (endotherm) or produced (exotherm) as a function of time or temperature. In the DSC method, the sample and reference are placed in thin metal (aluminum) pans, with the thermocouple sensors below the pans. There are two methods that can be used in DSC measurements, these are: by measuring the electrical energy provided to heaters below the pans necessary to maintain the two pans at the same temperature (power compensation), or by measuring the heat flow (differential temperature) as a function of sample temperature (heat flux).

T_g is not an intrinsic thermodynamic property; hence, it is affected partly by the test method. The most commonly encountered techniques to evaluate T_g include dilatometry, differential scanning calorimetry (DSC), and physical yielding. DSC is an easier and more widely applied method for determining the T_g. In DSC, the heat capacity of the polymer sample is measured relative to that of a reference material. The actual location of the glass transition curve depends on the heating rate of the DSC analysis, because relaxation rate effects become significant at about the T_g. For this reason, heating rate is generally specified with DSC results [21, 34, 35].

Differential scanning calorimeter has been used for quality control and degree of cure studies of different commercial products. In this study, the effects of fillers on the Tg were investigated.

2.2.6.4.2 Thermogravimetric Analysis (TGA)

Thermogravimetric analysis is used to measure weight loss of a material as a function of temperature and time. In a TGA analysis, a polymer sample is heated from room temperature to above its decomposition or pyrolysis temperature. Test is performed under

nitrogen atmosphere. The oxidative stability of polymers in air or oxygen can also be investigated by TGA. Thermal stability determination of a material is one of the most important applications of TGA [22].

Moisture, volatile, and filler contents are also determined by thermogravimetric analysis. So, effects of additives are investigated and separation of some components (for example, rubber from carbon black) can be obtained. If TGA is coupled with spectroscopic techniques, polymer degradation can be obtained in more detail.

A typical TGA curve of a thermoset composite is shown in Figure 2.19. In addition to the normal decomposition profile, there is another benefit of obtaining the filler that remains as the residue. On the other hand, to investigate residue amount, fillers should not get oxidized or form other compounds those cause a weight gain [14].

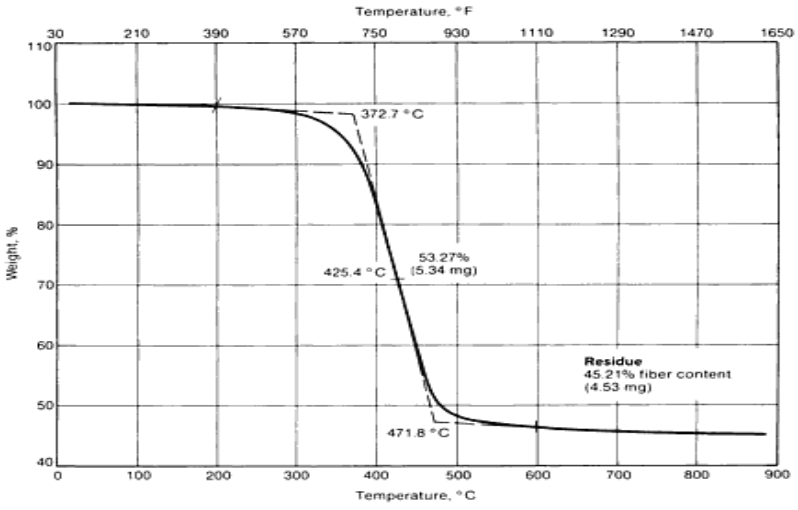

Figure 2.19 Typical thermogravimetric analysis curve for fiberglass-vinyl ester prepreg [14]

Because decomposition mechanisms are often diffusion controlled, sample geometry and fillers can affect the observed test results.

Therefore, the data obtained on small test specimens may not be extrapolated to larger structures. This type of information should be used judiciously as a guide for further studies until TGA or other thermal techniques are developed that give better correlation [14].

2.2.6.5 Flammability Test

Flammability test is performed to determine the comparative burning characteristics of polymeric materials. There are different test standards to determine the flammability property of polymeric materials. Cone calorimeter can be used to compare the combustion rate of nanocomposites with neat polymeric materials, while the other tests such as UL-94 is a qualitative pass/fail test. In the present study, ASTM D3801-06 standard is used and this is equivalent to the vertical burning test of ANSI/UL 94 standard (Test for Flammability of Plastic Materials for Parts in Devices and Appliances).

2.3 Previous Studies on Epoxy-Clay Nanocomposites

Park et al. showed that to achieve better interaction between clay surface and polymer matrix, surface treatment of the clay is necessary. In the study, surface modification of clay by dodecylammonium chloride led to increase of about 8 Å in the distance between the silicate layers. As a result, improved interfacial adhesion was achieved between basic epoxy resin and acidic clay interlayers. Thermal stability of nanocomposites was increased with the addition of the modified clay [7].

Chen and Curliss synthesized an organoclay and used it to make epoxy based nanocomposites. The degree of exfoliation and dispersion of the clays were confirmed by SAXS and TEM. Large d-spacings were

accomplished with the synthesized organoclay. But, Tg of the epoxy stayed almost at the same value [37].

Guo et al. investigated the effect of organically modified clay minerals on the thermal stability of the nanocomposite material. Thermal stability of the resultant nanocomposite was found to depend on the dispersion of the organoclays in the epoxy matrix, because well dispersed clay minerals increase the barrier properties of the nanocomposites to heat and oxygen. Hence, it was understood that thermal stability of the epoxy matrix increases by degree of exfoliation of the clay layers [8].

Chen et al. synthesized epoxy layered-silicate nanocomposites. The nanocomposites were developed to be used as coatings on aluminum surfaces in aerospace industry. The nanocomposites were characterized by the morphology analysis techniques. Also, solvent absorption and corrosion properties were investigated. The solvent absorption value was significantly decreased by the addition of the clay. On the other hand, the anticorrosion property of the nanocomposite was slightly improved. Beside these, it was observed that an increase in the processing temperature leads to higher d-spacing in the galleries [2].

Most epoxy resins are intrinsically brittle. So, some of the properties are affected negatively. Researchers investigated ways of increasing toughening properties of the epoxy resins. Ratna and Becker investigated the nanocomposites based on epoxy and toughened epoxy. Toughened epoxy is the blend of functionalized hyperbranched polymer (HBP) and epoxy resin. In that study, strengthening and toughening of the epoxy resin were accomplished by the addition of the HBP and clay [4].

Isık *et al*. studied the effect of the impact modifier (polyether polyol) on the properties of the epoxy/clay nanocomposite. In that study, it

was found that clay addition increased the T_g of epoxy based nanocomposite system. In addition to this, addition of the impact modifier without clay increased the impact strength. On the other hand, with the addition of both clay and impact modifier, maximum tensile strength and impact strength was achieved at 1 wt. % clay and 1 wt.% impact modifier loading [5].

Baran et al. synthesized two types of nanocomposites with sodium montmorillonite as well as organically modified montmorillonite. The effects of organically modified and unmodified clay on the mechanical properties of the polyester resin were investigated. In that study, Tg of the unsaturated polyester resin increased by the addition of the modified clay. This was attributed to the improved adhesion between the polymer and layered silicate surfaces. Also, addition of the organoclay had positive effects on the properties of the nanocomposites. Addition of 3 wt% organoclay increased the flexural modulus of unsaturated polyester by 35 %. Tensile strength of pristine polyester was also improved by addition of 5% organoclay loading. Finally, the effect of ultrasonic bath was also investigated. It was proved that by using ultrasonic mixing, the mechanical properties of nanocomposites were improved [9].

Nigam et al. prepared a nanocomposite with an epoxy resin and the modified clay in the study. Nanocomposites were obtained with 0, 1.5, 3, 4.5 and 6 % clay loadings based on epoxy matrix. At 6% clay loading, mechanical properties attained maximum value. Beyond this point, mechanical properties decreased. Thermal stability of nanocomposite with natural clay was higher than that with the modified clay. This was apparently due to lower thermal stability of organic clay [38, 39].

Salahuddin modified natural clay by intercalating ammonium cations of polyoxyalkyleneamines (jeffamine) through an ion exchange process. Then, the effects of different organoclay on the epoxy resin were

compared. Finally, it was concluded that the nature and molecular weight of jeffamine as well as percentage of modified clay affect the synthesis of epoxy/clay nanocomposites. The incorporation of the organoclay increased the hardness. Beside this, impact strength value of the nanocomposite with 7 % organoclay addition was found to be three times higher than that of pure epoxy [40].

Seo et al. investigated the curing behavior and structure of an nanocomposite system containing DGEBA epoxy with an aromatic amine curing agent and different amounts of organoclay. It was shown that clay loading increased curing rate of epoxy based nanocomposite. Also, the glass transition temperature of the epoxy was increased slightly by the incorporation of the clay [41].

Yasmin et al. showed that a three roll mill can be used to increase the degree of exfoliation the clay in an epoxy matrix. This technique was found to be quite efficient and environmentally friendly (no solvent is required) for high exfoliation and dispersion within a short period of time. In the study, higher tensile strength was obtained with better degassing. On the other hand, shear mixing produced foamy and viscous mixture and made degassing quite difficult [42].

Becker et al. investigated improvement of thermal stability and water uptake behavior in epoxy resin with different clay content. In the study, it was observed that by the addition of the clay mineral, water uptake of nanocomposites was reduced compared to pristine epoxy resin. On the other hand, water uptake of the epoxy resin was not proportionally correlated with the clay content. Also, it was concluded that thermal stability of the nanocomposite decreased compared to that of pure epoxy resin. The decrease in the thermal stability was very low, therefore it was not considered as a drawback [43].

CHAPTER 3

EXPERIMENTAL

3.1 Materials

3.1.1 Epoxy

A three-component epoxy resin system was used in this study. Diglycidyl ether Bisphenol A (DGEBA) type epoxy resin (Araldite LY 556) with an epoxy content of 183-188 was procured from Huntsman Inc. The hardener and accelerator is methyl-tetrahydrophthalic anhydride (Aradur 917, Huntsman Inc.) and 1-methyl imidazole (DY 070, Huntsman Inc.), respectively. The resin system is a low viscosity matrix system with a long pot life. Also, it has good fiber wetting properties. This epoxy resin is used generally for the filament winding application. Physical properties of epoxy resin, hardener and accelerator are given in the following tables respectively.

Table 3.1 Physical properties of the epoxy resin

Properties	**Data**
Appearance	Clear, Pale yellow liquid
Viscosity at 25^{O}C (ISO 12058-1)	10000 -12000 mPa.s
Density at 25 ^{O}C (ISO 1675)	1.15-1.20 g/cm^3

Table 3.2 Physical properties of the hardener

Properties	**Data**
Appearance	Clear liquid
Viscosity at 25^{O}C (ISO 12058-1)	50-100 mPa.s
Density at 25 ^{O}C (ISO 1675)	1.20-1.25 g/cm^3

Table 3.3 Pyhsical properties of the accelerator

Properties	**Data**
Appearance	Clear liquid
Viscosity at 25^{O}C (ISO 12058-1)	≤ 50 mPa.s
Density at 25 ^{O}C (ISO 1675)	0.95-1.05 g/cm^3

3.1.2 Clay

The clay mineral used in this study was Cloisite 30B, an organophilic clay obtained from Southern Clay Products. Cloisite 30B is produced by the modification of natural montmorillonite with methyl tallow bis-2-hydroxyethyl quaternary ammonium chloride (MT2EtOH). Chemical structure of the modifier is given in Figure 3.1. In the structure, T is tallow and includes ~65% C18; ~30% C16; ~5% C14. Chloride is used as the anion in this modifier.

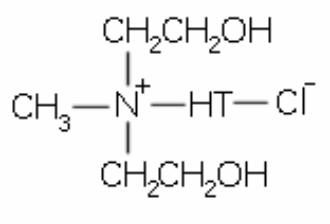

Figure 3.1 Chemical structure of a ternary ammonium salt

The physical properties of the Cloisite 30B are shown in Table 3.4.

Table 3.4 Properties of Cloisite 30B

Modifier concentration	90 meq/100g clay
% Moisture	< 2 %
% Weight loss on ignition	30 %
d_{001}	18.5 Å
Color	White
Density	1.98 g/cc

3.1.3 Mold Release Agent

Poliwax SV-6 (Poliya AŞ), mold release agent, was used to remove the nanocomposite test specimens from the aluminum molds. It is a silicone type release agent and applied to the mold before the mixed nanocomposite material is poured into the mold.

3.2 Preparation of nanocomposite test specimens

In this study, in-situ polymerization technique was followed to prepare the polymer nanocomposite test specimens. The experimental set-up is prepared as shown in Figure 3.2.

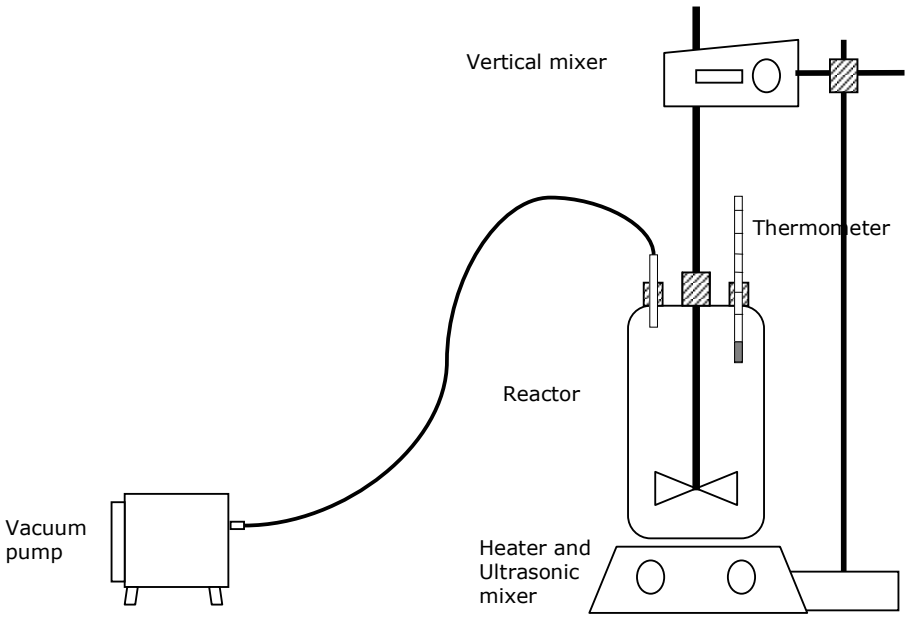

Figure 3.2 Experimental set-up

Prior to nanocomposite production process, the clay (Cloisite 30B) was dried at 90 °C for 8 hours. Also, the right reactor set-up was decided after some trials. The epoxy resin (Araldite LY 556) was placed into the reactor and heated to 40 °C to decrease the viscosity. Then, the desired amount of clay was added into the reactor during stirring. During the clay addition, the stirring rate was arranged not to let dust in the reactor. Cloisite 30B particles were dispersed in the epoxy resin by mechanically mixing for 1.5 hours at 40 ° C. The mixing rate was

approximately 700 rpm at this stage. While the mixture was mixed mechanically, ultrasonic mixing was applied for 30 minutes. Ultrasonic mixing is necessary to increase the distance between layers as well as dispersion of the clay in the matrix. During the mixing process, the mixture was degassed by a vacuum pump to eliminate the bubbles in it. After the mixing and vacuum processes, curing agent and accelerator were added at the ratios 100/90/0.5 (epoxy/curing agent/accelerator) by weight respectively. After addition of the curing agent, mixture was stirred for 30 minutes and 40 ^{o}C. At this stage, the mixing rate was arranged according to amount of clay loading not to let bubbling in the mixture. The nanocomposite mixture was cast into the test molds which were coated with mold release agent. Molds were put into the furnace carefully not to let nanocomposite resin spillage. If the epoxy resin spills out of molds, test samples are not standard. The cast polymer was cured. Curing cycle was in two steps which are pre-curing and post-curing. In the pre-curing step, the cast was heated to 80 ^{o}C, and held at 80 ^{o}C for 3 hours. Then, in the post-procuring step, the cast mixture was heated to 120 ^{o}C and held at 120 ^{o}C for 5 hours. After this period, the cast was cooled in the furnace to ambient temperature. Finally, molds were taken out from the furnace and test specimens were removed gently from the molds. The flow chart of the preparation of the epoxy/clay nanocomposite is given in Figure 3.3. In the production of nanocomposite test samples, different clay amounts (1, 3, 5, 7 and 9 % by weight) were used.

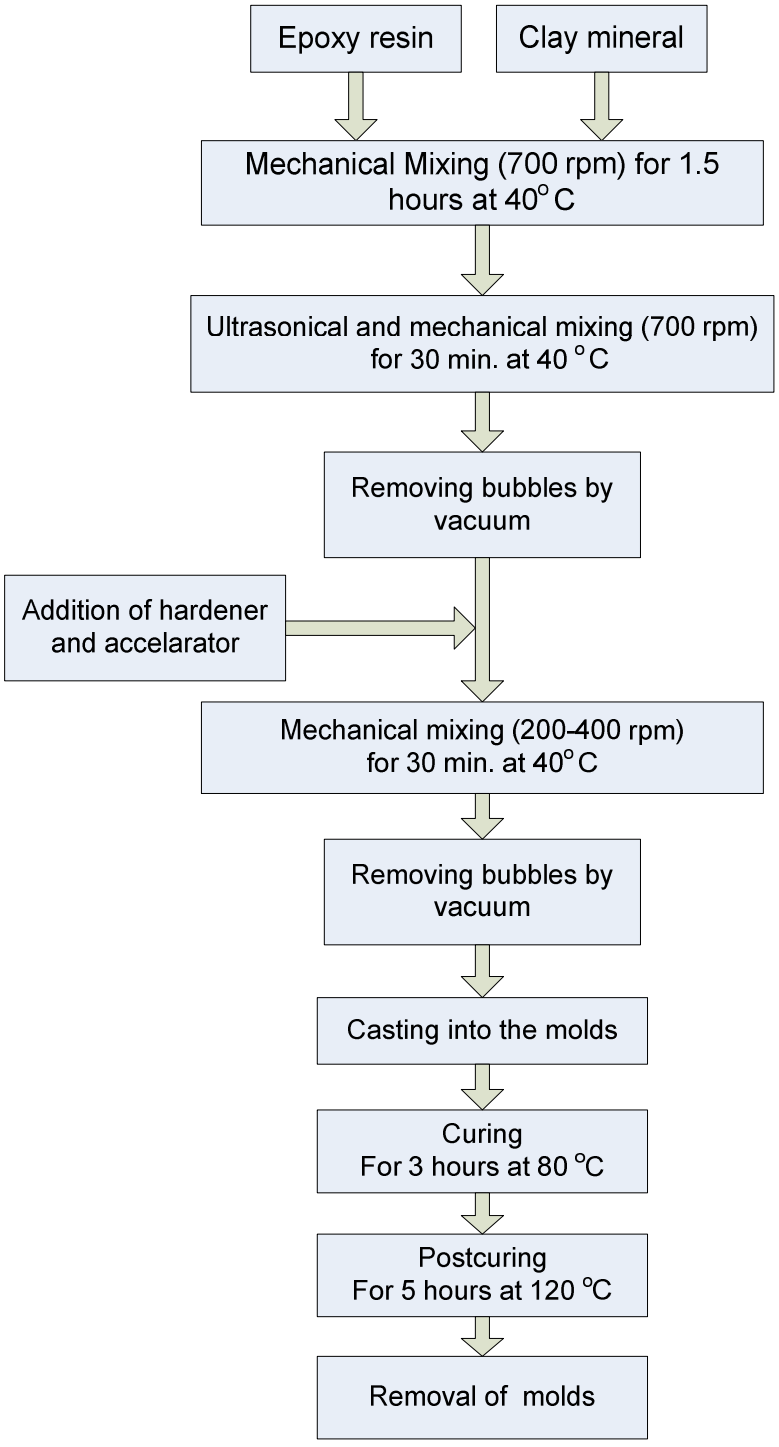

Figure 3.3 Procedure for the production of the epoxy clay nanocomposites

After the production of the test samples, mechanical, thermal and flammability properties of the nanocomposite materials were determined. Following tests were performed for the test samples:

- XRD analysis
- SEM analysis
- Tensile test
- Impact test
- Flexural test
- DSC analysis (Determination of Tg)
- TGA analysis (Decomposition temperature, weight loss)
- Flammability test

Mechanical tests were performed using the test specimens prepared according to Amercan Society for Testing and Materials (ASTM) and International Organisation for Strandardization (ISO) standards. Other tests were conducted with the pieces of specimens used in mechanical tests. Test details are explained in the following paragraphs.

3.3 Characterization

3.3.1 Scanning Electron Microscopy (SEM) Analysis

The fracture surface of the tensile specimens was examined by using FEI QUANTA 400- Field Emission Scanning Electron Microscope (FESEM). Before the SEM studies were performed, a thin section was cut from the fracture surfaces and it was coated with thin layer of gold–palladium. Then, SEM micrographs of tensile fractured surfaces were obtained with an accelerating voltage of 20 kV.

3.3.2 X-Ray Diffraction (XRD) Analysis

Exfoliation behavior of the organoclay in epoxy matrix was determined by XRD analysis. Analyses were conducted by a Rigaku DMAX 2200 diffractometer. Diffraction patterns of nanocomposite were measured for 2θ from 1^{o} to 10^{o} using CuK_{α} (λ = 1.5418 Å). The generator voltage and current were set to be 40 kV and 40 mA respectively. Before the analysis, samples were cleaned with methyl alcohol to remove residual clay from the surface.

3.3.3 Mechanical Testing

In order to characterize the mechanical properties of the test samples, tensile, flexural and impact tests were performed. All the tests were done at ambient temperature. At least, seven test specimens were used in each type of tests. The standard deviations for all the tests were calculated and the error bars are shown in the graphs. The tensile tests were performed two times with new test samples, because tensile test results of first production batch samples had a lot of fluctuation. However, tensile tests values of the second production batch also fluctuated. The big differences between the values can be attributed to several reasons and these will be explained in the following paragraphs.

3.3.3.1 Tensile Testing

Tensile tests were performed according to ASTM D 638-03 standard (Standard Test methods for Tensile Properties of Plastics). Tensile properties were obtained with a tensile testing machine (BESMAK A.Ş., U-test) using a test speed of 1 mm/min. The test specimens were prepared as Type I dimensions specified in ASTM D 638-03. Test

specimen of Type I dimensions are suitable for the hard materials as epoxy and its nanocomposites. Shape of the test specimens and dimensions are given in Figure 3.4. Tests were conducted at ambient temperature. As a result of the tests; tensile strength, strain at break and Young's modulus data were obtained.

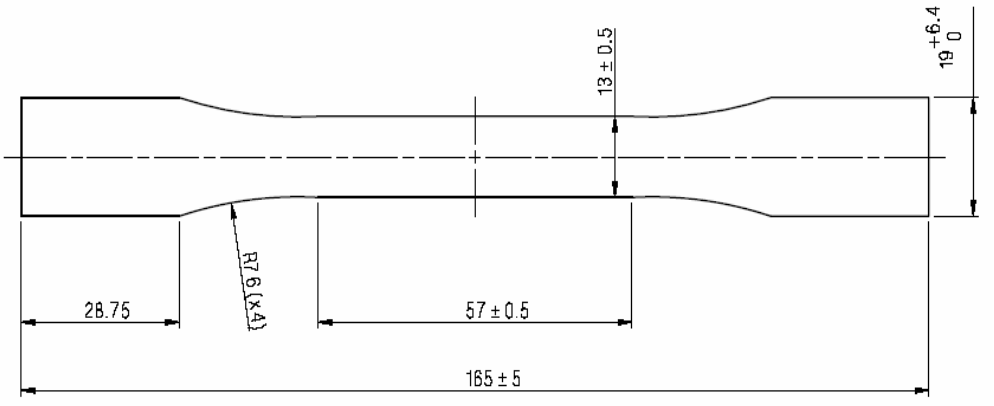

Figure 3.4 Dimensions of tensile test specimen

3.3.3.2 Flexural Testing

Flexural properties of the nanocomposite test samples were determined according to ASTM D 790-03 standard. Shape and dimensions of test specimen are given in Figure 3.5. Nanocomposite and epoxy test specimens are rigid materials, so procedure A of ASTM D 790-03 was followed. Procedure A is designed for materials broken at comparatively small deflections. Tests were conducted by using the U-test testing machine.

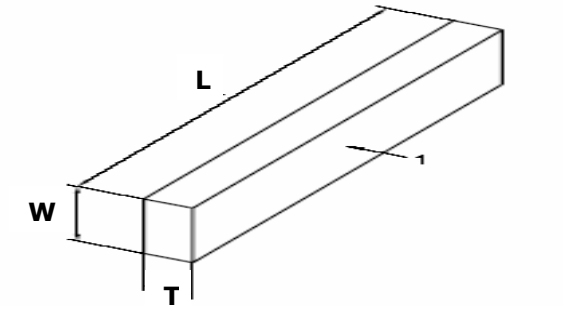

L (cm)	W (cm)	T (cm)	Span (cm)
80±2	10.0± 0.2	4.0±0.2	64±0.5

Figure 3.5 Flexural test specimen

The test specimen rests on two supports and is loaded by a loading nose to the middle of the test specimen. In this test, span-to-depth ratio was taken as 16:1.

The loading nose and supports have cylindrical surfaces. The radii of the loading nose and supports were taken as 5.0 ± 0.1 mm in the range as stated in ASTM D790.

Prior to performing tests, crosshead speed was calculated according to following equation.

$$R = ZL^2/6d \qquad (3.1)$$

where,

R= rate of crosshead motion, mm/min,

L= support span, mm

d = depth of beam

Z = rate of straining of the outer fiber, mm/mm/min, 0.01

Crosshead speed (R) was calculated as 1.71 mm/min. At least 7 samples were tested and average of them is reported as the test result. After load data were taken, flexural strength was calculated. For a test specimen with rectangular cross-section, the flexural strength is equal to

$$S=3PL/2bd^2 \quad (3.2)$$

where,

S = stress in the outer fibers at midspan (Mpa)
P = the load at fracture (N)
L = the distance between support points (mm)
b = the width of the specimen (mm)
d = the depth of specimen (mm)

The flexural strain at break in the outer fibres occurs at midspan, is calculated as follows.

$$r = \frac{6Dd}{L^2} \quad (3.3)$$

where,

r = the maximum strain in the outer fibers (mm/mm)

D = the maximum deflection of the center of the beam (mm)

L = the support span (mm)

d = the depth of specimen (mm).

D was taken as the point where specimen breaks so that strain at break value was calculated.

Tangent modulus of elasticity (flexural modulus) is the ratio, within the elastic limit of stress to corresponding strain and shall be expressed as MPa. It is calculated by drawing a tangent to the steepest initial straight-line portion of the load-deflection curve and by using Equation (3.4).

$$E_B = \frac{L^3 m}{4bd^3} \tag{3.4}$$

where,

E_B = modulus of elasticity in bending (MPa)

L = length of support span (mm)

b = the width of the beam tested (mm)

d = the depth of beam tested (mm)

m= the slope of the tangent to the initial straight-line portion of the load deflection curve, N/mm of deflection [37].

3.3.3.3 Impact Testing

Charpy impact tests were performed according to ISO 179-1 standard. Test specimens were prepared by casting of nanocomposites into the molds meeting the dimensions specified for the impact tests. In each test, a set of 5 unnotched specimens were tested. Impact test were conducted by using a Pendulum Impact Tester manufactured by Ceast SpA.

Tests were carried out at ambient temperature (25 ^{o}C). Pendulums were selected as sufficient to break the test specimens. The pendulum was lifted to the prescribed height. Specimen was placed on the

supports of test apparatus. Then, the pendulum was released. Finally, impact energy absorbed by the specimen was recorded in J/m unit. Results were determined as the average of at least 5 samples.

3.3.4 Differential Scanning Calorimetry (DSC) Analysis

Differential Scanning Calorimeter (DSC) experiments were conducted to investigate the change in the glass transition temperature of epoxy resins with different clay contents. Tests were performed with a DSC 131 instrument (Setaram Instrument). The samples were cut from the cast specimens used in mechanical tests. Heating rate was 20 ^{o}C/min and heating range was 25 ^{o}C to 240 ^{o}C under nitrogen atmosphere.

3.3.5 Thermogravimetric Analysis (TGA)

Thermal gravimetric analysis (TGA) was performed to determine the thermal stability of the epoxy resin with different clay contents by using Perkin Elmer Pyris 1 TGA analyzer. Tests were conducted at a heating rate of 10^{o}C/min from ambient temperature to 600 ^{o}C under nitrogen atmosphere. In TGA analysis, the test samples were cut from the cast specimens used in mechanical tests. Heat decomposition temperature of nanocomposite and amount of material remaining were determined.

3.3.6 Flammability Testing

The flammability tests were performed according to ASTM D3801-06. Test apparatus and test specimens were prepared according to this standard. The chamber is convenient to observe the tests in progress. During the test, induced or forced draft in the chamber was prevented.

Test specimens are burned by gas supply which should be uniform through the test.

Test specimens had the dimensions of 10.0±0.5 mm in thickness and 100±5 mm in length. Their surfaces were smooth and unbroken. Three test specimens were used.

Flammability test was done by using vertical burning test set-up shown in Figure 3.6.

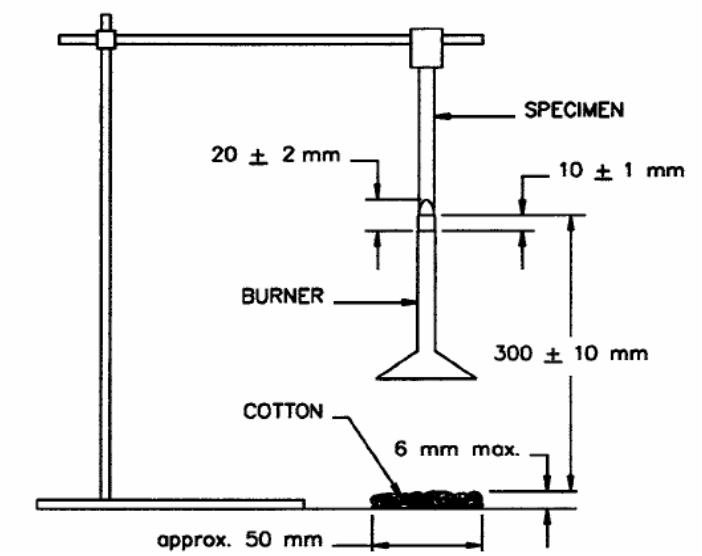

Figure 3.6 Vertical burning test setup according to ASTM D 3801-06

Test specimen is clamped from the upper 6 mm of the length. Distance between the lower end of the specimen and horizantal layer of cotton is arranged to be 300 mm.

Burner is placed remote from the test specimen and then ignited. Flame is arranged to be 20 ±2 mm height. Then, the valve is adjusted to produce 20 ±2 mm yellow-tipped blue flame. The flame approaches to the specimen from the wide side in a horizantal plane. Flame is

placed under the center of the specimen. Test specimen is exposed to flame from 10±1 cm distance and 10.0± 0.5 s time period. Then test flame is withdrawn from the specimen. Then, the afterflame time is measured in seconds. When the flaming ceases, specimen is again exposed to the flame from 10±1 mm distance and for 10.0± 0.5 s time period. After the second flame application, afterflame time and afterglow times are recorded, in seconds. Then, the flammability behavior of polymers are classified according to Table 3.5.

t1: Afterflame time after the first flame application

t2 : Afterflame times after the second flame application

t3 : Afterglow times after the second flame application

The total afterflame time for each set of three specimens is calculated by the following formula:

$$t_f = \sum_{i=1}^{5} (t_{1,i} + t_{2,i}) \tag{3.5}$$

where:

t_f = total flaming time

$t_{1,i}$ = afterflame time after the first flame impingement, s, of the i^{th} specimen

$t_{2,i}$ = afterflame time after the second flame impingement, s, of the i^{th} specimen

Table 3.5 Classification of flammability behavior

Criateria Conditions	V-0	V-1	V-2
Afterflame time	≤ 10s	≤30s	≤30s
Total afterflame time (for five specimens)	≤ 50s	≤250s	≤250s
Afterflame plus afterglow time for each individual	≤30s	≤60s	≤60s
Afterflame or afterglow of any specimen up to holding clamp	No	No	No
Cotton indicator ignited by flaming particles or drops	No	No	Yes

CHAPTER 4

RESULTS AND DISCUSSION

4.1 Morphological Analysis

4.1.1 Scanning Electron Microscopy (SEM) Analysis

The tensile fractured surfaces of the neat epoxy resin and epoxy-clay nanocomposites were examined by the scanning electron microscope. The SEM micrographs of test specimens are shown in Figures 4.1 through 4.6.

Figures 4.1.a and 4.1.b represent the microstructure of the pristine epoxy resin at low and high magnifications respectively. Very smooth and featureless surface is observed even at high magnification. This indicates the presence of brittle fracture in the neat resin. Also, there are some black spots representing the micro voids which may act as crack propagation sites.

Figures 4.2.a and 4.2.b show the fracture surface of nanocomposite with 1 wt. % organoclay. River line markings and sharp surfaces are the evidence for the brittle fracture of nanocomposite. These river lines formed during the crack propagation. No obvious agglomerates were observed in the micrographs. This can be attributed to exfoliation of the clay particles. In exfoliated state, individual clay layers may not be observed by SEM analyses.

In Figures 4.3.a and 4.3.b, micrographs of nanocomposite having 3 wt.% clay are shown. River line markings and sharp surfaces are also observed in these micrographs. The bright spots, corresponding to clay agglomerates, appeared here.

At 5 wt. % clay loading, no river line markings are seen in the SEM micrographs (Figures 4.4.a and 4.4.b). It was observed that the distance between the aggregates decreased and the size of clay aggregates increased.

The microstructures of nanocomposites with 7 and 9 wt.% clay content are represented in Figures 4.5.a, 4.5.b, 4.6.a and 4.6.b. At these clay contents, larger agglomerates were observed.

SEM micrographs showed that by the addition of the clay loading, the size of the clay aggregates increased. Average sizes of clay aggregates were measured and given in Table 4.1. At low clay loading, clay particles were more uniformly dispersed. On the other hand, at high clay contents, clay aggregates lead to crack initiation and stress concentration. These may lead to premature failure in mechanical tests.

Table 4.1 Average particle sizes of clay aggregates in nanocomposites

Clay content (wt. %)	Clay aggregate size (μm)
3	7
5	13
7	20
9	34

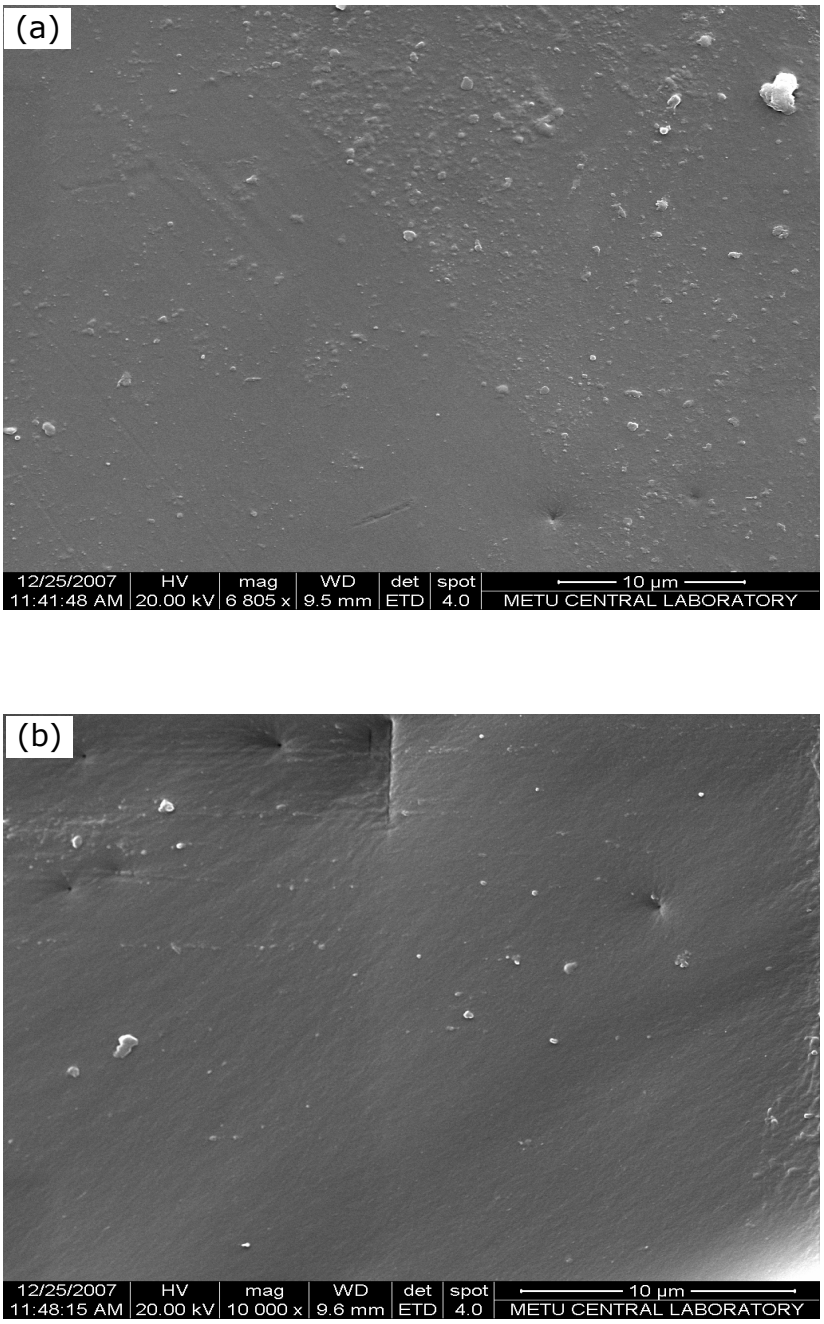

Figure 4.1 SEM micrographs of the tensile fractured surface of pristine epoxy resin: (a) low magnification and (b) high magnification

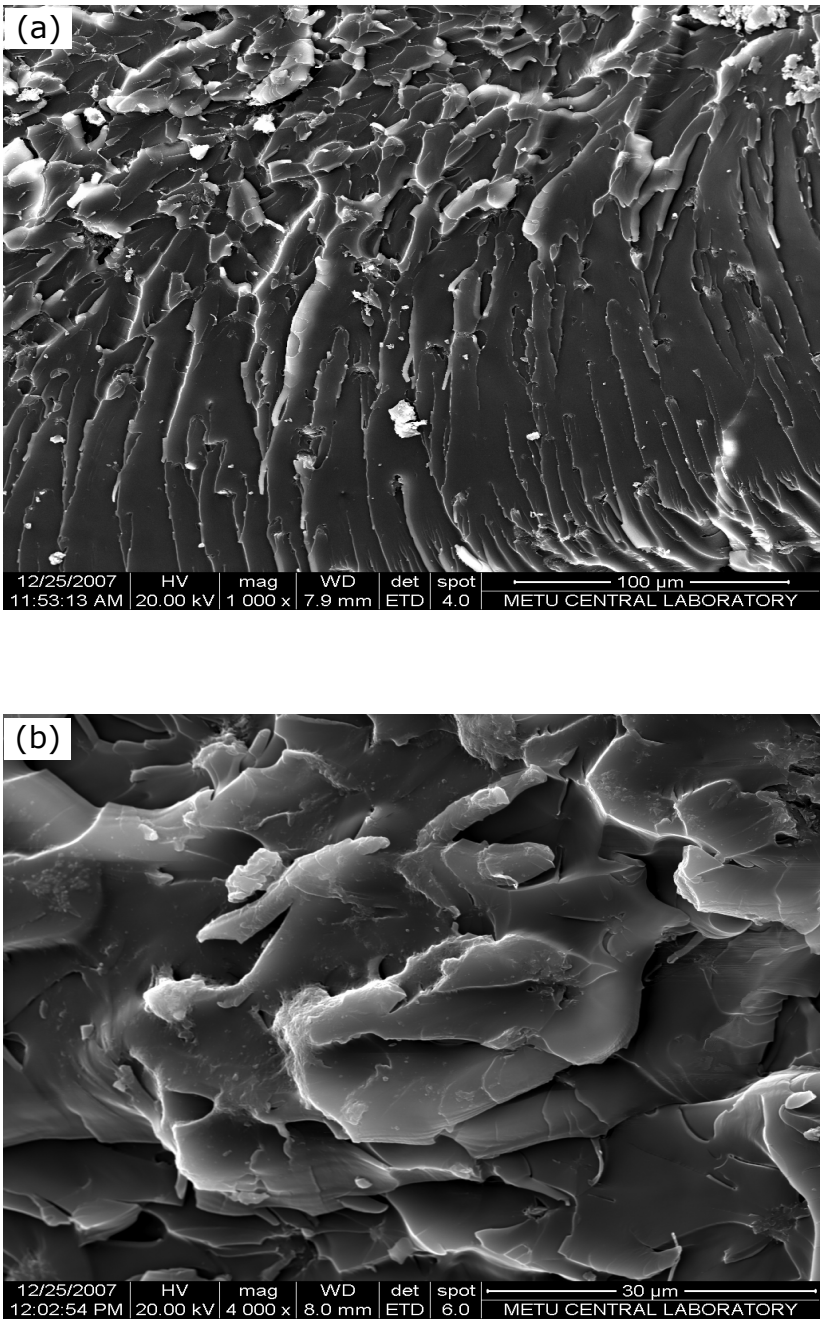

Figure 4.2 SEM micrographs of the tensile fractured surface of nanocomposite with 1 wt. % Cloisite 30B:
(a) low magnification and (b) high magnification

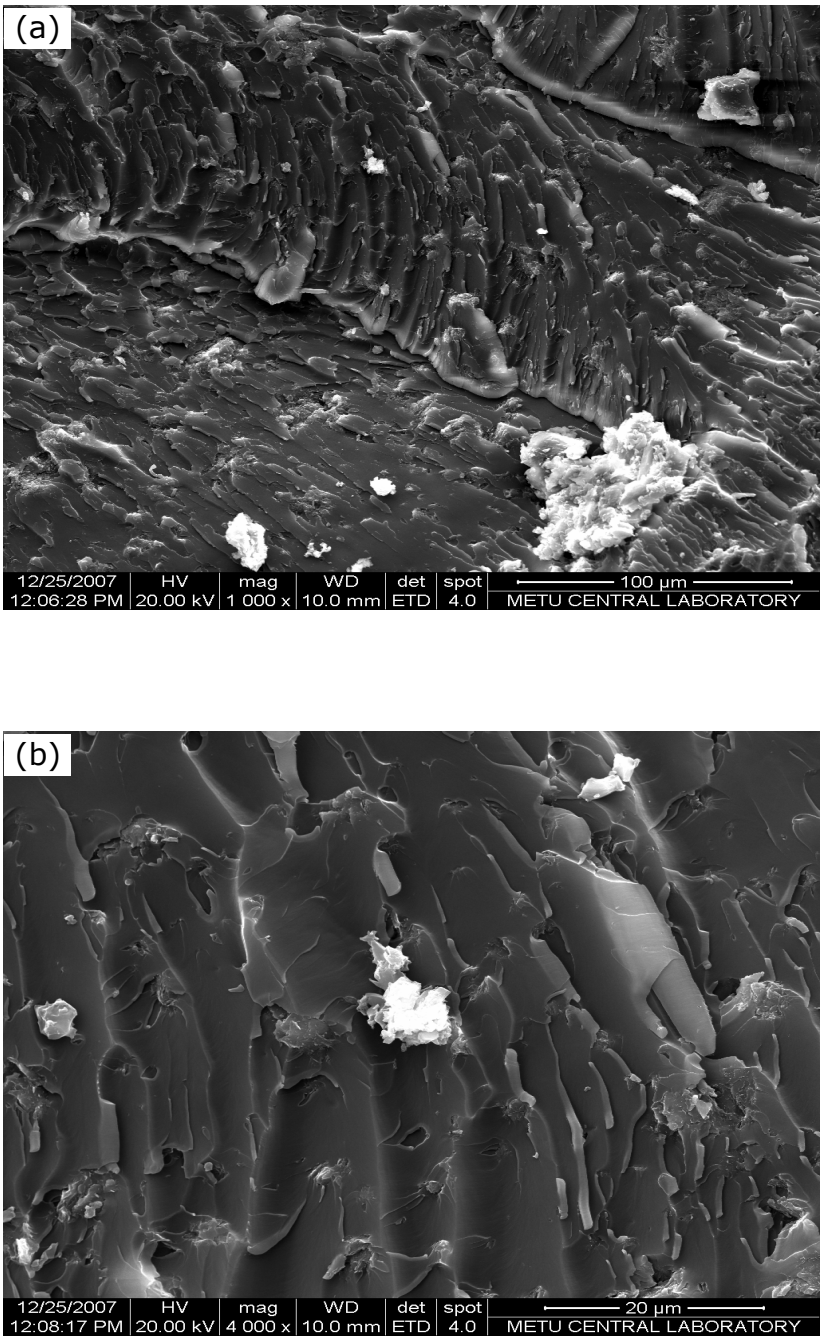

Figure 4.3 SEM micrographs of the tensile fractured surface of nanocomposite with 3 wt. % Cloisite 30B:
(a) low magnification and (b) high magnification

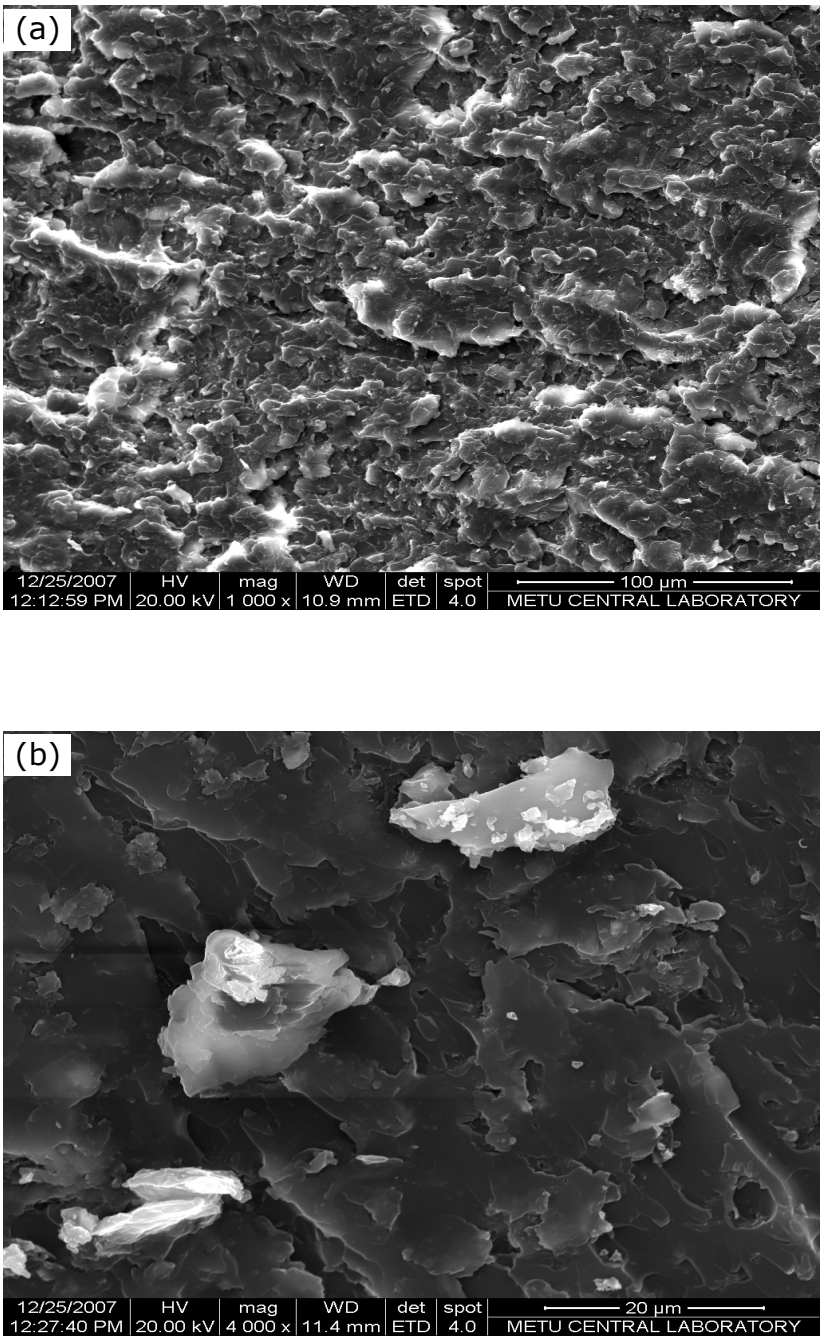

Figure 4.4 SEM micrographs of the tensile fractured surface of nanocomposite with 5 wt. % Cloisite 30B:
(a) low magnification and (b) high magnification

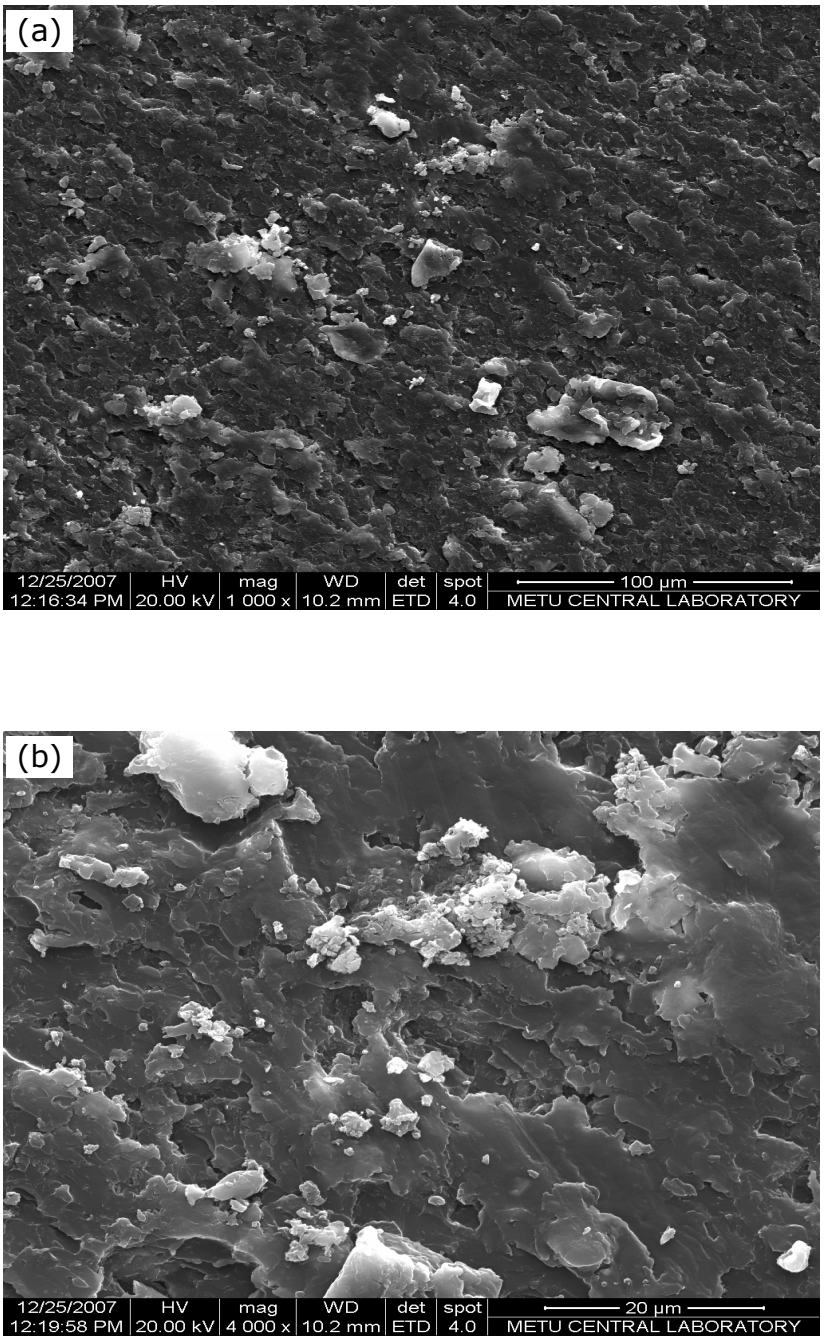

Figure 4.5 SEM micrographs of the tensile fractured surface of nanocomposite with 7 wt. % Cloisite 30B:
(a) low magnification and (b) high magnification

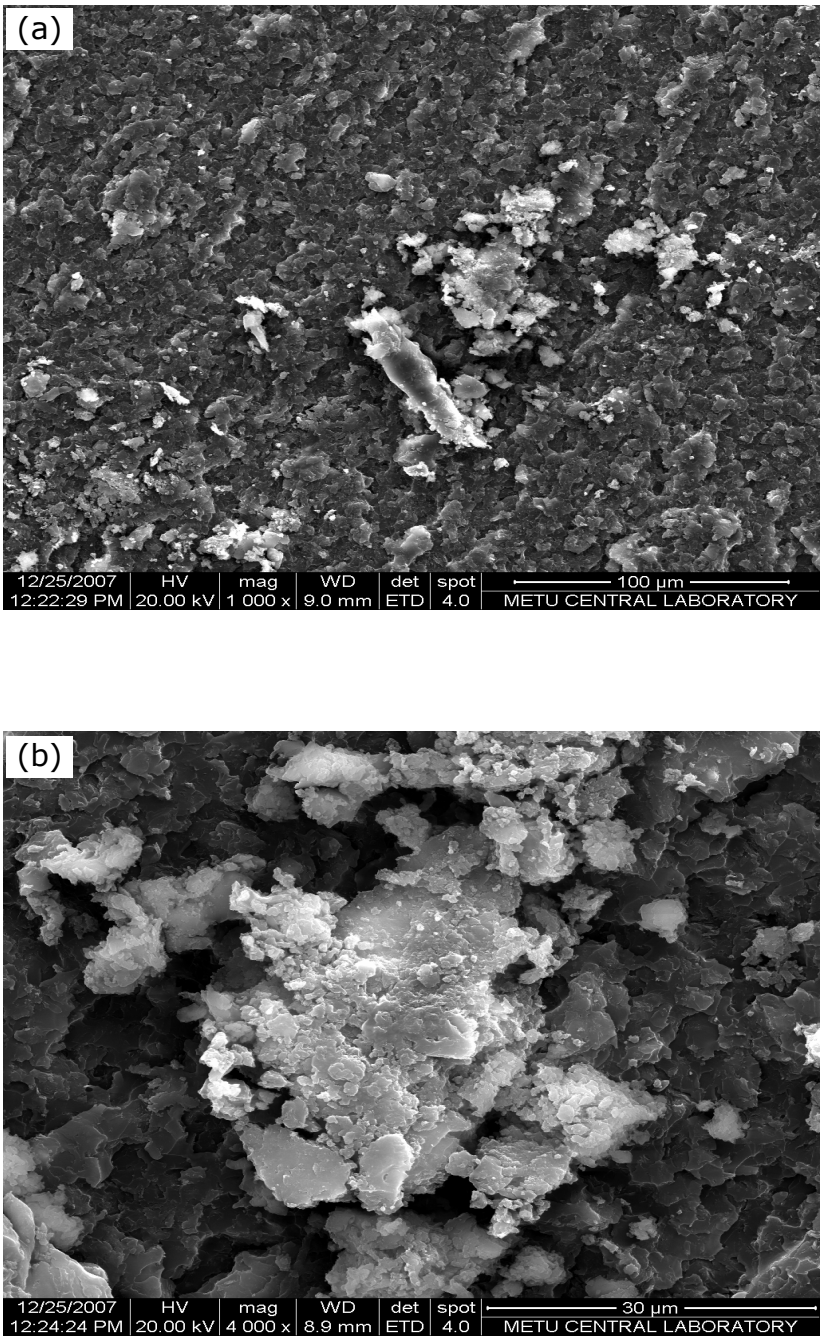

Figure 4.6 SEM micrographs of the tensile fractured surface of nanocomposite with 9 wt. % Cloisite 30B:
(a) low magnification and (b) high magnification

4.1.2 X-Ray Diffraction (XRD) Behavior

XRD was performed to determine d-spacing (also called as basal or interlamellar spacing) between the silicate layers of the clay in the nanocomposite resin.

Figures 4.7 and 4.8 show the diffraction patterns of the organoclay (Cloisite 30B) and pure epoxy resin respectively. The characteristic diffraction peak of Cloisite 30B was observed at $2\theta = 4.94^{o}$ and basal spacing is calculated as 17.89 Å. This value is approximately the same as the data determined by the manufacturer. The calculation of the basal spacing was done by using Bragg's Law given in Equation 4.1,

$$n\lambda = 2d\text{Sin}\theta \qquad (4.1)$$

where the following values are used:

n = 1

λ = 1.5418 Å

θ = the diffraction angle where the peak is observed.

In the diffractogram of pure epoxy resin, no peak was observed as expected. Because, there was no ordered or crystalline structure to be detected in the pure resin. On the other hand, at some clay concentrations, peaks appeared on the diffractograms at some diffraction angles. These are tabulated in Table 4.2 below.

Table 4.2 Diffraction peaks of the neat epoxy resin and nanocomposites

Clay Content	First Diffraction Angle	Second Diffraction Angle
The neat resin	Not observed	Not observed.
Cloisite 30B	4.94°	Not observed
1 wt. %	Not observed	Not observed
3 wt. %	2.20°	Not observed
5 wt. %	2.00°	5.59°
7 wt. %	2.12°	5.53°
9 wt. %	2.24°	5.16°

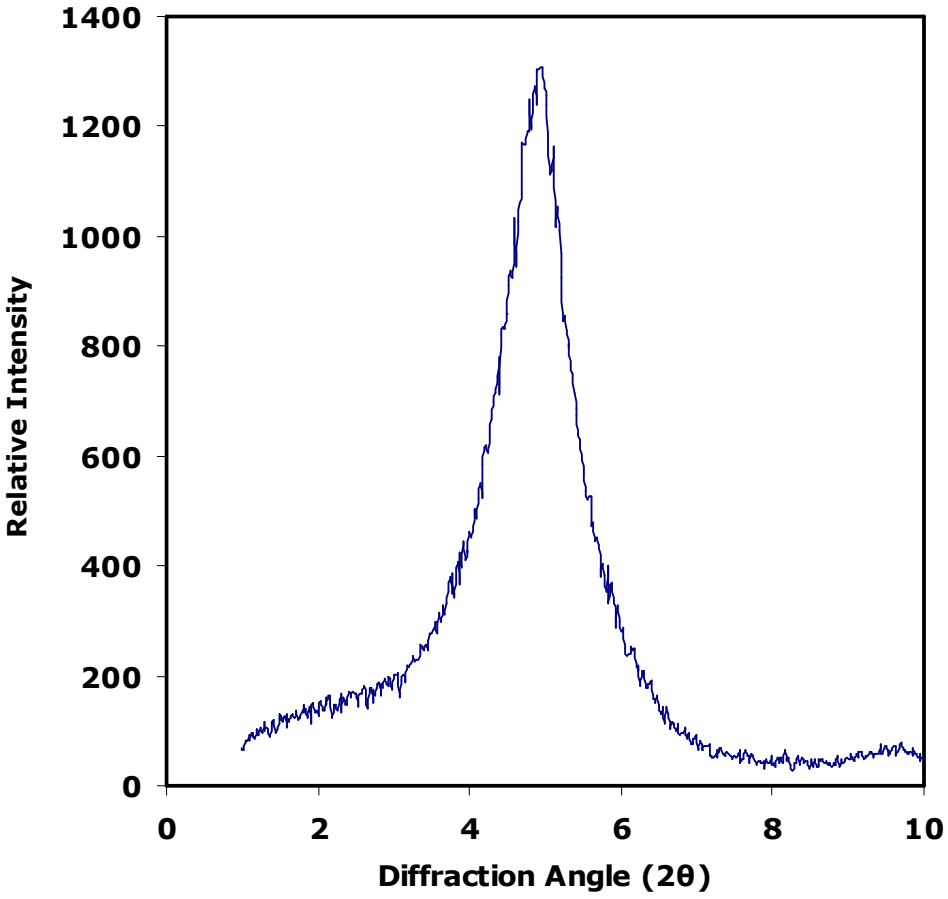

Figure 4.7 X-ray diffaction pattern of Cloisite 30B

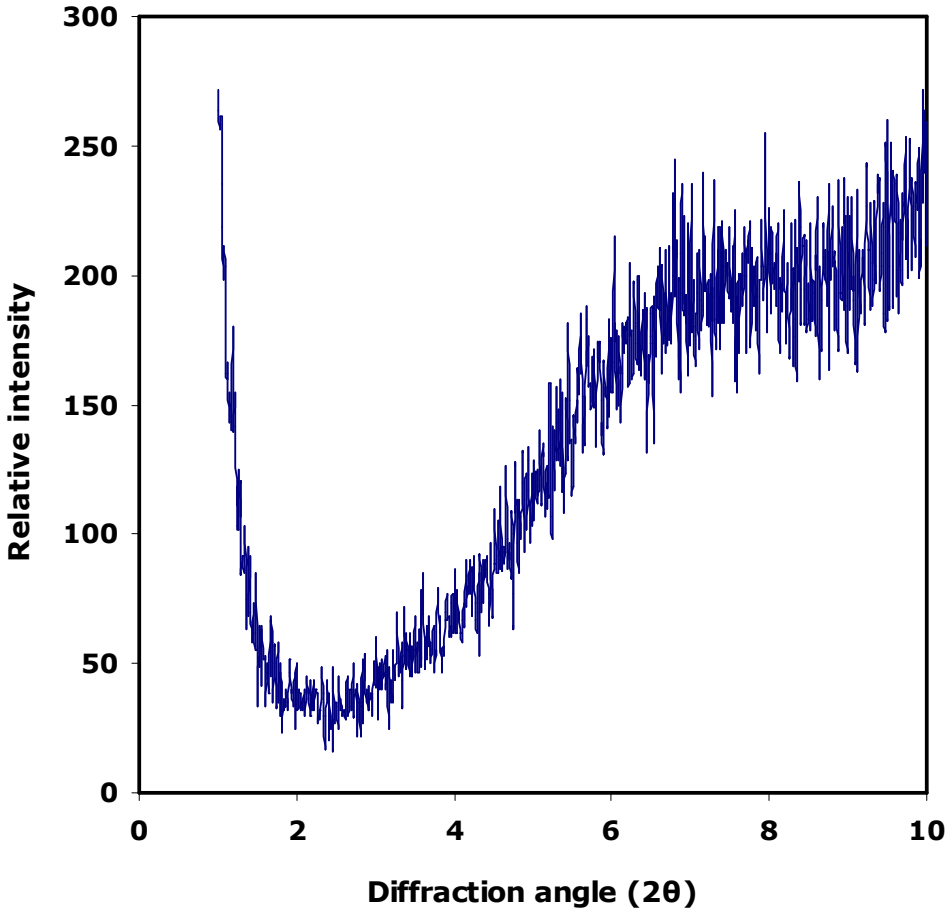

Figure 4.8 X-ray diffaction pattern of pure epoxy resin

It is very important to start the XRD analyses with the correct angle at which diffraction peaks can be observed. In order to observe d-spacing greater than 30 Å, analyses must be started from $2\theta=1^{o}$. Otherwise, with $2\theta=2^{o}$ starting angle, some of the peaks would not be observed in the XRD diffractogram. Hence, this would cause to draw wrong conclusions implying that complete exfoliation is achieved.

The distance between the clay layers increases as they are mixed in the epoxy resin. According to degree of dispersion, either exfoliated or intercalated nanocomposites can be achieved. However, at high clay loadings, both intercalated and agglomerated structures can be present in the polymeric matrix. In the present study, nanocomposites having one peak around $2\theta=2^{o}$ (d-spacing:4.4 nm) indicate that intercalated structures are obtained. Because, when the d-spacing between the layers is around the 1 and 4 nm, the nanocomposite is usually called as intercalated [26].

XRD pattern of the nanocomposite with 1 wt.% clay content is shown in Figure 4.9. Here, no peak was observed. This can be explained by well exfoliation of the clay particles. In exfoliated state, the distance between the clay layers is so long that each silicate layer moves independently. Clay layers do not interact with each other. On the other hand, at 3 wt. % clay content (Figure 4.10), the distance between the silicate layers (d-spacing) decreased and a peak appeared at $2\theta = 2^{o}$ diffraction angle which corresponds to the d-spacing of 4.42 nm. This indicates that at 3 wt. % clay content, intercalated nanocomposite was achieved. When clay loading increases further, a second peak was observed in the diffraction patterns at around $2\theta = 5^{o}$ (Figure 4.11). This second peak corresponds to agglomerated structures in the matrix. After 5 wt. % clay loading, both clay agglomeration and intercalation were achieved. First peak indicates the presence of intercalated structures and second one indicates the presence of agglomerated clay particles. The nanocomposite resin with 7 and 9 wt.% clay content are shown in Figures 4.12 and 4.13

respectively. Diffraction peaks at 2θ = 2.12° and 5.53° appeared in case of 7 wt. % clay content, and the peaks appeared at 2θ = 2.24° and 5.16° were obtained in case of 9 wt. % clay content. These two clear peaks indicated that both intercalated and agglomerated clays were present in the epoxy resin.

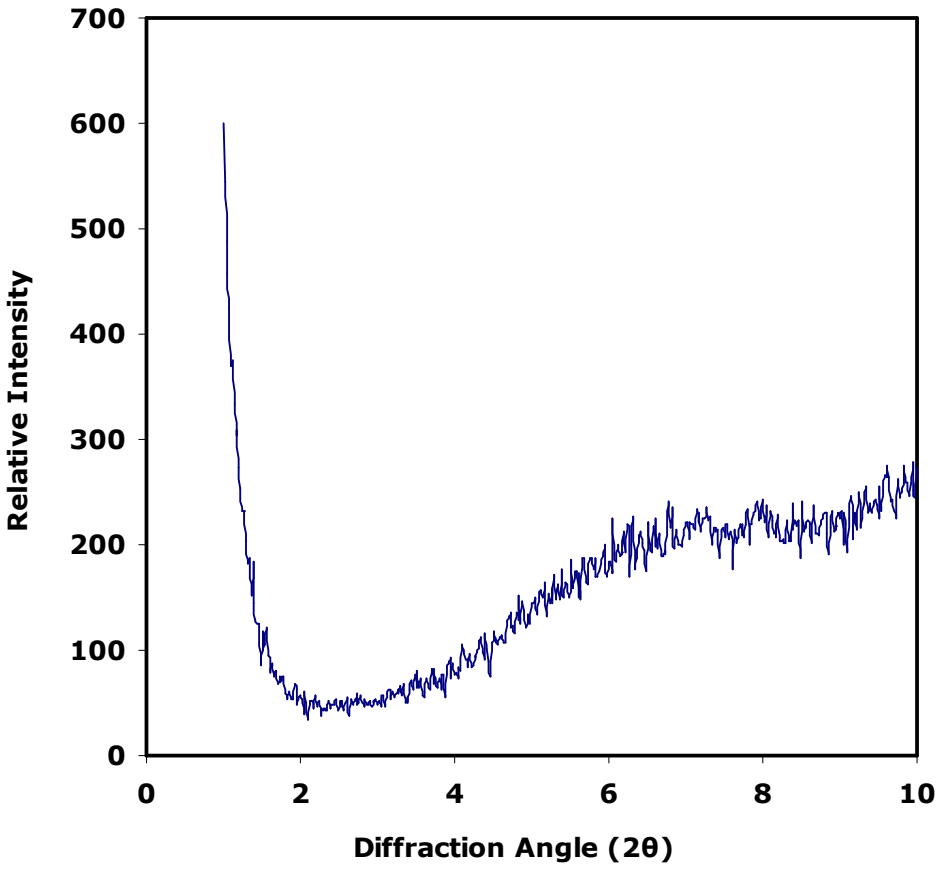

Figure 4.9 X-ray diffraction pattern of the nanocomposite containing 1 wt % Cloisite 30B

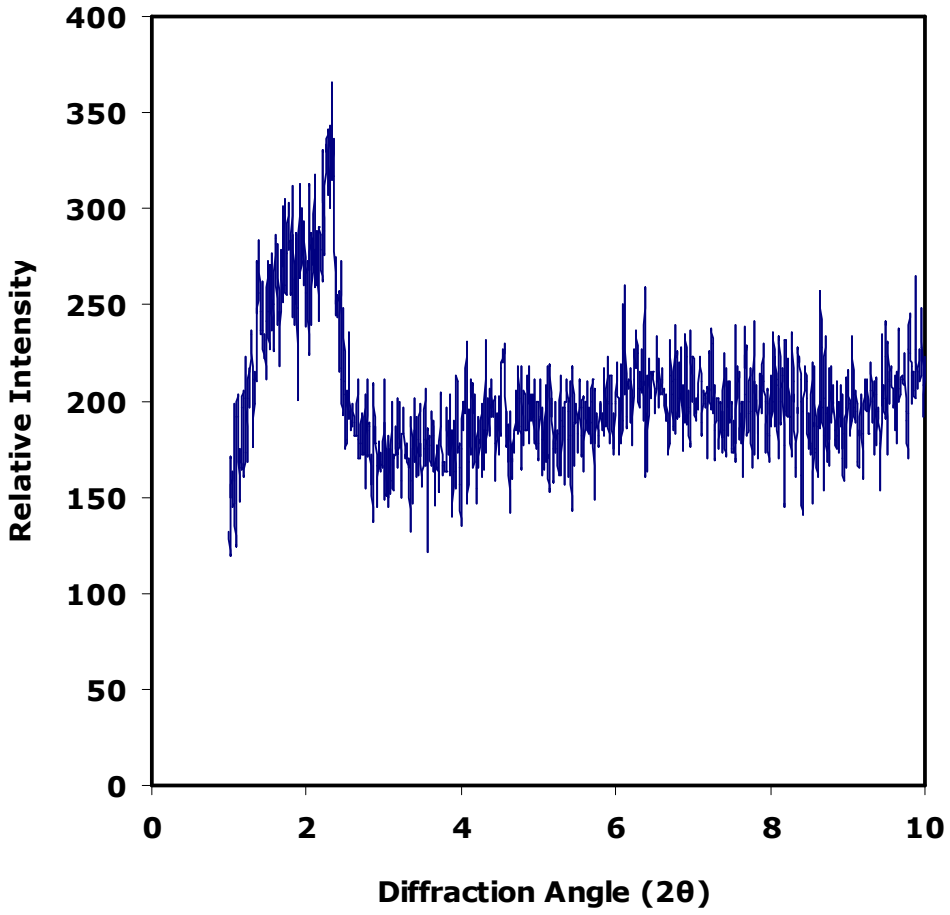

Figure 4.10 X-ray diffraction pattern of the nanocomposite containing 3 wt % Cloisite 30B

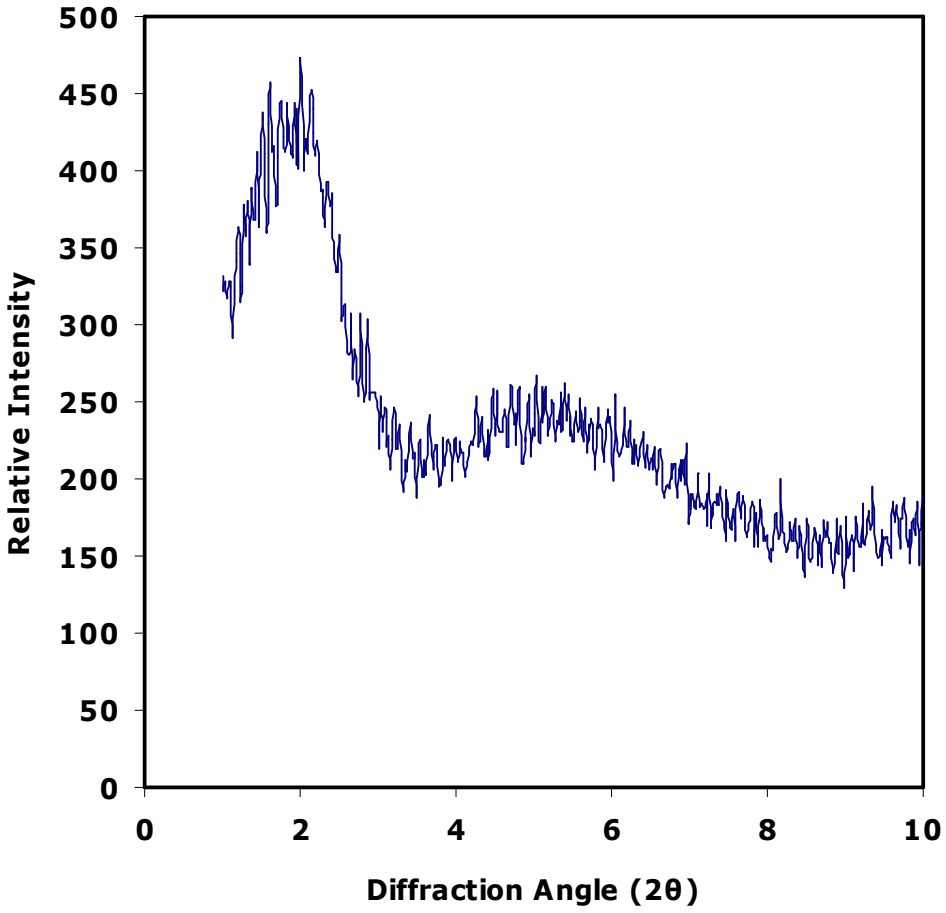

Figure 4.11 X-ray diffraction pattern of the nanocomposite containing 5 wt % Cloisite 30B

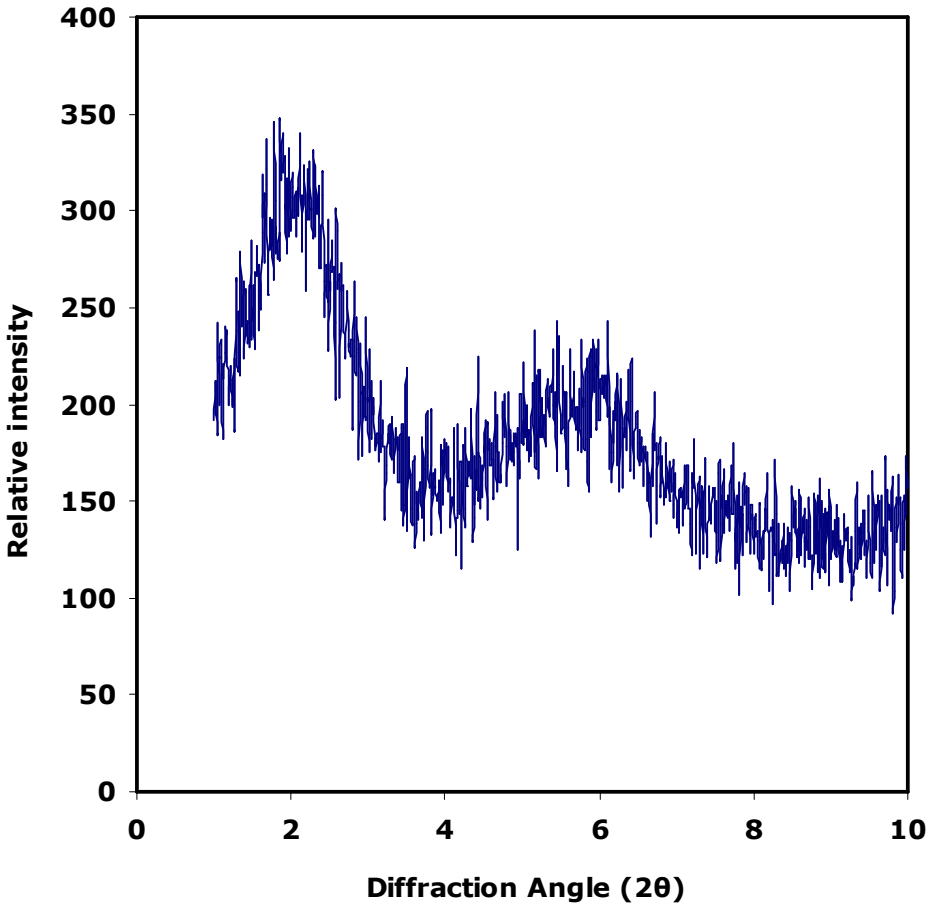

Figure 4.12 X-ray diffraction pattern of the nanocomposite containing 7 wt % Cloisite 30B

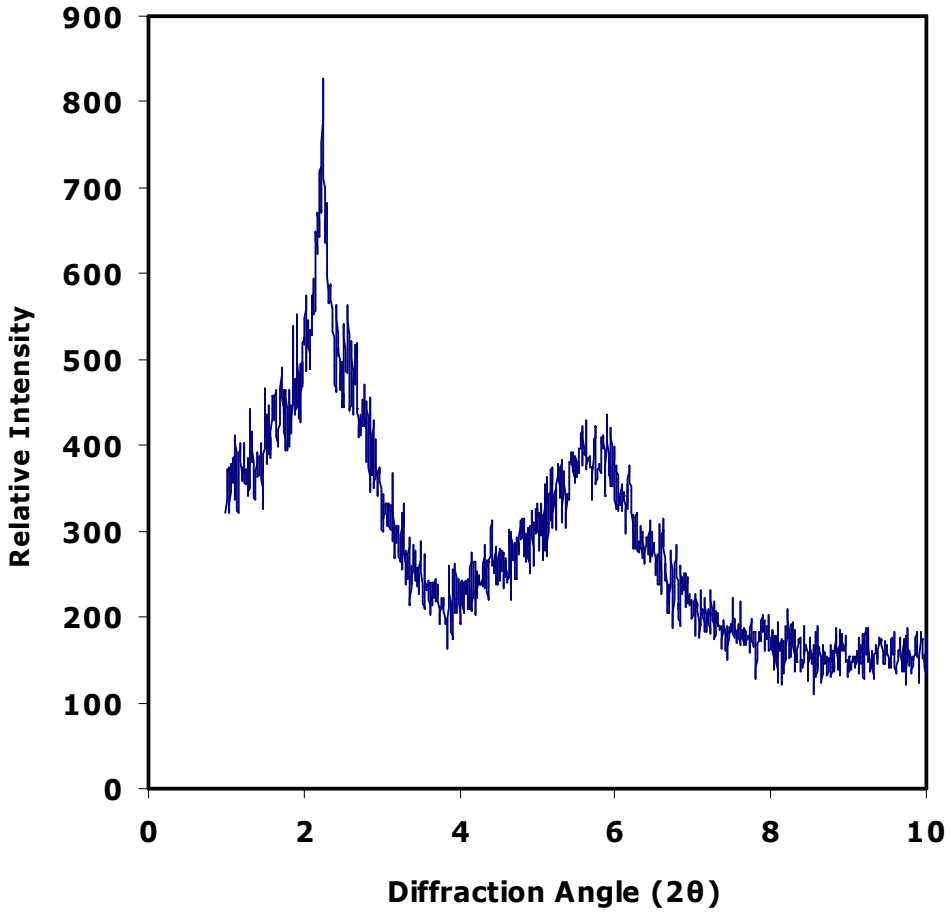

Figure 4.13 X-ray diffraction pattern of the nanocomposite containing 9 wt % Cloisite 30B

4.2 Mechanical Behaviours

In the present study, tensile, flexural and impact tests were done to characterize the mechanical properties of the synthesized epoxy-clay nanocomposites. The mechanical properties of nanocomposites were compared with those of neat epoxy resin.

4.2.1 Tensile Properties

Tensile properties of all nanocomposite materials as a function of clay loading are given in Figures 4.14 through 4.16 (Appendix A1.1, A1.2 and A1.3). It was observed in Figure 4.14 that tensile strength values of nanocomposites decrease steadily with clay loading. The tensile strength value of the neat epoxy resin decreased from 55 MPa to 29 MPa with 9 % clay loading. There is no improvement in the tensile strength values of neat epoxy resin with the addition of clay. This is in contrast to the results reported in the previous studies by other researchers [42]. For example; In the study of Isık et al. [5], tensile strength was improved by following the same process steps and with the same type of clay, Cloisite 30B. In the present study, decrease in tensile strength values may be both material and process related. Type of epoxy system (resin, curing agent, and accelerator) and clay could be incompatible. So, the poor interaction between the clay and epoxy resin could lead to poor adhesion. Beside clay type, clay loading could be too high (even 1 wt. %), then clay platelets would not intercalate or exfoliate in the epoxy resin. During dispersion of clay particles in the epoxy matrix, the viscosity of the resin system increase and that can prevent the easy movement of clay particles. This could lead to uneven distribution of clay particles in the matrix.

The other reason of the decrease in the tensile strength values may also be attributed to micro bubbles which arose during processing.

Stirring rate of mechanical mixer, stirring time period, mixing temperature, stirrer type, and clay percentage could cause micro bubbles. The micro bubbles observed in the test specimens may have negative effects on the tensile strength. Although degassing was applied to the epoxy-clay mixture during and after the production, it is very hard to eliminate them totally. Some micro bubbles could not be observed during the production step, because of their very small sizes. On the other hand, heating of nanocomposite resin caused the micro voids to expand during the production step. Beside these, reduction of the stirring rate did not solve the bubbling problem thoroughly. The time of mixing affected the amount of micro voids in the resin. It was observed that as the mixing time period increased, more micro voids were formed. The addition of the clay increased the viscosity of the mixture and hindered complete degassing before molding. Especially, by the addition of more than 5 % clay, more micro voids were observed in the produced nanocomposites. Voids can also be resulted from trapped air during pouring of the viscous epoxy-clay mixture onto the mold. Although curing process was carried out under vacuum furnace, micro voids are not totally eliminated. Because of the micro voids, cracks can be initiated and can cause failure of the test specimen at lower strain values. Hence, it is very important to eliminate voids in the nanocomposite materials. Improved and more consistent tensile strength values can be accomplished by applying better degassing processes.

The aggregation of clay layers may also be another reason for the lower tensile strength values. At higher clay loading, unexfoliated nanoparticles may act as additional crack initiation sites by splitting up easily under applied load.

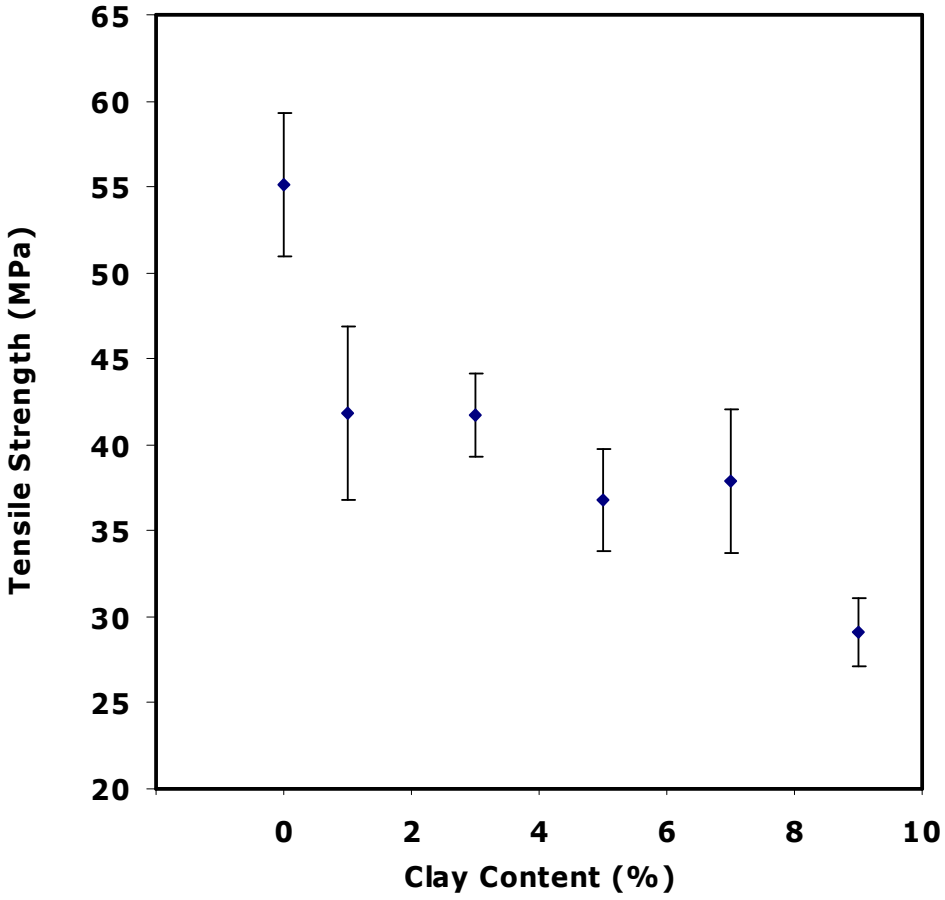

Figure 4.14 The tensile strength of the neat resin and nanocomposites with Cloisite 30B

The tensile modulus of the nanocomposites shown in Figure 4.15 has a maximum value with 5 wt.% clay addition. At this clay loading, Young's modulus value of nanocomposite is 26 % higher than that of pristine epoxy resin. This improvement in Young's modulus can be attributed to exfoliation and good dispersion of the clay particles in the matrix as well as to the good interfacial adhesion between the clay particles and the epoxy matrix. Up to 5 wt. % clay loading, mobility of the polymer chains can be restricted by well dispersed nanoclay particles and by the adhesion at polymer-clay interface. So, nanocomposite resin becomes stiffer and leading to higher modulus. Beyond 5 wt.% clay addition, the tensile modulus value of the nanocomposites decreased. This may have been resulted from lower degree of exfoliation. Unexfoliated aggregates of clay layers can lead to reduction in the Young's modulus value by splitting up under load. Moreover; addition of more than 5 wt.% clay may also lower the cross-link density. Hence, nanocomposite resin may become less stiff and polymer chains can move more easily. Consequently, this leads to a decrease in Young's modulus value. The stiffness value of clay particles is very high compared to the polymer matrix. As a result, by the rule of mixture, resultant nanocomposites would have higher stiffness than pure epoxy resin. On the other hand, the increase in stiffness can not be explained only by rule of mixture. There are some other factors affecting final nanocomposite properties. These are: aspect ratio of filler, volume ratio, direction of particles, adhesion between the clay and polymer.

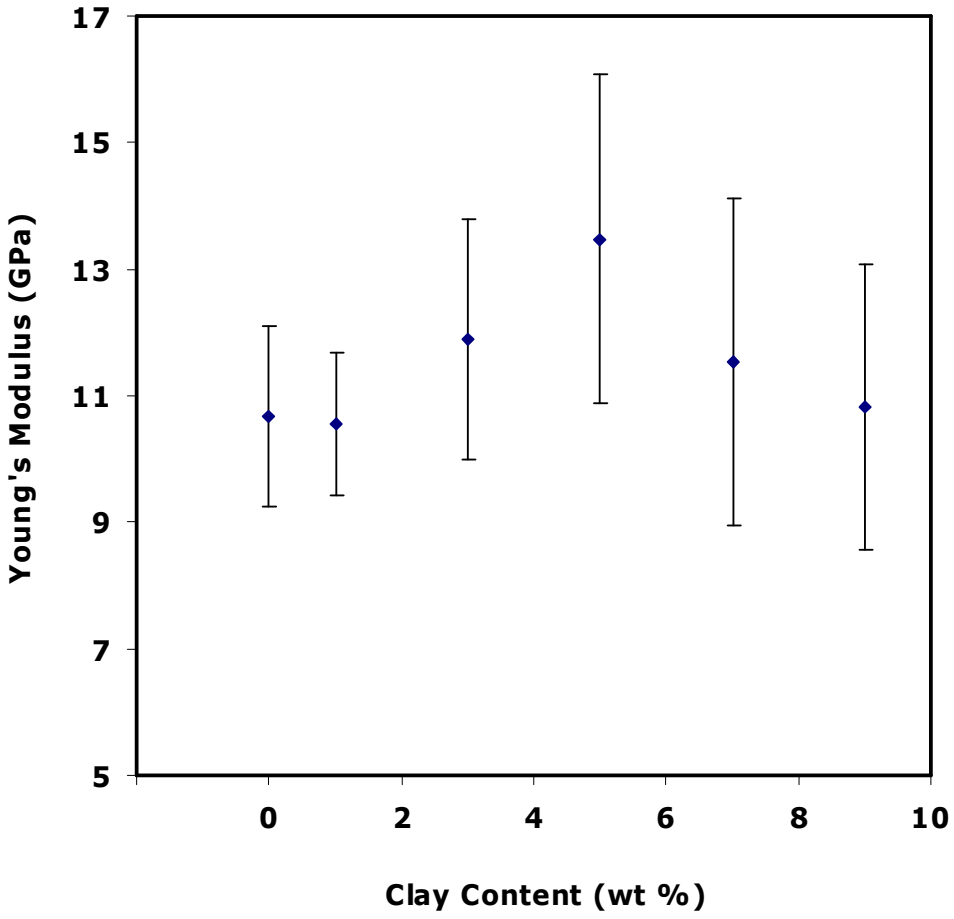

Figure 4.15 The Young's modulus of the neat resin and nanocomposites with Cloisite 30B

Strain at break values decreased by the addition of clay as shown in Figure 4.16. Stiffness of the clay particles is higher than that of epoxy resin, so the strain value at break can decrease by the clay addition. Beside this, with the addition of clay nanocomposite resins become more brittle because of micro voids and this may lead to failure of test specimens at relatively low strain at break values. Also, strain at break values are in a wide range. This may have resulted from cracks caused by several defects, since defects can act as crack initiation sites which can also lead the material to break at lower strain values than that of pristine epoxy. As stated before, unexfoliated clays may also act as crack initiator by splitting up under tensile loading.

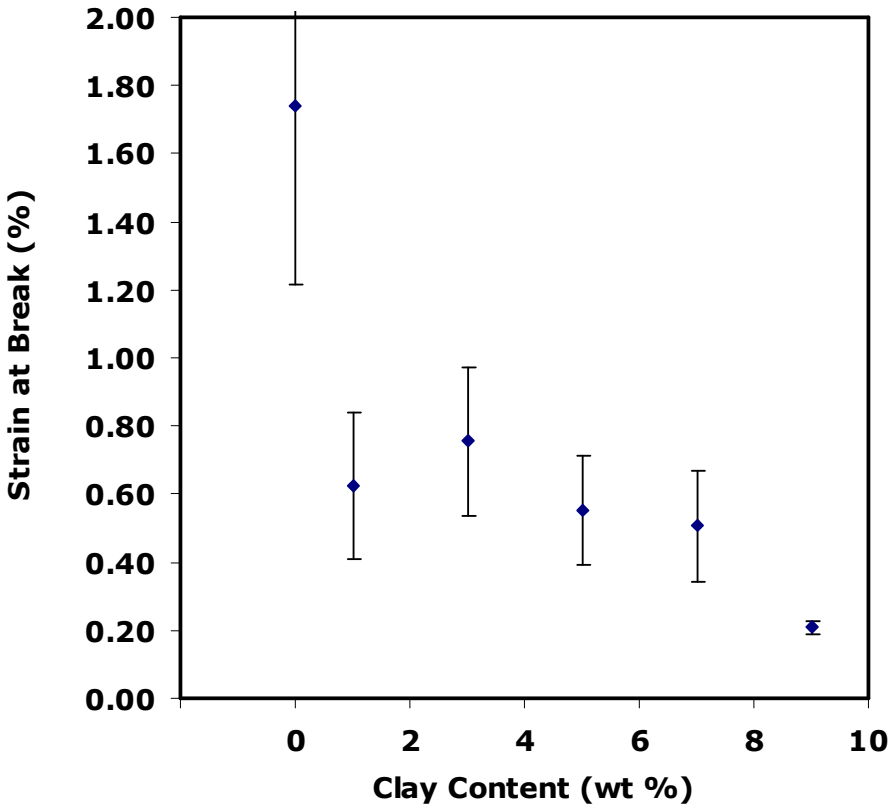

Figure 4.16 The tensile strain at break of the neat resin and nanocomposites with Cloisite 30B

4.2.2 Flexural Properties

The flexural strength, flexural modulus and flexural strain at break values of neat epoxy resin and epoxy/clay nanocomposites with different clay loading are shown in Figure 4.17 through 4.19 (see Appendix A.1.3). Flexural strength property exhibits similar trend with flexural strain property. They have a minimum value at 5 % clay loading. On the other hand, flexural modulus increases continuously.

Figure 4.17 shows the flexural strength values of nanocomposites with different Cloisite 30B contents. Flexural strength of the nanocomposites has a minimum value at 5 % clay loading. The flexural strength values exhibit similar behavior as seen in the tensile strength. At 5 % clay loading, flexural strength value is approximately 43 % lower compared to the flexural strength of the neat epoxy resin. Beyond this point, little increase is observed in the flexural strength values of the nanocomposites, but they are still lower than those of pristine epoxy resin. Reduction in the flexural strength values can be attributed to the incompatibility between the epoxy resin and clay particles. This can lead to poor bonding between the epoxy resin and nano particles. Hence, lower flexural strength values are obtained. If they were compatible, we would expect an increase in flexural strength value. Beside this, unexfoliated clay layers and some defects (voids, cracks) can cause premature failure of the nanocomposite resins as explained for the tensile strength behavior.

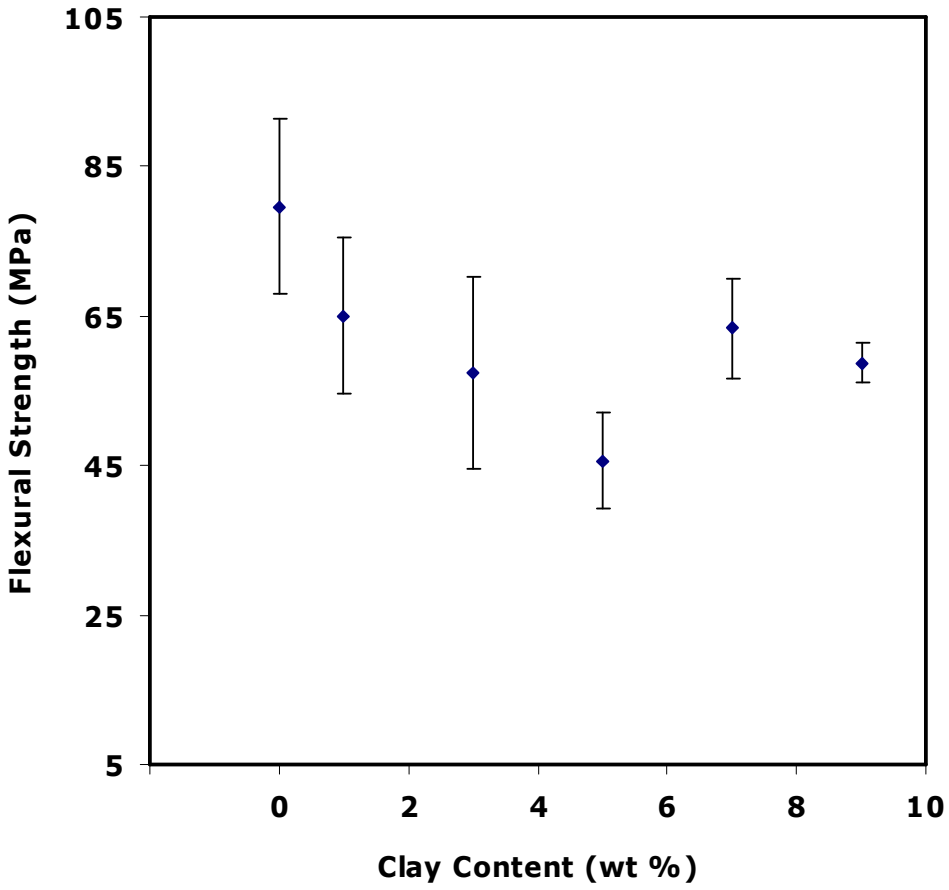

Figure 4.17 The flexural strength of the neat resin and nanocomposites with Cloisite 30B

Figure 4.18 shows the behavior of flexural modulus with clay loading. It was observed that the flexural modulus of the epoxy/clay nanocomposites increased continuously with increasing clay content. Maximum improvement was achieved at 9 % clay content. At this point, flexural modulus value increased about 48 % compared to the pure epoxy resin. The increase in flexural modulus can be attributed to exfoliation of Cloisite 30B particles in the epoxy resin. Exfoliation of clay particles increases rigidity in the resultant nanocomposite. The increase in the rigidity may lead to high flexural modulus of nanocomposite resin. In this study, although flexural modulus increases, flexural strength values decrease. Brittleness and crack initiation sites lead to lower flexural strength values as discussed before.

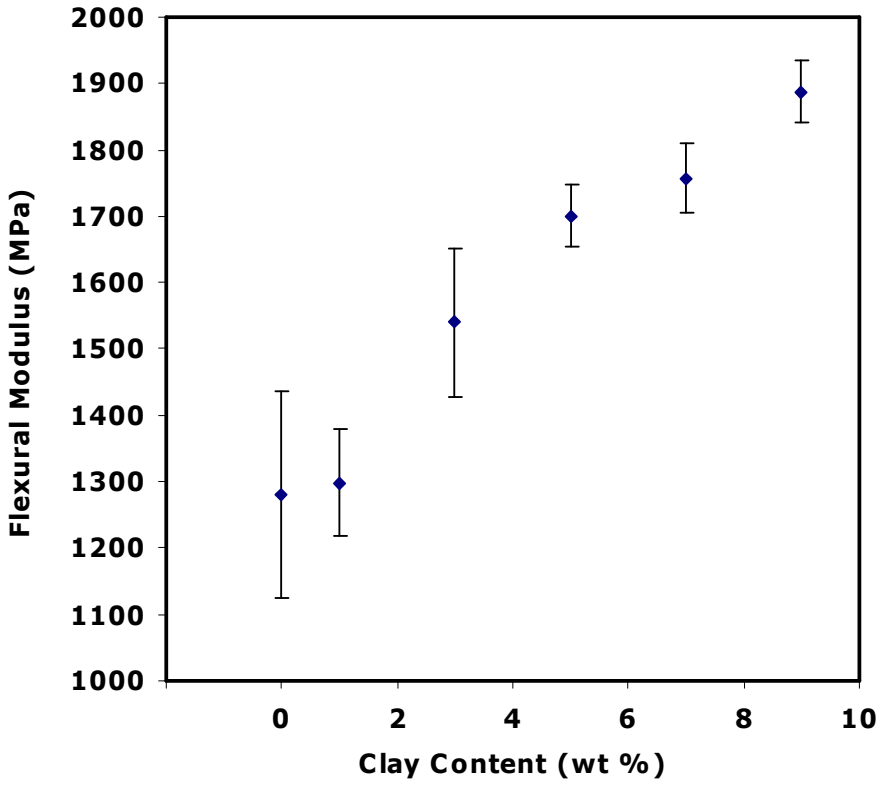

Figure 4.18 The flexural modulus of the neat resin and nanocomposites with Cloisite 30B

Flexural strain at break value of neat epoxy and nanocomposites are shown in Figure 4.19. As expected, the flexural strain exhibits similar behavior as the tensile strain. Flexural strain has a minimum value at 5 wt. % clay loading, then it slowly increases beyond this point. The flexural strain values also depend on the same factors as explained for the tensile strain.

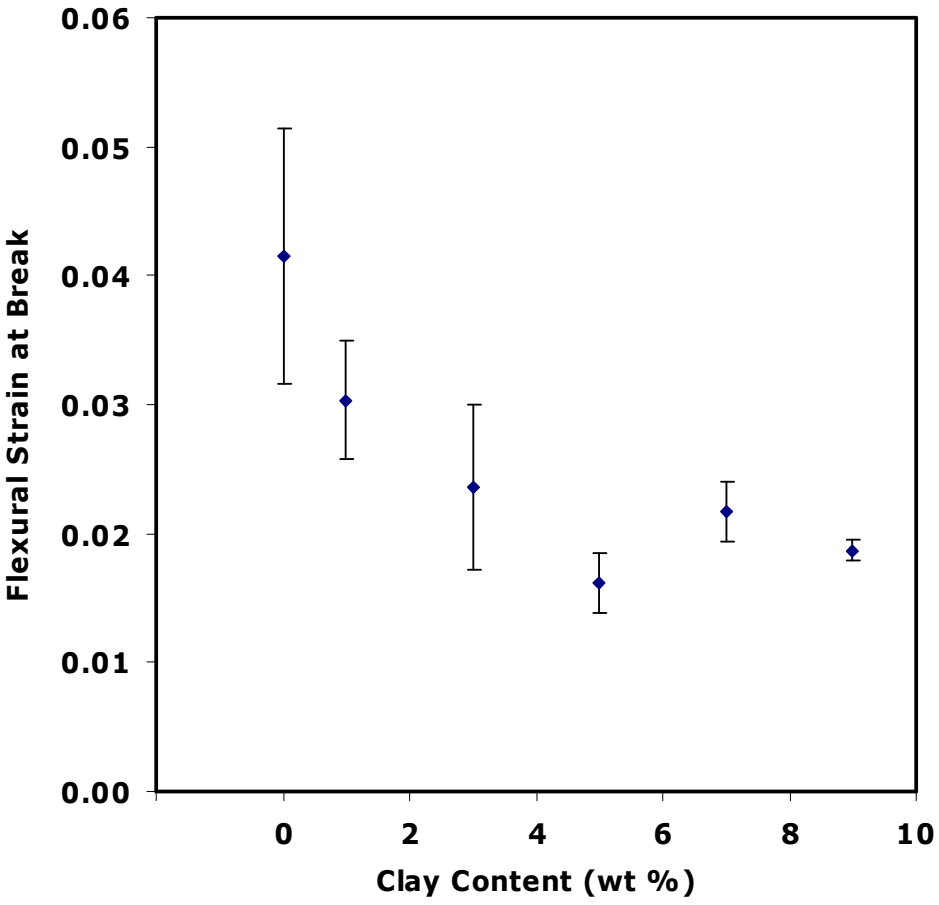

Figure 4.19 The flexural strain at break of the neat resin and nanocomposites with Cloisite 30B

4.2.3 Impact Strength

Impact strength values of the neat epoxy and epoxy/clay nanocomposites with different clay loadings are shown in Figure 4.20. Impact strength of the nanocomposites has similar behavior as their flexural strength.

Impact strength of the neat epoxy resin decreased continuously up to 7 wt.% clay loading. At this clay content, a minimum of 46 % deterioration in impact energy was obtained. Beyond this point, the impact energy showed an increasing trend. But, impact strength value with 9 wt.% clay content was still lower than that of the neat epoxy resin. The neat epoxy resin has the maximum impact strength. In this study, no improvement in impact strength was achieved by the addition clay.

Unexfoliated clay particles in the resin may lead to crack initiation sites and these cracks result with premature failure of test specimens. Also, there may be tiny voids as stated above that may also act as a crack initiator.

Above 7 % clay loading, clay particles may prevent the continuation of cracks. This can be achieved by formation of tortuous crack propagation path with clay particles in the nanocomposite. Hence, the impact energy value displays an increase. However, it is not enough to draw a conclusion with only one clay loading. So, additional experiments with higher clay loadings may help to draw more accurate conclusions.

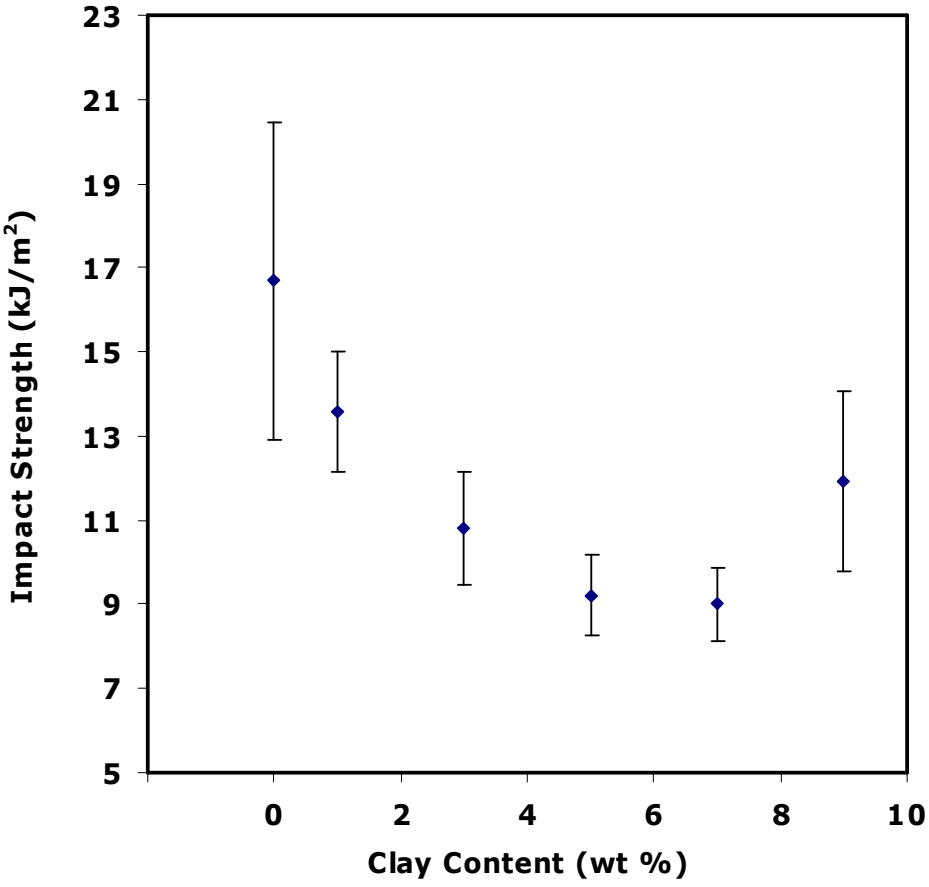

Figure 4.20 The impact strength of the neat resin and nanocomposites with Cloisite 30B

4.3 Thermal Analysis

4.3.1 Differential Scanning Calorimetry (DSC)

The glass transition temperatures (T_g) of neat epoxy resin and epoxy/clay nanocomposites were determined by differential scanning calorimeter (DSC). Figure 4.21 presents effects of the organoclay on the T_g of the developed nanocomposites. DSC analyses indicated that T_g of the cured nanocomposite resins decreased continuously with clay loading. On the other hand, in previous studies both reduction and increase have been observed in the T_g for different resin systems. The neat epoxy resin has T_g of 147 ^oC. Addition of 9% organoclay into the epoxy resin has an effect of lowering T_g to 129 ^oC. The decrease in the T_g with clay addition may be attributed to consumption of unreacted monomers on the surface of the clay particles. Hence, crosslink density decreases by increasing clay loading of the resin. Finally, reduction in the crosslink density may result in lower T_g. Also, consumption of the free radicals may lead to excess unreacted curing agent in resin system. The excess curing agent has the plasticization effect on the resin system. This may lead to a reduction in T_g value. Consumption of unreacted monomers in the galleries and entanglements can lead to reduction in T_g. DSC graphs of neat resin and nanocomposites are given in Appendix B.

The T_g of the nanocomposite systems are affected by both the bulk epoxy properties and epoxy-clay interaction. In the case of conventional composites, T_g of the system is the same as the T_g of the bulk matrix system. But in nanocomposites, motion of the epoxy monomers is restricted by clay layers. So, the T_g values with epoxy-clay interaction are different. Well exfoliated clay layers lead to the same or higher T_g values than the neat resin, but intercalated clay layers result with lower T_g values. The T_g of the nanocomposite system will be affected by the epoxy-clay interaction.

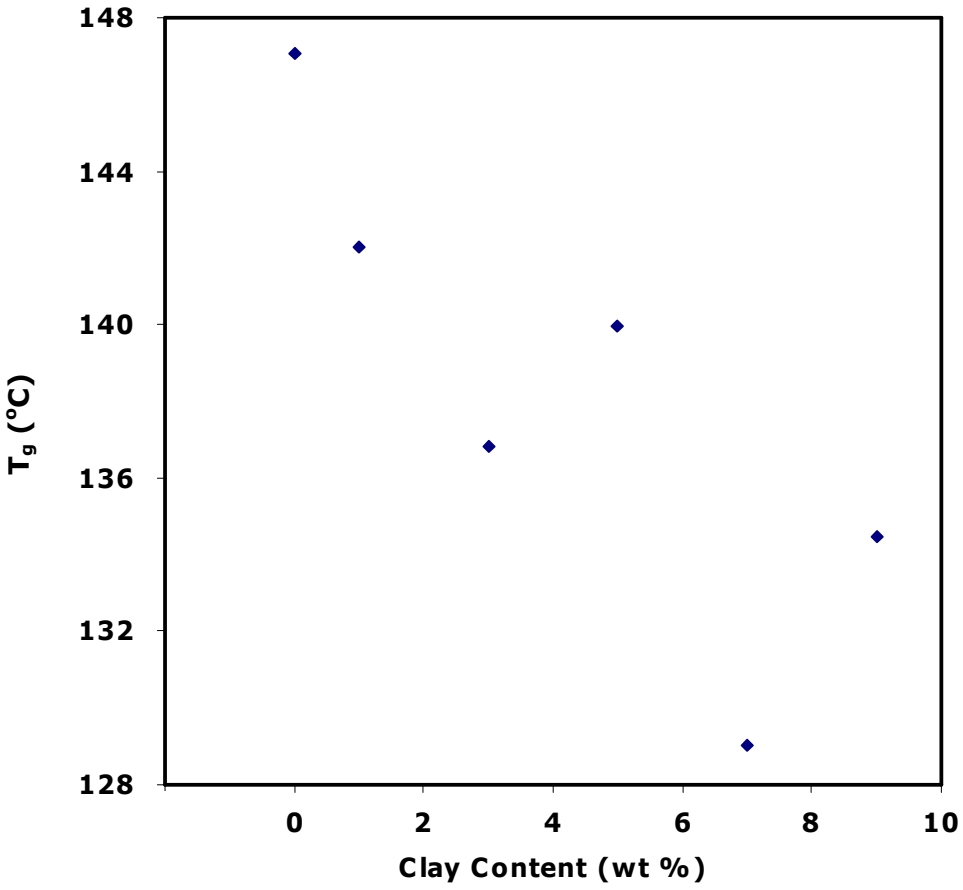

Figure 4.21 The glass transition temperature (T_g) of the neat resin and nanocomposites with Cloisite 30B

4.3.2 Thermogravimetric Analysis (TGA)

Thermal stability of epoxy/clay nanocomposites with different clay loadings were determined by thermogravimetric analyse (TGA) as shown in Figure 4.22 (see in Appendix C). Thermal stability is related with degradation of organoclay and epoxy resin. The initial decomposition temperature of pure epoxy resin was increased in the order of 5-10 ^{o}C by clay loading. Degradation resistance of epoxy resin was slightly improved by the addition of the organoclay up to 7% as shown in Table A-1. The initial decomposition temperature of the neat epoxy resin increased from 302^{o}C to 310^{o}C with 7% clay loading. This slight improvement may have been achieved by the barrier properties of the layered silicates and the tortuous path for the removal of volatile decomposition products preventing the diffusion out of decomposition products. Also, clay particles act as insulator reducing conduction heat transfer within the nanocomposite.

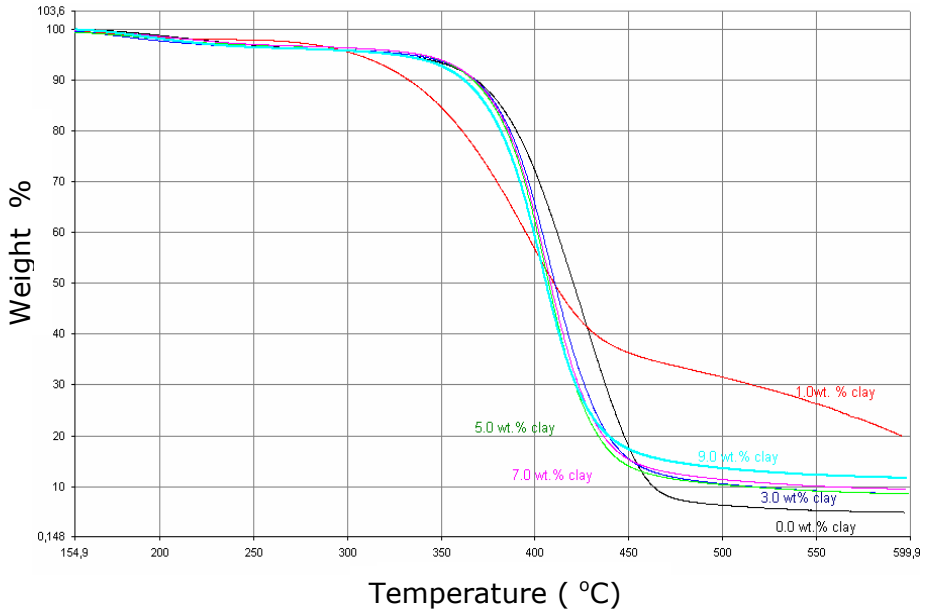

Figure 4.22 TGA thermograms of the neat resin and nanocomposites with Cloisite 30B

Initial decomposition temperature and the weight remaining after decomposition are shown in Table 4.3. After the decomposition of the epoxy/clay nanocomposite, char formation takes place. The weight remained shows the char formation after decomposition. Char acts as an insulator material and enhances decomposition temperature of the nanocomposite material. Clay loading has an effect of increasing the char formation. Neat epoxy resin has char formation of 4.94% whilst char formation is 11.68 % for nanocomposite with 9% clay content. The amount of char formation increases continuously with clay loading.

Table 4.3 Initial decomposition temperature and weight remaining after decomposition

Clay Content (%)	Initial Decomposition Temperature (^{o}C)	Weight Remaining (%)
0 %	302	4.94
1 %	270	6.18
3 %	294	8.63
5 %	304	8.57
7 %	310	9.52
9%	290	11.68

4.4 Flammability Properties

Vertical burning test according to ASTM D 3801-06 for neat epoxy resin and its nanocomposites were failed. The test specimens were burned up to the holding clamp. They did not self-extinguish. The neat epoxy resin used in the study was very flammable by itself. Also, organoclay (Cloiste 30B) addition does not change the flammability

property of neat epoxy resin. Neat epoxy resin drips on to the cotton during burning. But, polymer dripping decreases by the addition of organoclay. Amount of char formed after burning increases by increasing clay content. Char formation is promoted by the organoclay and acts as a binder between the clay platelets. This prevents the dripping of the nanocomposite resin.

During the combustion of the neat epoxy resin, a little bubbling was observed. These bubbles include degradation products of the epoxy resin. Addition of the organoclay decreases bubbling of the epoxy resin, because char formed during burning may also act as a heat insulator and mass transfer barrier. Hence, release of degredation products slows down.

Flammability characteristics of nanocomposites also depend on the degree of exfoliation and the distribution of nanoclays within the polymeric matrix. But, here because the neat epoxy resin is very flammable, clay addition between 0 and 9 wt% is not sufficient to have self-extinguishing materials. At high clay concentration, flammability of epoxy resin may be decreased to a reasonable level. As a result, the epoxy-clay (Cloisite 30B) nanocomposite developed here is not useful because of their high flammability.

CHAPTER 5

CONCLUSIONS

Epoxy/clay nanocomposites were prepared by in-situ polymerization and characterized by mechanical tests (tensile, flexural, impact), morphological analysis (WAXD, SEM), thermal analysis (TGA, DSC) and flammability test. The test results of the synthesized nanocomposites are compared with those of neat epoxy resin.

SEM micrographs indicated that the best degree of dispersion was achieved at 1 wt.% clay loading. Beyond this point, agglomerated structures were observed in the micrographs.

XRD patterns showed that exfoliated structures were achieved at 1 wt. % clay content. At 3 wt. % clay loading, intercalated nanocomposites were achieved. When clay addition is higher than this point, agglomerated structures were observed. Two peaks appearing at 5, 7 and 9 wt. % clay contents show the presence of agglomerated Cloisite 30B and intercalated clay structures.

Tensile strength and tensile strain at break values of nanocomposites exhibited no improvement with clay addition. These values decreased steadily with clay loading. On the other hand, Young's modulus increased with clay content and a maximum was achieved at 5 wt. % clay loading. Beyond this point, Young's modulus started to decrease. Impact strength values exhibited no improvement with respect to neat epoxy resin. It has a minimum at 7 wt. % clay content and then increases a little, but the value is still lower than that of neat epoxy resin. Flexural strength property exhibited similar trend with the flexural strain property. They both have a minimum value at 5 % clay

loading. On the other hand, flexural modulus increased continuously. Mechanical properties of composites with organoclay exhibited improvement only for flexural modulus and tensile modulus. Clay particles have higher modulus than the epoxy resin, hence the resultant nanocomposites also have a higher modulus than the resin.

T_g value and thermal stability values were not affected much with the clay addition. T_g of the cured nanocomposite resins decreased little with clay loading. Initial decomposition temperature of epoxy resin was slightly improved by the addition of the organoclay up to 7%. The amount of char formation increased continuously by increasing clay content. There is no improvement in flammability properties of the epoxy-clay nanocomposites. They are as flammable as the neat epoxy resin. However, total burning time decreased slightly. Amount of clay loading may be insufficient to have a self-extinguishing material.

Epoxy-clay nanocomposite material was achieved by in-situ polymerization. The final properties of resultant epoxy-clay nanocomposites were not improved as much as expected. This type of epoxy resin (suitable for the filament winding process) is not convenient to have nanocomposites having improved properties. A new study is required by proper selection of epoxy system and/or nano filler.

REFERENCES

[1] Wing Mai, Y., Zhen Yu, Z., *Polymer Nanocomposites*, Woodhead Publishing Limited, 29-54 (2006)

[2] Chen, C., Khobaib, M., Curliss, D., *Epoxy Layered-Silicate Nanocomposite*, Progress in Polymer Coatings 47, 376 -383 (2003)

[3] Liu, W., Hoa, S.V., Pugh, M., *Organoclay-Modified High Performance Epoxy Nanocomposites*, Composite Science and Technology, 65, 307-316 (2005)

[4] Ratna, D., Becker, O., Krishnamurthy, R., Simon, G.P., Varley, R.J., *Nanocomposites Based on a Combination of Epoxy Resin, Hyperbranched Epoxy and Layered Silicate*, Polymer 44, 7449-7457 (2003)

[5] Isik, I., Yilmazer, U., Bayram, G., *Impact Modified Epoxy/Montmorillonite Nanocomposite: Synthesis And Characterization*, Polymer, 44, 6371-6377 (2003)

[6] Inceoglu, A.B., Yilmazer, U., *Synthesis and Mechanical Properties of Unsaturated Polyester Based Nanocomposites*, Polymer Engineering and Science, 43, 661-669 (2003)

[7] Park, S.-J., Seo, D.-I., Lee, J.-R., *Surface Modification of Montmorillonite on Surface Acid-Base Characteristics of Clay and Thermal Stability of Epoxy/ Clay Nanocomposites,* Journal of Colloid and Interface Science 251, 160-165 (2002)

[8] Guo, B., Jia, D., Cai, C., *Effects Of Organo-Montmorillonite Dispersion on the Thermal Stability of Epoxy Resin Nanocomposites*, European Polymer Journal 40, 1743-1748 (2004)

[9] Morgan, A.B., Harris, J.D., *Effects of Organoclay Soxhlet Extraction on Mechanical Properties, Flammability Properties and Organoclay Dispersion of Polypropylene Nanocomposites*, Polymer, 44, 2313 – 2320 (2003)

[10] Kohlhass, K.M., Stach, E.A., Stankovich, S., Ruoff, R.S., *Transmission Electron Microscopy of Polymer-graphene Nanocomposites*, Microsc Microanal (2006), 12

[11] Usuki, A., Kawasumi, M., Kojima, Y., Okada, A., Kuruachi, T., Kamigaito, O., S*welling Behaivor of Montmorillonite Cation Exchanged*

for ω-amino Acids by ε-caprolactam, Journal of Material Research, (1993);8:1174-8

[12] Gorrasi, G., Tortora, M., Vittoria, V., Pollet, E., Bénédicte, L., Alexandre, M., Dubois, P., *Vapor Barrier Properties of Polycaprolactone Montmorillonite Nanocomposites: Effect of Clay Dispersion,* Polymer, Vol. 44, 2271-2279 (2003)

[13] Miyagama, H., Rich, M.J., Drzal, L.T., *Amine Cured Epoxy/clay nanocomposites: I. Processing and Chemical Characterization*, Journal of Polymer Science Part B: Polymer Physics, Vol. 42, (2004), pp:4384-4390

[14] Miracle, D. B., Donaldsan, S.L., *Introduction to Composites, ASM Handbook, Vol. 21,* ASM International Online, (2003)

[15] Akovali, G., *Handbook of Composite Fabrication*, Rapra Technology, Limited, Shawbury, (2001)

[16] Kelly, A., *Concise Encyclopedia of Composite Materials*

[17] Sheldon, R. P.*, Composite Polymeric Materials,* Elsevier Science, New York, (1982)

[18] Davis, J.R., Davis & Associates, *Applications of Ceramic-Matrix Composites,* ASM Handbook, Vol. 21, ASM International Online, (2003)

[19] Miller, T.E., *Introduction to Composites, 4th Ed.,* Composites Institute, New York, 1990

[20] Pilato, L.A., Michno, M.J., *Advanced Composite Materials*, Springer-Verlag, Berlin, (1994)

[21] Linda L., *Polymer Science for Engineer,* C & C Technologies

[22] Billmeyer, F.W., *Textbook of Polymer Science,* Wiley-Interscience Publication, New York, (1984)

[23] Challa, G., *Polymer Chemistry: An Introduction,* Ellis Horwood Limited, New York, (1993)

[24] Hart, H., Hart, D.J., Craine, L.E., *Organic Chemistry*, Ninth Edition, Houghton Mifflin Company (1995)

[25] Seymour, R. B., *Polymer Composites*, Utrecht, the Netherlands, (1990)

[26] Okamoto M., *Polymer/Layered Silicates*, Rapra Review Reports, Vol. 14, (2003)

[27] Xanthos, M., *Functional Fillers for Plastics*, WILEY-VCH Verlag GmbH&Co. KGaA (2005)

[28] Gao, F., *Clay/Polymer Composites: The Story,* Materials Today, (2004)

[29] Fisher, L. W., *Selection of Engineering Materials and Adhesives*, Taylor & Francis Group (2005)

[30] ASTM D 638: *Standard Test Method for Tensile Properties of Plastics*, USA (2003)

[31] ASTM D 790: *Standard Test Methods for Flexural Properties of Unreinforced and Reinforced Plastics and Electrical Insulating Materials*, USA (1995)

[32] http://www.matweb.com/reference/flexuralstrength.asp

[33] ISO 179-1: *Plastics - Determination of Charpy Impact Properties*, USA (2000)

[34] http://us.mt.com/mt/userCom/TA_UserCom13_0240929710242401.jsp

[35] http://hekabe.kt.dtu.dk/~vigild/2005_04_melitek/dsc.htm

[36] Jenkins, R., Snyder, R., *Introduction to X-Ray Powder Diffractometry,* John Wiley, (1996)

[37] Chen C., Curliss D., *Processing and Morphological Development of Montmorillonite Epoxy Nanocomposites*, Nanotechnology (2003); 14, 643,48

[38] Nigam, V., Setua, D.K., Mathur, G.N., Kar,K.K., "*Epoxy –MMT Clay Nanocomposites: Synthesis and Characterization*", Journal of Applied Polymer Science (2004), Vol 93, pp:2201-2210

[39] Chen, K.H., Yang, S.M., *Synthesis of Epoxy-Montmorillonite Nanocomposite*, Journal of Applied Polymer Science (2002), vol 86, pp:414-421

[40] Salahuddin, N.A., Lay*ered Silicate/epoxy Nanocomposites: Synthesis, Characterization and Properties*, Polymers for Advanced Technologies 15, (2004), pp:251-259

[41] Seo, K.S., Kim, D.S., *Curing Behavior and Structure of the Epoxy/Clay Nanocomposite*, Polymer Engineering and Science, (2006), pp:1318-1325

[42] Yasmin, A., Abot, J.L., Daniel, I.M., *Processing of Clay/epoxy Nanocomposites by Shear Mixing*, Scripta Materialia 49, (2003), pg: 81-86

[43] Becker, O., Varley, R.J., Simon, G.P., *Thermal Stability and Water Uptake of High Performance Epoxy Layered Silicate Nanocomposites*, European polymer journal 40, (2004), pp:187-195

APPENDIX A

A.1. Tensile Test Results for All Samples

Table A1.1 Tensile strength test results for all samples

No	Tensile Strength (MPa)					
	Neat Resin	1 wt.%	3 wt.%	5 wt.%	7 wt.%	9 wt.%
1	62.59	43.94	43.64	35.66	45.93	23.08
2	56.56	49.70	35.15	30.00	38.58	31.59
3	59.47	57.97	39.41	39.33	29.26	35.44
4	50.06	28.04	41.83	44.57	36.39	29.68
5	41.95	32.79	45.30	40.99	51.89	27.60
6	65.56	37.69	49.47	30.25	30.88	30.29
7	49.42	42.89	37.36	-	32.45	26.22
Average	55.09	41.86	41.74	36.80	37.91	29.13
Standard Deviation	4.17	5.07	2.45	2.96	4.17	1.99

Table A1.2 Young's modulus test results for all samples

No	Modulus (GPa)					
	Neat Resin	1 wt.%	3 wt.%	5 wt.%	7 wt.%	9 wt.%
1	9.01	8.37	13.96	7.80	3.31	6.97
2	7.49	11.16	16.18	15.93	14.09	10.33
3	15.76	12.01	7.33	12.72	9.38	11.45
4	9.79	15.26	9.76	9.24	10.00	19.36
5	10.57	10.66	15.36	12.90	16.61	9.31
6	11.46	11.24	8.53	22.28	16.77	7.55
7	-	5.17	12.13	-	10.60	-
Average	10.68	10.55	11.89	13.48	11.54	10.83
Standard Deviation	1.42	1.12	1.89	2.59	2.59	2.25

Table A1.3 Tensile strain at break results for all samples

No	Tensile Strain at Break %					
	Neat Resin	**1 wt.%**	**3 wt.%**	**5 wt.%**	**7 wt.%**	**9 wt.%**
1	1.23	1.00	0.86	1.15	0.72	0.17
2	0.58	0.86	0.53	0.30	0.22	0.20
3	2.04	1.19	0.62	0.36	1.00	0.25
4	3.67	0.31	0.83	0.62	0.42	0.20
5	1.48	0.25	0.48	0.55	0.34	0.14
6	1.45	0.22	1.67	0.34	0.14	0.23
7		0.55	0.30		0.72	0.25
Average	1.74	0.62	0.76	0.55	0.51	0.21
Standard Deviation	1.05	0.39	0.45	0.32	0.31	0.04

A.2 Flexural Test Results for All Samples

Table A2.1 Flexural strength test results for all samples

No	Flexural Strength (MPa)					
	Neat Resin	1 wt.%	3 wt.%	5 wt.%	7 wt.%	9 wt.%
1	42.46	49.87	44.56	44.60	57.12	58.80
2	82.75	56.78	96.61	26.78	78.59	61.41
3	93.40	64.71	43.22	41.36	63.37	60.49
4	99.25	70.06	80.06	38.47	73.84	49.36
5	38.74	34.61	76.53	41.10	58.28	57.67
6	101.93	60.92	90.48	59.11	37.80	64.12
7	99.73	83.58	26.48	39.14	57.02	49.39
8	81.20	65.93	43.78	73.05	84.94	61.41
9	92.39	52.54	37.87	51.23	62.03	65.56
10	64.89	111.34	33.88	41.40	60.76	59.41
Average	79.67	65.03	57.35	45.63	63.38	58.76
Standard Deviation	8.02	12.37	7.42	4.56	5.41	4.90

Table A2.2 Flexural modulus test results for all samples

No	Flexural Modulus (MPa)					
	Neat Resin	1 wt.%	3 wt.%	5 wt.%	7 wt.%	9 wt.%
1	1624.3	1023.4	1715.5	1696.0	1613.6	1871.6
2	1433.4	1340.0	1446.5	1659.7	1796.4	1902.1
3	825.6	1316.2	1793.8	1632.2	1701.9	1822.8
4	947.5	1126.3	1126.4	1797.9	1697.0	1880.9
5	1506.6	1440.0	1259.7	1658.3	1692.6	1889.6
6	1107.9	1529.7	1691.4	1878.7	1687.2	1932.2
7	1162.7	1215.8	1726.2	1583.7	1946.9	1835.7
8	1599.3	1196.4	1555.0	1612.5	1703.8	1727.6
9	970.5	1313.2	1409.3	1690.7	1858.3	2083.6
10	1626.2	1481.0	1683.4	1798.5	1870.8	1931.9
Average	1280.4	1298.2	1540.7	1700.8	1756.8	1887.8
Standard Deviation	155.6	80.2	111.7	47.3	52.7	45.8

Table A2.3 Flexural strain at break results for all samples

No	Flexural Strain at Break %					
	Neat Resin	**1 wt.%**	**3 wt.%**	**5 wt.%**	**7 wt.%**	**9 wt.%**
1	0.0157	0.0292	0.0156	0.0158	0.0212	0.0188
2	0.0346	0.0254	0.0401	0.0097	0.0263	0.0194
3	0.0679	0.0295	0.0145	0.0152	0.0223	0.0199
4	0.0628	0.0373	0.0426	0.0128	0.0261	0.0157
5	0.0154	0.0144	0.0365	0.0149	0.0207	0.0183
6	0.0552	0.0239	0.0321	0.0189	0.0134	0.0199
7	0.0515	0.0412	0.0092	0.0148	0.0176	0.0161
8	0.0305	0.0331	0.0169	0.0272	0.0299	0.0213
9	0.0571	0.0240	0.0161	0.0182	0.0200	0.0189
10	0.0239	0.0451	0.0121	0.0138	0.0195	0.0185
Average	0.0415	0.0303	0.0236	0.0161	0.0217	0.0187
Standard Deviation	0.0099	0.0046	0.0064	0.0023	0.0024	0.0008

A.3. Impact Test Results for All Samples

Table A3.1 Impact strength test results for all samples

No	Impact Strength (kJ/m2)					
	Neat Resin	**1 wt.%**	**3 wt.%**	**5 wt.%**	**7 wt.%**	**9 wt.%**
1	28.58	15.00	14.65	8.88	8.03	5.33
2	17.38	13.48	9.30	12.23	11.78	12.00
3	8.35	11.05	8.03	9.88	7.23	16.95
4	12.73	10.70	12.38	7.65	9.23	13.95
5	16.38	17.58	9.75	7.48	8.78	11.45
Average	16.68	13.56	10.82	9.22	9.01	11.94
Standard Deviation	3.77	1.43	1.33	0.97	0.86	2.14

APPENDIX B

DSC Graphs of Neat Epoxy Resin and its Nanocomposites

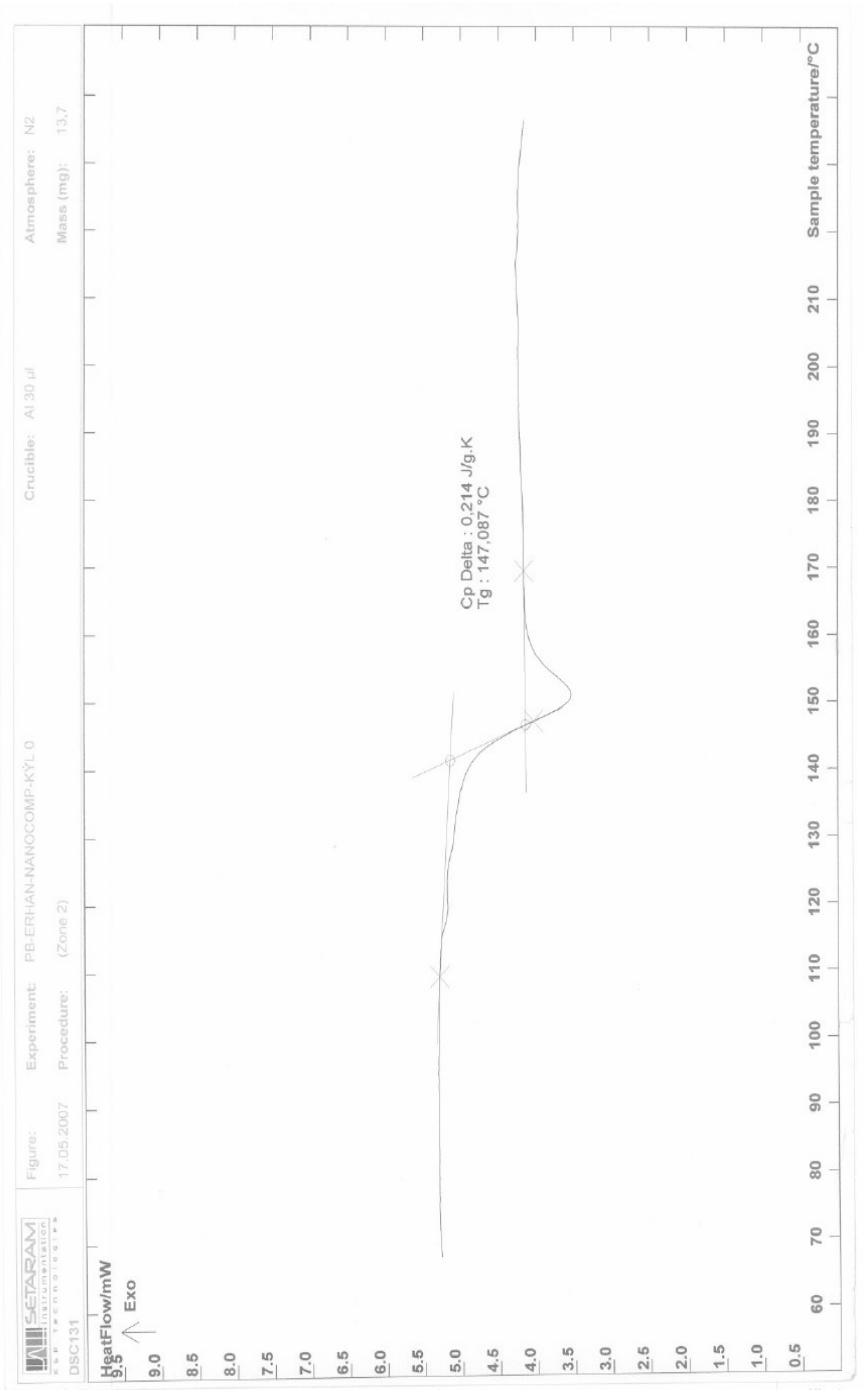

Figure B1. DSC graph of neat epoxy resin

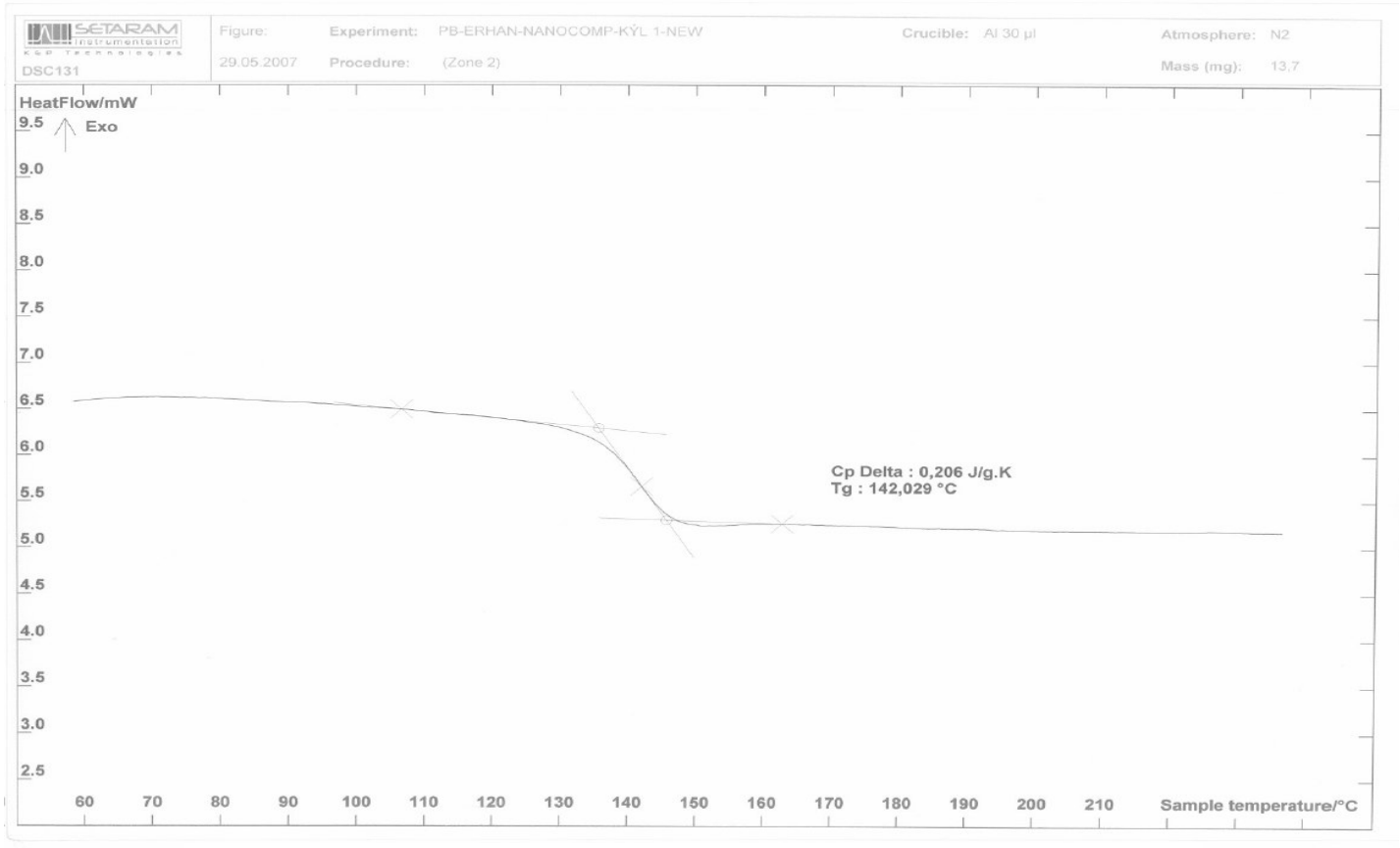

Figure B2. DSC graph of nanocomposite with 1 weight % Cloisite 30B

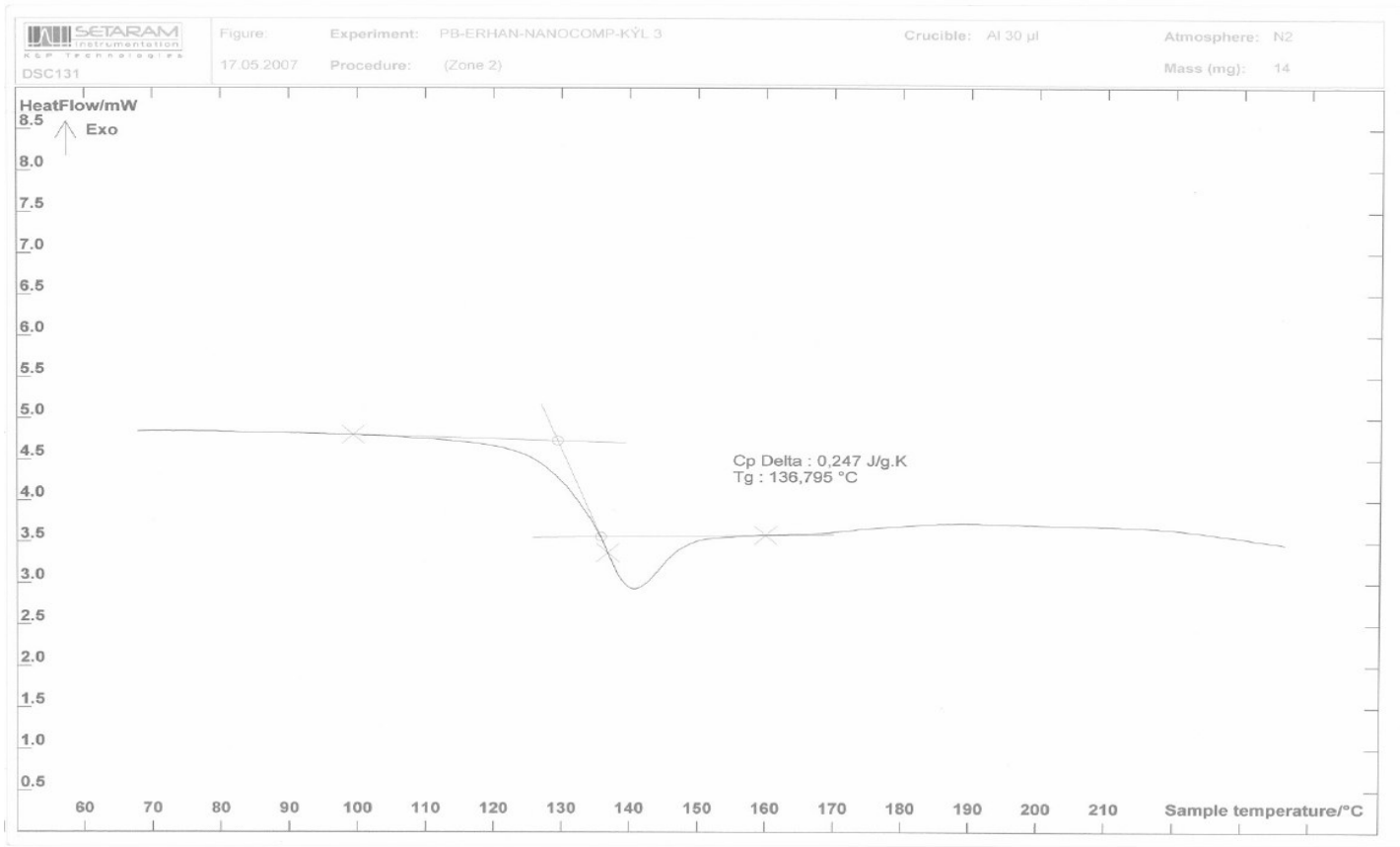

Figure B3. DSC graph of nanocomposite with 3 weight % Cloisite 30B

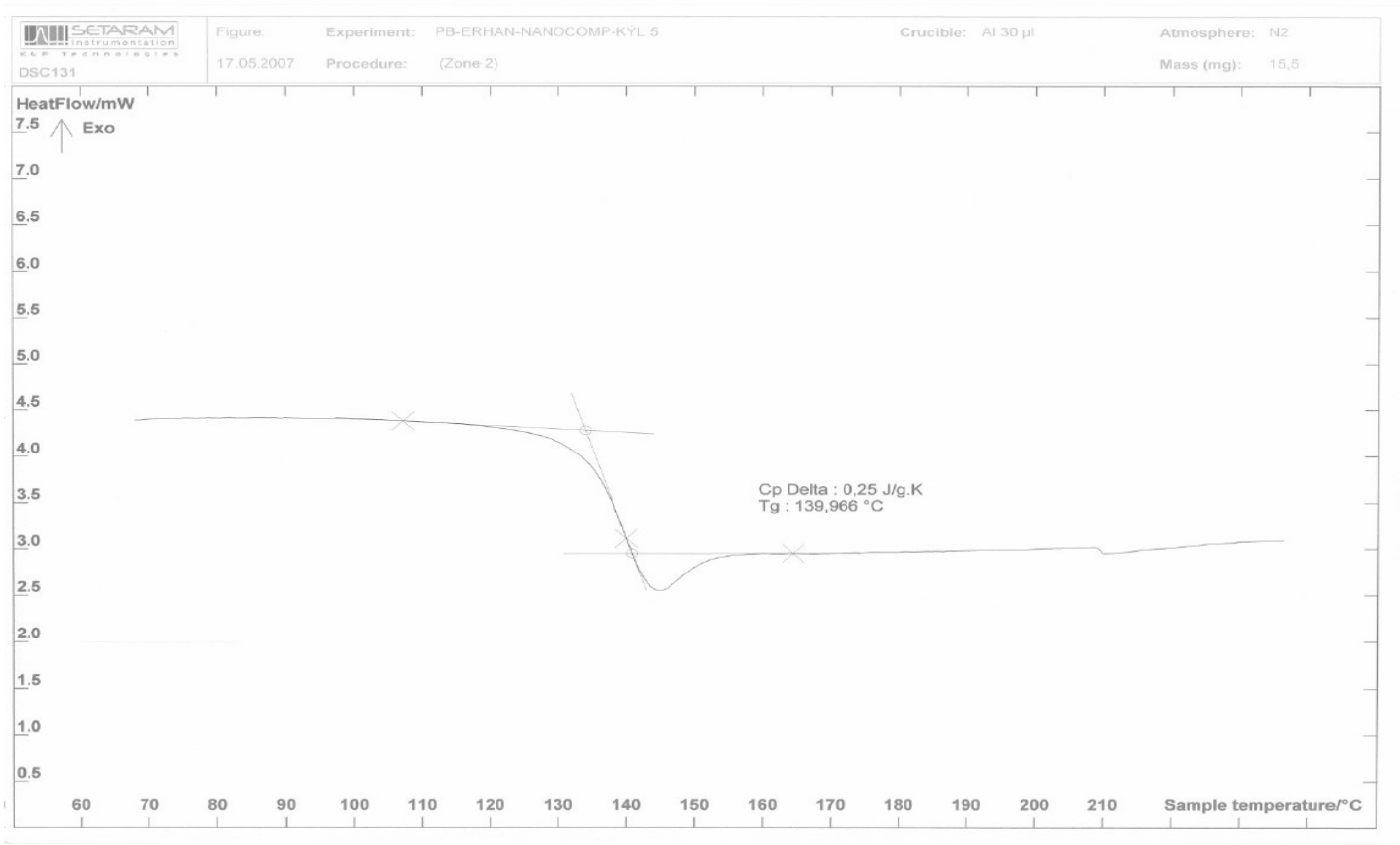

Figure B4. DSC graph of nanocomposite with 5 weight % Cloisite 30B

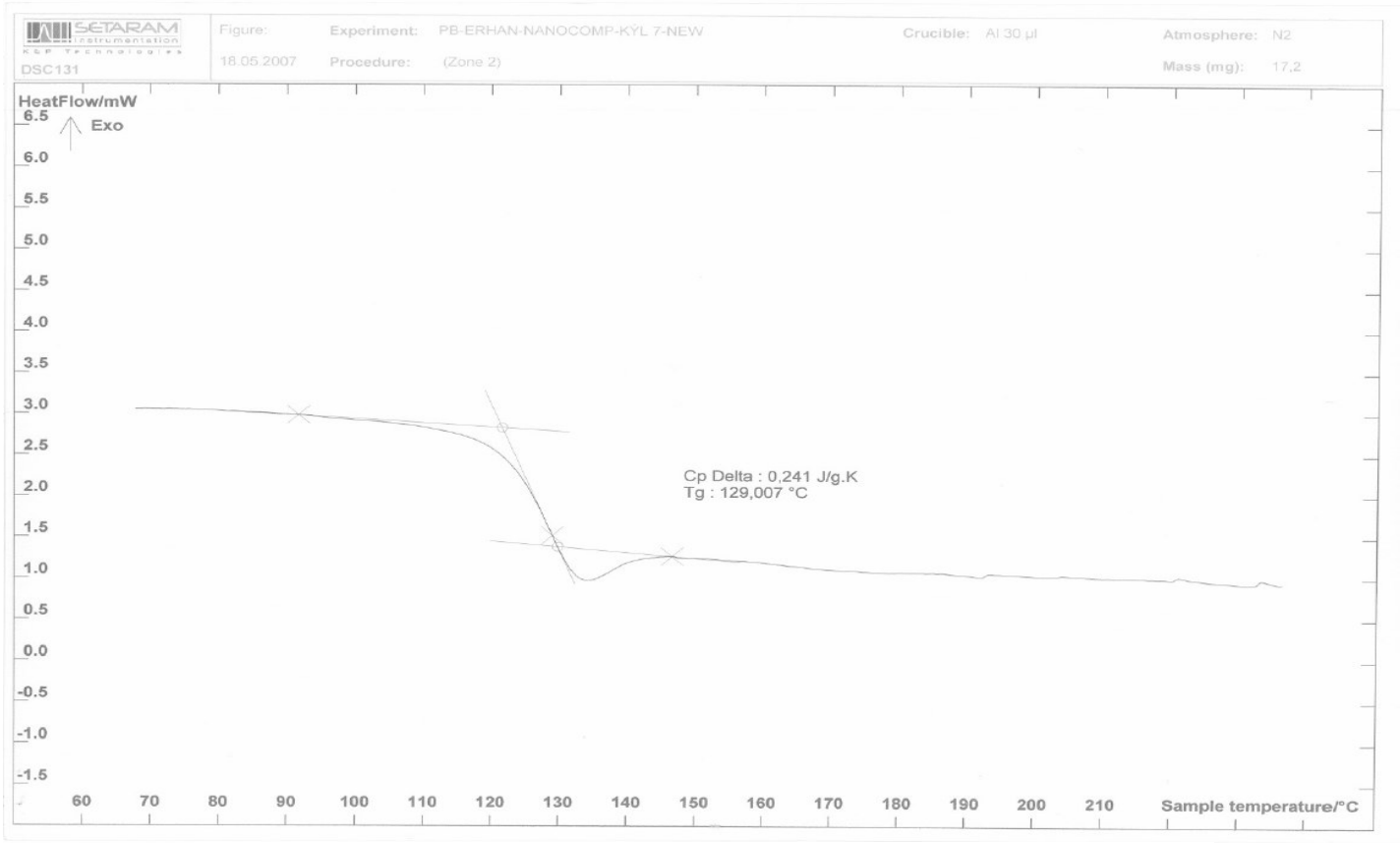

Figure B5. DSC graph of nanocomposite with 7 weight % Cloisite 30B

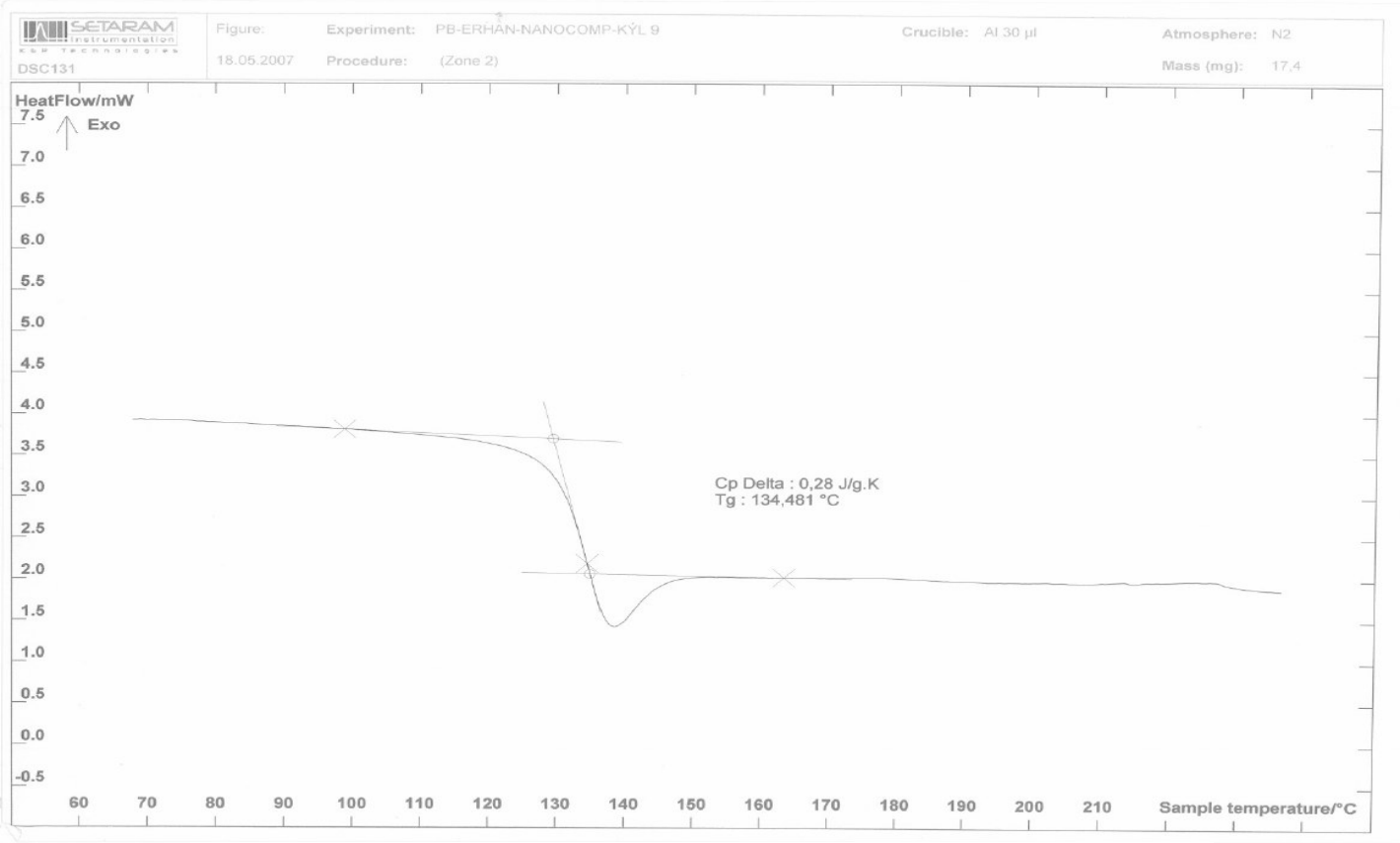

Figure B6. DSC graph of nanocomposite with 9 weight % Cloisite 30B

APPENDIX C

TGA Thermograms of Neat Epoxy Resin and its Nanocomposites

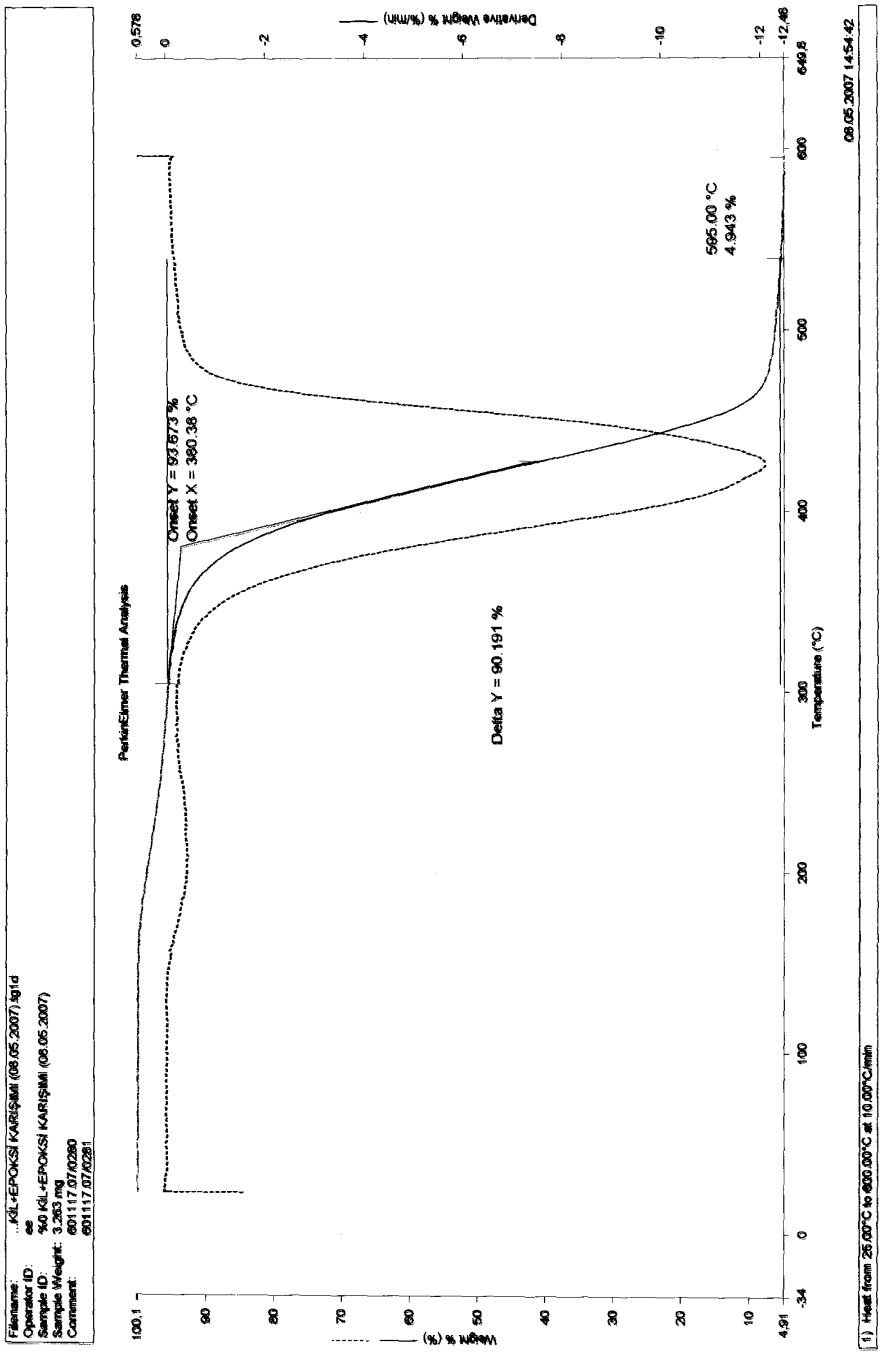

Figure C1. TGA thermogram of neat epoxy resin

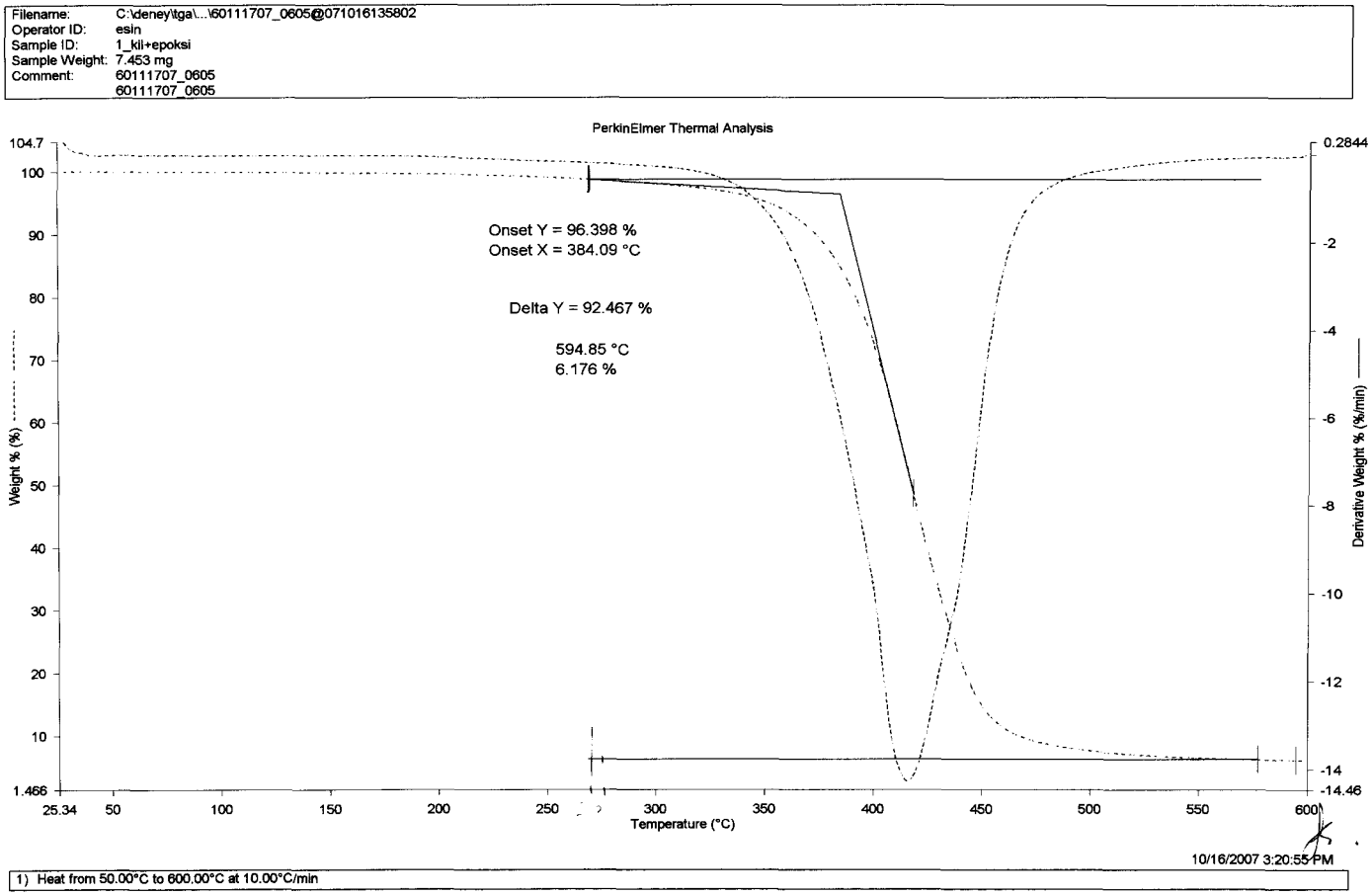

Figure C2. TGA thermogram of nanocomposite with 1 weight % Cloisite30B

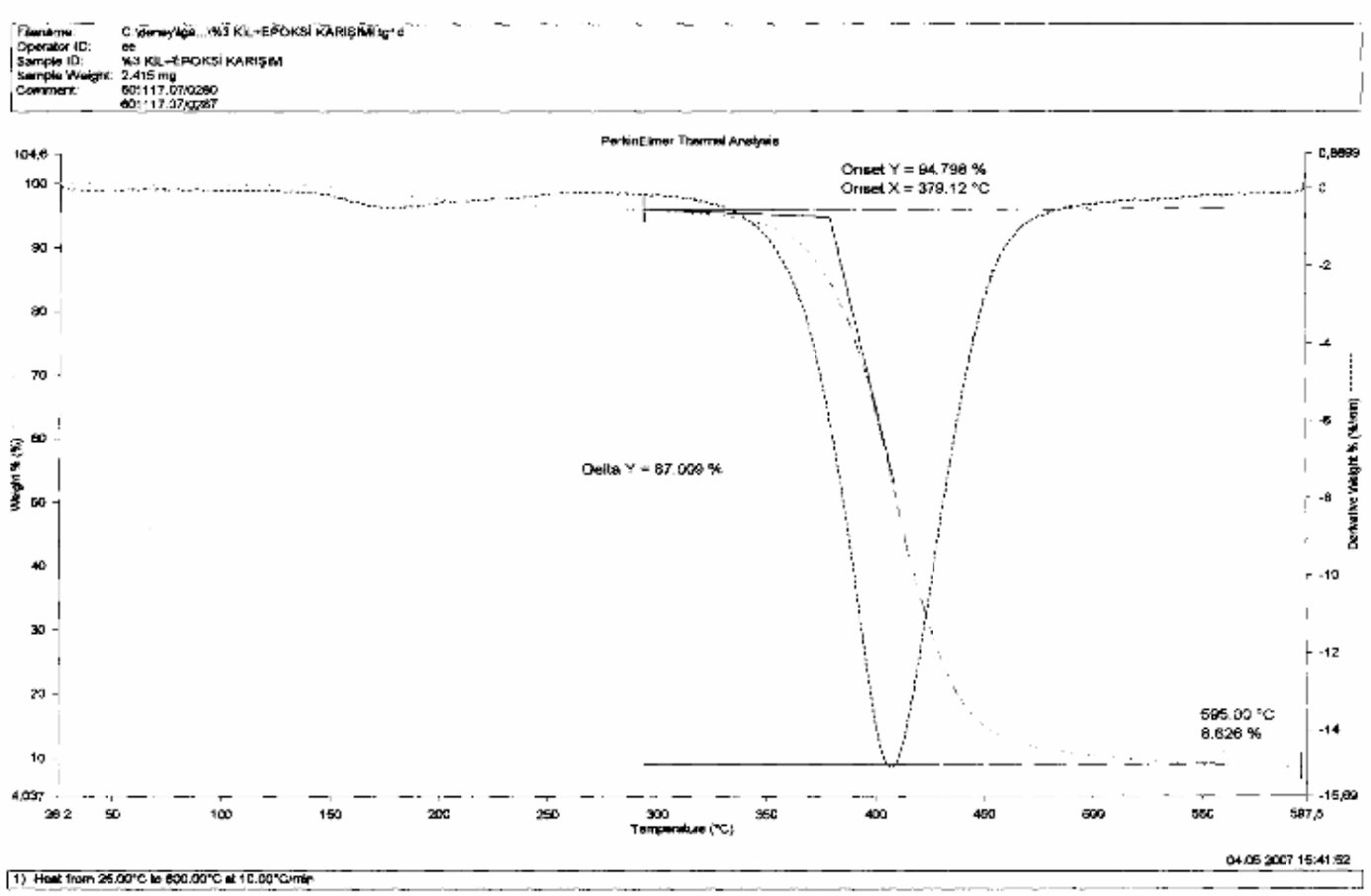

Figure C3. TGA thermogram of nanocomposite with 3 weight % Cloisite30B

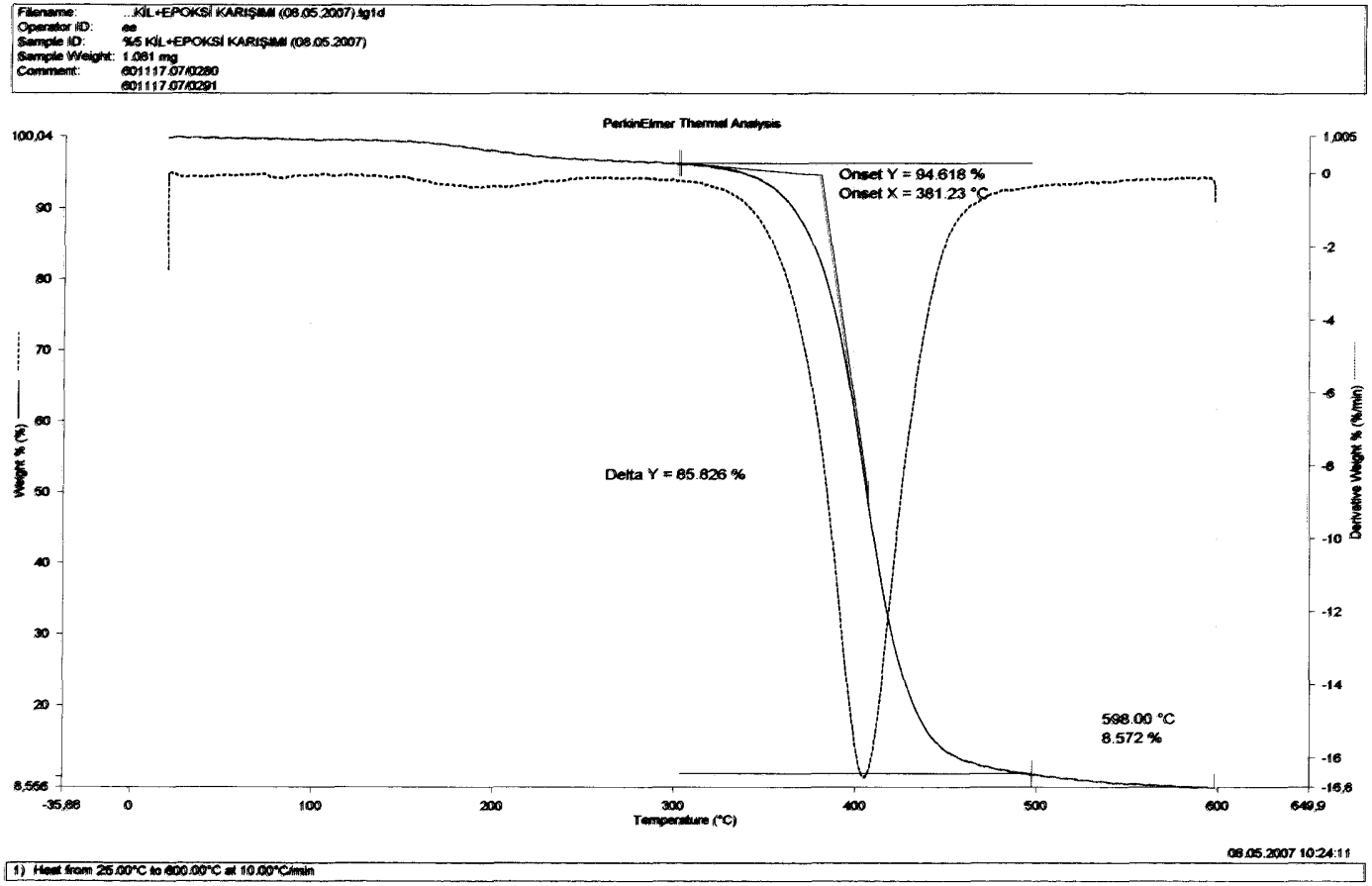

Figure C4. TGA thermogram of nanocomposite with 5 weight % Cloisite30B

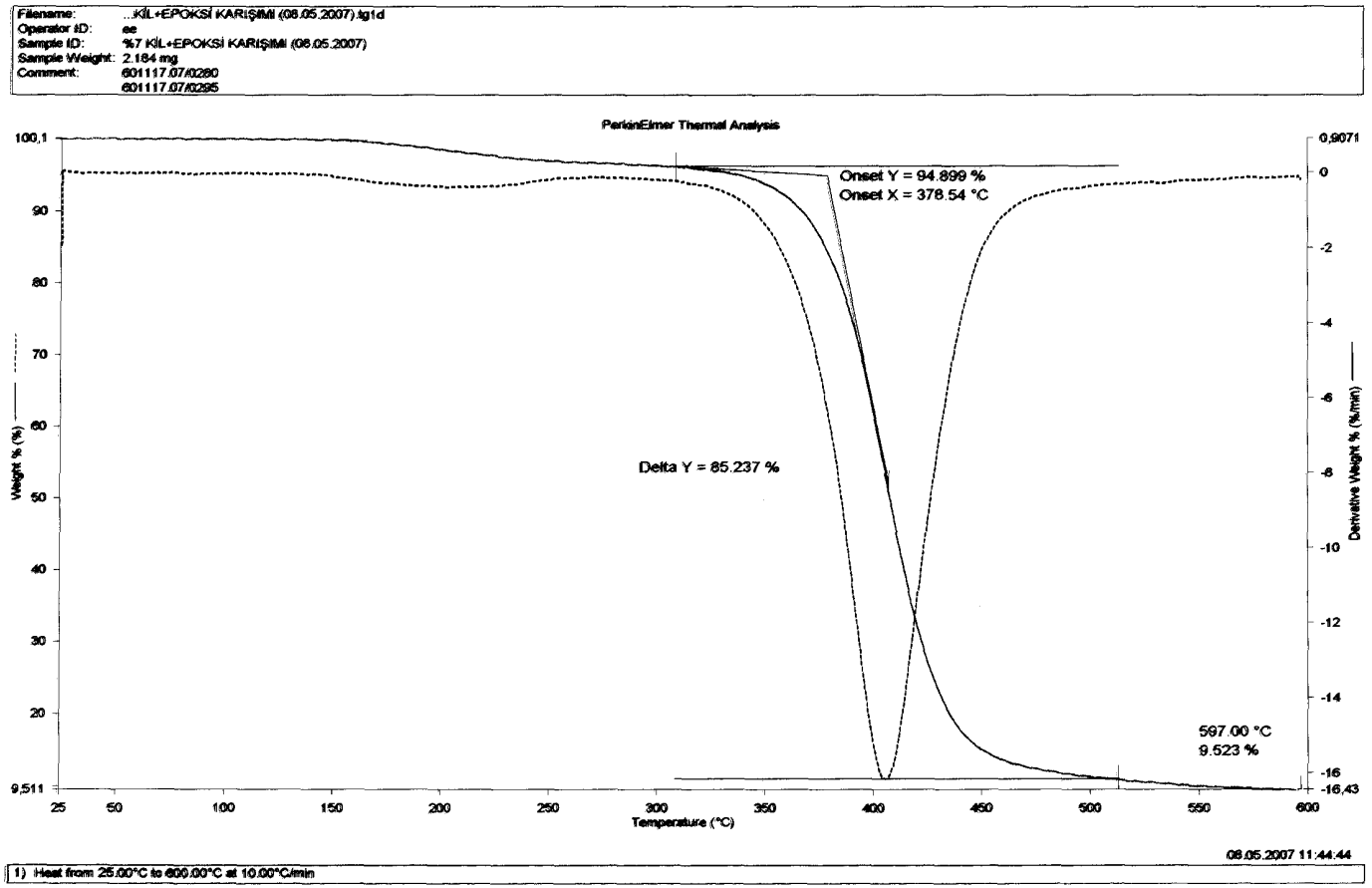

Figure C5. TGA thermogram of nanocomposite with 7 weight % Cloisite30B

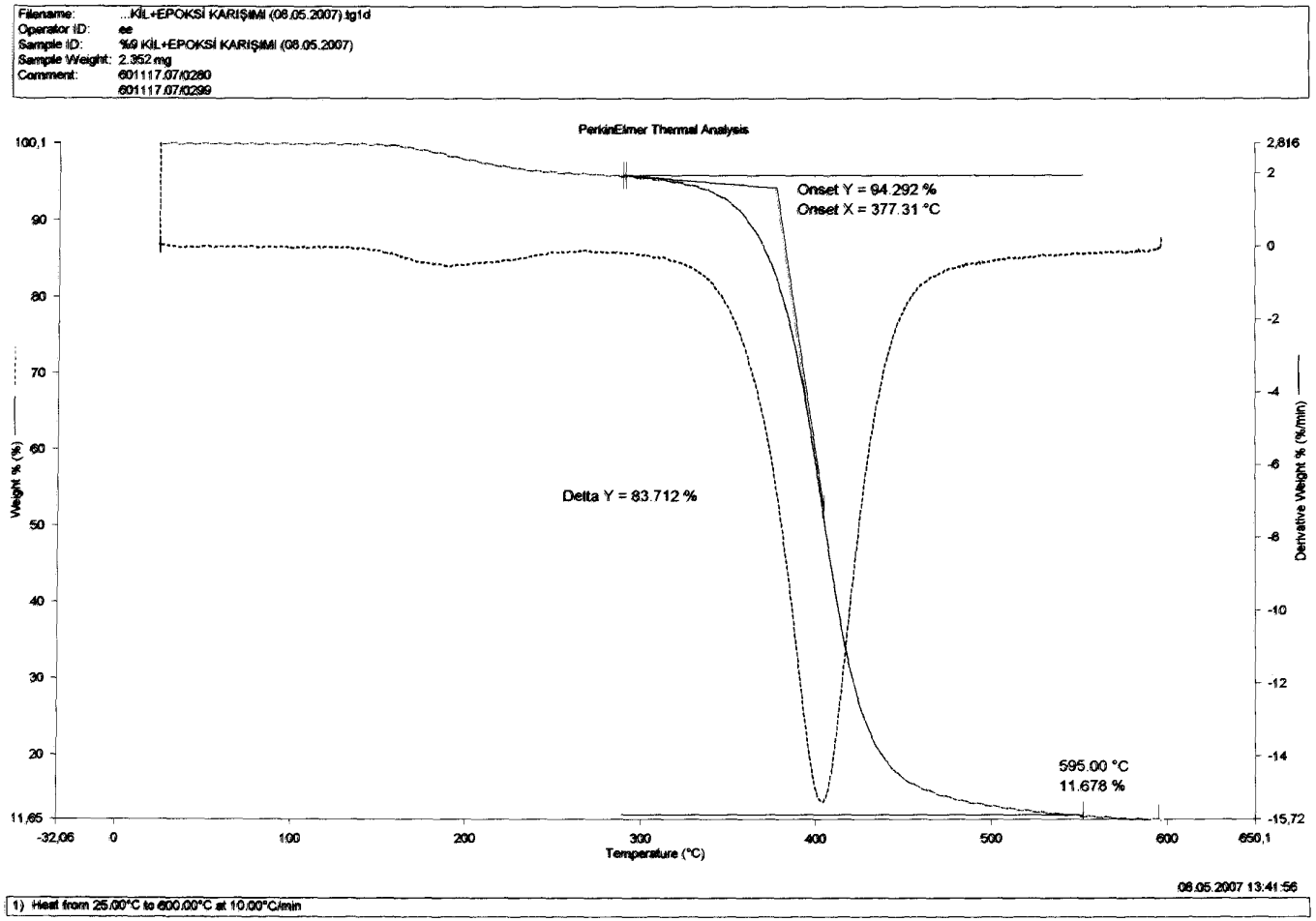

Figure C6. TGA thermogram of nanocomposite with 9 weight % Cloisite30B